Electronic Supplementary Information (ESI)

Mitochondria Targeted De Novo Designed Aggregation-Induced Emission Probe for Selective Detection of Neurotoxic Amyloid-β Aggregates

Tapas Bera, Aniruddha Mondal, Samiran Kar, Ayan Mukherjee, Somenath Banerjee and Samit Guha*

Department of Chemistry, Organic Chemistry Section, Jadavpur University, Kolkata 700032, India.

*E-mail: samitfsu@gmail.com, samit.guha@jadavpuruniversity.in

Table of Contents

Experimental Section

Materials: Fmoc-amino acid building blocks: Fmoc-Gly-OH, Fmoc-Ser(tBu)-OH, Fmoc-Asn(Trt)-OH, Fmoc-Lys(Boc)-OH, Fmoc-Glu(OtBu)-OH, Fmoc-Ala-OH, Fmoc-Ile-OH, Fmoc-Leu-OH, Fmoc-Met-OH, Fmoc-Val-OH, Fmoc-Tyr(tBu)-OH, Fmoc-His(Trt)-OH, Fmoc-Gln(Trt)-OH, Fmoc-Asp(tBu)-OH, Fmoc-Arg(Pbf)-OH, Fmoc-Phe-OH, Wang Resin LL (100-200 mesh), TLC silica gel 60 F_{254}, and XTT were acquired from Merck. 4-Diethylamino-salicylaldehyde, diethyl malonate, pyridine, Phosphorus oxychloride, 2-(4-Aminophenyl)acetonitrile, 1-[Bis(dimethylamino)methylene]-1*H*-1,2,3-triazolo[4,5-*b*]pyridinium 3-oxide hexafluorophosphate (HATU), *N*,*N*-Diisopropylethylamine (DIPEA), DMF, Thioflavin T, Uranyl acetate, *N,N,N′,N′*-Tetramethyl-*O*-(1*H*-benzotriazol-1-yl)uronium hexafluorophosphate (HBTU), 1-Hydroxybenzotriazole (HOBt), Trifluoroacetic acid (TFA), Triisopropylsilane (TIPS), 1,2-Ethanedithiol, Piperidine, Ethyl iodide, Tetrabutylammonium hydroxide 30-hydrate, Hoechst 33342, all the HPLC grade solvents and spectroscopic grade solvents were bought from Sigma-Aldrich. 1,1,1,3,3,3-Hexafluoro-2-propanol (HFIP) was bought from SRL Chemicals. $CDCl_3$ was attained from Cambridge Isotope Laboratories, Inc. Rhodamine B was procured from TCI chemicals. SH-SY5Y cells were obtained from the NCCS, India. XTT, DMEM, Trypsin EDTA mixture, and FBS were procured from HiMedia Laboratories. Mitochondrion targeting commercially available dye MitoTracker Deep Red FM and Ham's F-12K (Kaighn's) medium were acquired from Thermo Fisher Scientific. JC-1 based mitochondrion membrane potential and Annexin V-FITC/PI apoptosis detection kits were procured from BD Biosciences. *Millipore* ultra-pure H_2O was used for all the experiments.

METHODS

Microwave Synthesizer: Aβ40 peptide was synthesized by a manual microwave solid phase peptide synthesizer using the Fmoc-SPPS protocol (CEM corporation, model discover bio, USA make).

NMR Spectroscopy: 1D (^{1}H and ^{13}C NMR) and 2D NMR experiments were executed on Bruker DPX300 and DPX400 MHz spectrometers at 298 K in $CDCl_3$. The manufacturers' supplied Bruker TopSpin 3.6.2 software was utilized to process the data. NMR chemical shifts were recorded in δ ppm by locking and calibration with appropriate deuterated NMR solvents.

High-Resolution Electrospray Ionization Mass Spectrometry (HRMS-ESI): A Q-Tofmicro mass spectrometer from Waters Corporation was used to record the HRMS-ESI in positive mode. Manufacturers' supplied mass application software MassLynx V4.1 was utilized to process the data.

Matrix-Assisted Laser Desorption/Ionization Time-Of-Flight Mass Spectrometry (**MALDI-TOF MS)**: The mass of the Aβ40 protein was determined by MALDI-TOF MS using a Bruker Daltonics ultrafleXtreme instrument. Here, for the matrix preparation, α-cyano-4-hydroxy-cinnamic acid was used.

Absorption Spectroscopy: A Shimadzu UV-1800 spectrometer (double beam) with a wavelength range of 190-1100 nm was used to record the absorption spectra in various spectroscopy grade solvents. All inspections were accomplished in a quartz cuvette (1 cm path length).

Fluorescence Spectroscopy: In order to acquire fluorescence spectra in different spectroscopic grade solvents, a Horiba Jobin Yvon FluoroMax-4 spectrofluorometer operated by FluorEssence Version 3.9.0.1 software was utilized. Both the ex/em bandwidths were fixed at 5 nm.

Fluorescence Lifetime Measurement using Time-Correlated Single Photon Counting (TCSPC) Assay: The time-correlated single photon counting (TCSPC) method was utilized to achieve the fluorescence lifetimes (τ) of the synthesized Cou-AIE-TPP$^+$ fluorophore along with Cou-AIE-TPP$^+$ in the presence of Aβ40 peptide in PBS on the Horiba DeltaFlex lifetime device. The solutions of the Cou-AIE-TPP$^+$ probe and Cou-AIE-TPP$^+$ in the presence of Aβ40 peptide were distinctly excited with a 510 nm DeltaDiode laser (Horiba Scientific, model: DD-510L) to obtain the τ value. Horiba EzTime decay analysis software was used for fluorescence lifetime measurements and data analysis.

pH Meter: To prepare PBS solutions with specific pH values, a Mettler Toledo pH meter was used.

Inspection of the Aggregation-Induced Emission (AIE) Property of Cou-AIE-TPP$^+$: The AIE property of Cou-AIE-TPP$^+$ was examined by determining their fluorescence emission intensity in THF/PBS mixtures with different volume percentages (vol%) of PBS fractions. Various solutions were prepared with changing PBS volume percentages between 0−90% and the total volume of THF/PBS mixtures remained constant. The final concentration of Cou-AIE-TPP$^+$ in each sample was 2 μM. The fluorescence emission of these THF/PBS solutions was noted at λ_{ex} = 480 nm. A THF solution of Cou-AIE-TPP$^+$ is nonfluorescent but showed orange fluorescence after adding PBS due to the aggregation induced emission of Cou-AIE-TPP$^+$.

Preparation of Aβ40 Monomers, Oligomers, Protofibrils, and Fibrils:

Aβ40 monomer was prepared by dissolving Aβ40 peptide in HFIP (concentration of the stock solution 250 μM).

For the preparation of oligomers, 1.0 mg of lyophilized Aβ40 was dissolved in 400 μL of HFIP at 25 °C and waited for 15 m. Next, D.I. H_2O (900 μL) was mixed to the resulting Aβ40 (100 μL) solution. Afterward incubation at 25 °C for an additional 15 m, the solution was centrifuged, and the supernatant was taken into a new tube to evaporate the HFIP using an N_2 stream. Next, the sample was stirred at 500 rpm for 12 h. For the protofibril preparation it was incubated for 24 h.

To prepare Aβ40 fibrils, 1.0 mg of Aβ40 peptide was suspended in a 1% ammonium hydroxide solution (1.0 mL). The resulting solution (100 μL) was 10-times diluted using PBS buffer (pH = 7.4) and stirred at 25 °C for 5 days. The ThT fluorescence experiment and TEM analysis were applied to confirm the formation of Aβ40 fibrils.

A freshly prepared stock solution was used in every experiment.

Determination of Relative Quantum Yields of Cou-AIE-TPP$^+$ in the Presence and Absence of Aβ40 Peptide: The relative method was utilized to quantify the fluorescence quantum yields (QY) of the synthesized Cou-AIE-TPP$^+$ probe in the presence and absence of Aβ40 peptide. Here, the integrated fluorescence intensities of the synthesized Cou-AIE-TPP$^+$ probe, Cou-AIE-TPP$^+$ + Aβ40 monomers, Cou-AIE-TPP$^+$ + Aβ40 oligomers, and Cou-AIE-TPP$^+$ + Aβ40 fibrils were correlated with the reference molecule Rhodamine-B by applying the succeeding equation:

$\Phi_f(x) = \Phi_f(st) \times [(A_{st} \times F_x \times \eta_x^2)/(A_x \times F_{st} \times \eta_{st}^2)]$

Φ_f(st) and Φ_f(x): Fluorescence QY of the standard and synthesized Cou-AIE-TPP$^+$ probes, respectively.

A_{st} and A_x: Absorbance of standard and synthesized Cou-AIE-TPP$^+$ probes at λ_{ex}.

F_{st} and F_x : The integrated emission ranges underneath the modified emission spectra for the standard and synthesized Cou-AIE-TPP$^+$ probes, respectively.

η_{st} and η_x : Refractive indices of the solvents where the standard & synthesized Cou-AIE-TPP$^+$ probes were recorded, respectively. Herein, the standard and synthesized Cou-AIE-TPP$^+$ probes were dissolved in EtOH and PBS, respectively. Refractive indices, $\eta_{EtOH} = 1.3614$ and $\eta_{PBS} = 1.335$.

st : standard.

x : synthesized probe.

Φ_f(st): QY of the reference probe Rhodamine-B in EtOH = 0.49. In PBS, the relative QY (Φ_f) of the Cou-AIE-TPP$^+$ probe, Cou-AIE-TPP$^+$ + Aβ40 monomers, Cou-AIE-TPP$^+$ + Aβ40 oligomers, and Cou-AIE-TPP$^+$ + Aβ40 fibrils were determined to be 0.45, 0.47, 0.52, and 0.70, respectively.

Circular Dichroism (CD) Spectroscopy: CD spectra were acquired on a JASCO instrument (Model J-815–150S) at 25°C. Data were taken using a 1 mm quartz cuvette in the 190-260 nm range with a 0.5 nm step, 2 s collection times per step, and a 1 nm bandwidth. The CD signal from the PBS as background was corrected from the CD signal of the peptide solution in PBS. The secondary structure of Aβ40 peptide at 10 μM concentration in PBS solution was monitored at the initial stage (0 hours) and after being aged for 7 days at 37°C. The average of three spectra was taken for each measurement.

Fourier Transform Infrared Spectroscopy (FT-IR): FT-IR spectra were acquired on a PerkinElmer Spectrum Two FT-IR spectrometer from 4000 to 400 cm^{-1} at room temperature in ATR mode. The Aβ40 peptide fibrils were isolated from solution by centrifugation at 12000 rpm for ten minutes, and the secondary structure of the peptides was monitored using FT-IR. FT-IR spectra of Aβ40 monomer and Aβ40 fibrils were recorded, which signify random coil and β-sheet secondary structure, respectively.

X-Ray Powder Diffraction: The X-ray diffraction from the dried fibers of Aβ40 peptide was recorded on a Bruker D8 Advance X-ray diffractometer by Cu Kα radiation (λ = 1.5418 Å) operating at 40 kV and 40 mA.

TEM Experiments: 10 μL of freshly prepared Aβ40 monomers, oligomers, protofibrils, and fibrils in PBS solutions were pipetted out separately onto 300 mesh carbon-coated copper grids. After 2 m the solvent on the grid was cautiously blotted by a tissue paper. For negative staining, 10 μL of an aqueous solution of uranyl acetate [2 % (w/v)] was added to the grid and allowed to float for 30 s. The excess solution was shocked using a blotting paper. The sample was air dried at room temperature and kept in a desiccator for 1 day before taking TEM images on a JEOL (Model: JEM 2100F) instrument operated at 120 kV.

In Vitro Binding Assays through the Cou-AIE-TPP$^+$ Kinetic Assay: To study the fluorescence response of Cou-AIE-TPP$^+$ towards Aβ40, a solution of Cou-AIE-TPP$^+$ (1 μM) was mixed with different concentrations (0-10 μM) of Aβ40 (a final volume of 2 mL) and incubated in a PBS solution at room temperature for different times (0-200 min). The emission spectra (500-800 nm) of the mixture were measured at an excitation wavelength of 480 nm for Cou-AIE-TPP$^+$. λ_{em} of Cou-AIE-TPP$^+$ was monitored at 604 nm. The ex/em slit widths were kept at 5 nm. Three independent tests were executed for the Cou-AIE-TPP$^+$ binding kinetic assay. Error bars indicate standard deviations from the mean of three independent runs. We found that Cou-AIE-TPP$^+$ could report the nucleation (lag phase), elongation (growth phase), and saturation stages of Aβ40 fibril formation. The lag phase designated Aβ40 monomers and soluble oligomers; the elongation phase denoted early aggregates and late aggregates; and finally, the aggregation progression reached the saturation stage, where the majority of the Aβ40 peptides were converted to mature fibrils.

Thioflavin T (ThT) Kinetic Assay: A stock solution of ThT (50 μM) in PBS (pH 7.4) was made freshly with proper precaution to evade degradation from light. A solution of Aβ40 (10 μM) in 20 mmol of PBS (pH 7.4) was prepared. Aliquots of the Aβ40 peptide solution and the concentrated solution of ThT were mixed in a solution of 20 mmol PBS (pH 7.4). λ_{em} of ThT was monitored at 485 nm with λ_{ex} at 440 nm. The data were collected at 5 min intervals for 200 min. Three independent tests were executed for each ThT assay. Kinetic curves were fitted by the sigmoidal curve fitting. Error bars indicate standard deviations from the mean of three independent runs. All samples were stirred constantly by a micro magnetic stir bar. The incubation conditions were kept the same for Cou-AIE-TPP$^+$ and ThT. The ex/em slit widths were retained at 5 nm.

Competitive Binding and Displacement Assay: A displacement experiment that titrates Cou-AIE-TPP$^+$ (0 to 400 nM) against ThT (400 nM) bound Aβ40 fibrils (10 μM) is used. When Cou-AIE-TPP$^+$ is gradually added to the ThT/ Aβ40 pre-fibrillar complex in PBS (pH 7.4), ThT's fluorescence (λ_{em} = 480 nm) gradually decreases whereas Cou-AIE-TPP$^+$'s red fluorescence intensity (λ_{em} = 604 nm) sharply increases with an increase in Cou-AIE-TPP$^+$ concentration. Before recording the fluorescence in the displacement assay, the mixture was incubated at 25 °C for 5 m. The emission intensity of ThT and Cou-AIE-TPP$^+$ was recorded under excitation at λ_{ex} = 440 nm and λ_{ex} = 480 nm, respectively.

Measurement of Binding Affinity (K_d): Pre-aggregated Aβ40 (10 μM final concentration) was mixed with various concentrations of Cou-AIE-TPP$^+$ (10, 20, 30, 40, 50, 60, 70, 80, 90, 100, 150, 200, 250, 300 nM) in PBS. The mixtures were incubated for 30 m at 25 °C. Next the fluorescence emission intensity at 604 nm was measured at each excitation wavelength (λ_{ex} 480 nm). Three independent experiments were accomplished. The dissociation constants (K_d) were obtained from the best-fit curve for each of the tested probe solutions.

The dissociation constant (K_d) was calculated from fluorescence titration data using the Hill-1 equation:

$$\frac{F-F_0}{F_0} = 1 + \frac{[F-F_0]\,[AIE]^n}{{K_d}^n\,[AIE]^n}$$

F and F_0 were the emission intensities of Cou-AIE-TPP$^+$ in the presence and absence of Aβ40

K_d was the dissociation constant

n was the Hill's coefficient

The relative fluorescence intensity (F/F_0) of Cou-AIE-TPP$^+$ in the absence of Aβ40 at the starting point was considered to be ~ 1.

***n*-Octanol/PBS Partition Coefficient Value of Cou-AIE-TPP$^+$:** The *n*-Octanol/PBS partition coefficient value of Cou-AIE-TPP$^+$ was calculated. To determine the partition coefficient of Cou-AIE-TPP$^+$, 1 mg of Cou-AIE-TPP$^+$ was dissolved in 2 mL of *n*-octanol. By proper dilution the absorbance of the stock solution of Cou-AIE-TPP$^+$ in *n*-octanol was measured on a UV/vis spectrometer. The stock solution in *n*-octanol (1 mL) and an equal volume of PBS (pH 7.4) were combined and vortexed for one minute, and incubated at 37 °C for one hour to attain equilibrium. The solution was centrifuged for 10 minutes at 4000 rpm in order to disperse the organic and aqueous layers. Subsequently to centrifugation, the absorbance in *n*-octanol (*A*o) part was recorded on a UV/vis spectrometer using proper dilution. The partition coefficient value is obtained by dividing the absorbance of the n-octanol layer (after mixing) by the absorbance of an aqueous PBS layer (as determined by comparing the absorbance values of the n-octanol layer before and after mixing with PBS).

Partition coefficient (P) = $(A\text{o})_f$ /[$(A\text{o})_i$ − $(A\text{o})_f$]

$(A\text{o})_i$ and $(A\text{o})_f$ were the initial and final absorbances in the *n*-octanol layer, respectively.

The partition coefficient (P) of Cou-AIE-TPP$^+$ was found to be 19.95, and the log P value was 1.3.

Diffusion-Ordered Spectroscopy (DOSY) and Diffusion by NMR: The proton diffusion-ordered NMR spectroscopy (DOSY-NMR) studies were executed on a 400 MHz Bruker NMR instrument equipped with an iProbe. To measure the diffusion coefficient of Cou-AIE-TPP$^+$ at 25 °C, a 5 μM concentrated solution of Cou-AIE-TPP$^+$ was prepared in a buffer encompassing 20 mM sodium phosphate (pH 7.4) and 20 mM NaCl. Cou-AIE-TPP$^+$ (5 μM) in both the absence and presence of Aβ40 (10 μM) solutions in PBS were loaded into standard 5-mm NMR tubes for the DOSY experiment. The data for diffusion measurements were collected at 25 °C with a diffusion delay time (Δ) of 50 ms, gradient pulse duration (δ) of 1.5 ms, and a gyromagnetic ratio (γ) of 26752 rad / (s*Gauss) with variable gradient strengths (gauss/cm). Data processing and analysis were executed by the

Bruker TopSpin 4.3.0 software. The collective FIDs were Fourier transformed using Bruker TopSpin 4.3.0 to obtain a pseudo-2D spectrum. The diffusion coefficient was calculated by fitting the experimental data to the Stejskal-Tanner formula: $I(G_z) = I(0)*\exp[-D\gamma^2\delta^2G_z^2(\Delta - \delta/3)]*10^4$.

$I(G_z)$ and $I(0)$ = The signal intensities obtained with the respective gradient strengths of G_z and $G_z = 0$

D = Diffusion coefficient

γ = Gyromagnetic ratio

δ = Gradient pulse duration

Δ = Diffusion time

The diffusion coefficient of a Cou-AIE-TPP$^+$ (5 μM) sample in PBS was $3.11\pm0.14 \times 10^{-10}$ m^2 s^{-1}, whereas the addition of Aβ40 (10 μM) to the Cou-AIE-TPP$^+$ (5 μM) sample in PBS caused a change in the diffusion coefficient of Cou-AIE-TPP$^+$ to $2.77\pm0.03 \times 10^{-10}$ m^2 s^{-1}.

Isothermal Titration Calorimetry (ITC): ITC experimentation was executed on a MicroCal PEAQ-ITC microcalorimeter (Malvern). ITC measures the heat released/absorbed in a biomolecular binding incident in solution and calculates the binding affinity and thermodynamic parameters of molecular interactions in a single test. It helps to understand why the interactions happen, including the binding mechanisms. Binding affinity (K_D), reaction stoichiometry (n), enthalpy (ΔH), and entropy (ΔS) disclose the forces that dictate biomolecular interactions and can also exemplify function and mechanism at a molecular level. Aβ40 solution was made in PBS solution and filtered via a 0.2 μm syringe filter before the ITC assay. The reference cell was loaded with a PBS solution. 280 μL of Aβ40 (20 μM) in PBS was transferred into the sample cell, and 200 μM Cou-AIE-TPP$^+$ (10 times more concentrated than Aβ40) in PBS was poured into the syringe. In every test, 2 μL × 19 injections with an overall volume of 38 μL of Cou-AIE-TPP$^+$ were transferred to the Aβ40 solution with a period of 4s per injection and 150s spacing among two injections. Mixing was performed automatically by stirring the syringe at a speed of 750 rpm at 25 °C. The titrations were performed in triplicate at 25 °C, and for all the titrations, almost indistinguishable outcomes were acquired. Blank titrations were performed by injecting PBS into PBS, Cou-AIE-TPP$^+$ into PBS, and Aβ40 dilutions were subtracted from the Aβ40/Cou-AIE-TPP$^+$ titration. Binding enthalpy was achieved by fitting the amended data into an appropriate binding model. A titration plot of kcal/mol vs molar ratio (Cou-AIE-TPP$^+$/Aβ40) was developed. The upper panels show the raw data for the Aβ40/Cou-AIE-TPP$^+$ titration, and the bottom panels signify the binding isotherm by plotting integrated peak areas vs the molar ratio for titration. The subsequent isotherm is best fitted to a binding model to attain the K_D, n, ΔH, ΔS, and ΔG of interaction. The ITC data and plots were examined by MicroCal PEAQ-ITC Analysis Software to measure the heat of interaction and thermodynamic parameters.

Computational Methods:

Density functional theory (DFT): The density functional theory (DFT) calculation for Cou-AIE-TPP$^+$ was performed with Gaussian 09 W software.[S1] The ground state geometries were optimized at the Becke 3-parameter exchange functional by the gradient-corrected correlation functional of Lee, Yang, and Parr (B3LYP) by the 6-31+G* basis set [B3LYP/6-31+G*]. The frontier molecular orbitals (FMOs) of Cou-AIE-TPP$^+$ were analyzed using Gaussian 09W under the B3LYP/6-31+G* level.

Molecular Docking Simulation: The obtained energy minimized structure of Cou-AIE-TPP$^+$ using B3LYP/6-31+G* was used for the molecular docking experiment. The crystal structure of Aβ40 fibrils (PDB ID: 2LMP) was achieved from the Protein Database (www.rcsb.org) and optimized by the AutoDock4.2 software.[S2] Molecular docking simulation was accomplished with Autodock Vina. Figures were developed through the Discovery Studio Visualizer software package. AutoDock4.2 was exploited for molecular docking experiments with the aid of the Lamarckian procedure inside the grid box of dimensions 60 × 60 × 60 Å^3 at the ligand binding pocket. The greatest docking pose of the molecules was anticipated through binding energy, inhibition constant, ligand efficiency, van der Waals forces, intermolecular energy, hydrogen bond, total internal energy, dissolve energy, torsional energy, and unbound energy.

The scoring function was written as: $\Delta G_{binding} = \Delta G_{vdW} + \Delta G_{elec} + \Delta G_{hbond} + \Delta G_{desolv} + \Delta G_{tors}$

The DFT energy-minimized conformer of the Cou-AIE-TPP$^+$ molecule in the Aβ40 peptide binding site was documented by .dlg file that was analyzed with the aid of AutoDockTools.

Cell Culture: SH-SY5Y was a three-time subcloned cell derived from the SK-N-SH human neuroblastoma cell line. The SH-SY5Y cell line was studied as a model for neurodegenerative disorders. A human neuroblastoma cell line SH-SY5Y was maintained in growth media encompassing DMEM:Ham′s F12 (1:1, pH 7.4), glutamine (2 mM), non-essential amino acids (1% NEAA), and 10% FBS. The SH-SY5Y cell line was preserved at 37 °C in the incubator with routine passage of 5% CO_2.

Cell Viability Assay using XTT Reagent: The cell viability test was performed on SH-SY5Y cells by 2,3-bis-(2-methoxy-4-nitro-5-sulfophenyl)-2*H*-tetrazolium-5-carboxanilide (XTT) reagent. The SH-SY5Y cells (5 × 10^4 cells/well) were seeded in a 96-well plate in 50% DMEM and F12K media (Invitrogen) with 10% FBS and grown to obtain > 80% confluency before treatment. SH-SY5Y cells were treated with various concentrations of Cou-AIE-TPP$^+$ (control, 0.5, 1.0, 2.0, 5.0, 10.0, 20.0, and 50.0 μM) and incubated for 72 h at 37 °C. After treatment, 25 μL of XTT solution with phenazine methosulfate (PMS) in 50% DMEM and F12K were mixed to each well and further incubated for 2 h at 37 °C, which was converted to H_2O-soluble highly colored formazan upon reduction in the presence of an electron mediator (dehydrogenases present in metabolically active cells). The microplate was shaken for 10 seconds, and the absorbance at 470 nm was recorded by an automated microplate reader (Thermo Fisher Scientific). The quantity of the formazan dye produced by the activity of

dehydrogenases in SH-SY5Y cells was directly proportional to the number of living SH-SY5Y cells. The SH-SY5Y cell viability was calculated based on the measured data (colorimetric assays). The consequences were reported by the following equation:

Viable cells (%) = (*A* of treated cells / *A* of untreated cells) × 100

All experiments were performed in parallel and in triplicate.

Evidence for the Accumulation of Cou-AIE-TPP$^+$ within the Live Human Neuroblastoma SH-SY5Y Cell Mitochondria Monitored through Confocal Laser Scanning Microscopy: Confocal laser scanning microscopy (CLSM) was performed to verify the accumulation of Cou-AIE-TPP$^+$ within the mitochondria of human neuroblastoma SH-SY5Y live cells. CLSM images were acquired using a Leica STELLARIS 5 platform with a HC PL APO 100×/ 1.40 OIL CS2 objective connected to a white light laser (WLL) along with an Acousto-Optical Beam Splitter (AOBS) and HyD S detector. For human neuroblastoma SH-SY5Y live cells CLSM imaging, the cells at a density of 5×10^4 cells/mL were seeded in a 35-mm glass-bottomed confocal dish (SPL Lifesciences, catalogue no. 200350) and permitted to obtain ~80% confluency in DMEM: F12K (1:1, pH 7.4) media at 37 °C for 24 h in a 5% CO_2 incubator. Next washing through 1× PBS, live SH-SY5Y cells were incubated with a 500 nM solution of Cou-AIE-TPP$^+$ in media for 20 min at 37 °C in a 5% CO_2 environment; subsequently, the media was discarded cautiously and washed caringly using 1× PBS. Successively, SH-SY5Y cells were incubated first with 0.2 μM MitoTracker Deep Red FM and then with Hoechst 33342 (0.1 μg mL^{-1}) for 20 and 15 min, respectively, at 37 °C in a 5% CO_2 setting. Later in the treatment process, SH-SY5Y cells were finally washed twice with media before capturing the CLSM images. Human neuroblastoma SH-SY5Y live cell confocal images were processed by LAS X software. In the course of the live SH-SY5Y cells CLSM imaging process, 37 °C and a 5% CO_2 setting were upheld (Figure S50).

For Hoechst 33342: laser λ_{ex} = 405 nm (blue channel, detection range of emission 415-480 nm); MitoTracker Deep Red FM: laser λ_{ex} = 638 nm (Cy-5 channel, detection range of emission 650-710 nm); Cou-AIE-TPP$^+$: laser λ_{ex} = 488 nm (green channel, detection range of emission 570-630 nm).

Live SH-SY5Y Cell 3D Confocal Imaging using Synthesized Cou-AIE-TPP$^+$ Dye: For the live cell 3D picture accomplishment, the CLSM images of human neuroblastoma SH-SY5Y live cells stained with the mitochondria targeting synthesized Cou-AIE-TPP$^+$ dye and nuclear staining dye Hoechst 33342 were captured every 0.4 μm on the Z-axis by a Leica STELLARIS 5 confocal microscope. 32 frames for each channel were taken over a 10 minute period and finally rebuilt with the aid of LAS X software to acquire the live SH-SY5Y cell 3D CLSM images.

In Vitro Fluorescence Imaging of Aβ40 Fibrils using Synthesized Cou-AIE-TPP$^+$ Dye: The SH-SY5Y cells were seeded and cultured in a dish at 5×10^3 cells/dish for 24 h at 37 °C. Next washing through 1 × PBS, live SH-SY5Y cells were incubated with Aβ40 (10 μM) for different times at 37 °C in a 5% CO_2 atmosphere. Subsequently, the media was discarded cautiously and washed caringly using 1 × PBS. Successively, SH-SY5Y cells were incubated first with 500 nM Cou-AIE-TPP$^+$ for 20 min and then stained with ThT (5 μM) for 20 min at 37 °C in a 5% CO_2 setting. Later in the treatment process, SH-SY5Y cells were finally washed twice with media before capturing the CLSM images. Confocal images of human neuroblastoma SH-SY5Y cells treated with Aβ40 (10 μM) over 0-48 h were obtained by a Leica STELLARIS 5 confocal microscope and the images were processed through LAS X software.

For ThT: laser λ_{ex} = 405 nm (blue channel, detection range of emission 450-500 nm); Cou-AIE-TPP$^+$:laser λ_{ex} = 488 nm (green channel, detection range of emission 570-630 nm).

Pearson's Correlation Coefficient (PCC) Determination: Pearson's correlation coefficient (PCC) is one of the classical statistical analyses in pattern recognition for matching one confocal image (green channel) with another (red channel). PC graphs can explain the extent of overlapping among two patterns in a dual-color colocalization image. PC coefficients were calculated by the examination of confocal micrographs by the LAS X software with the Quantify tool. To determine PC coefficients for CLSM images, all of the pixels having the same image coordinates were paired.

PC coefficient (PCC) was calculated (image comprising of two channels) according to the equation:

$$PCC = \frac{\sum_i (S1_i - S1_{avg}) * (S2_i - S2_{avg})}{[\sum_i (S1_i - S1_{avg})^2 * \sum_i (S2_i - S2_{avg})^2]^{(1/2)}}$$

S1 = signal intensity of pixels (pixel i) in the 1st channel

S2 = signal intensity of pixels (pixel i) in the 2nd channel.

$S1_{avg}$ = mean values of pixels in the 1st channel

$S2_{avg}$ = mean values of pixels in the 2nd channel.

Determination of Mitochondrial Membrane Potential Alteration after Incubation with Aβ40 Over Time Using the JC-1 Assay: Amendments in mitochondrial membrane potential were measured using a lipophilic cationic JC-1 probe (mitochondrion membrane potential detection kit) on a fluorescence-activated cell sorting (FACS) flow cytometer. For healthy mitochondria, the $\Delta\Psi_m$ value was highly negative. JC-1 dye was incorporated to the mitochondria, and the J-aggregates of JC-1 were observed. Conversely, when the membrane

depolarized, the J-aggregates of JC-1 seepage from the mitochondria into the cytosol as monomers were detected. The excitation of JC-1 was 494 nm, and the emission was detected at 527 nm (green emission, JC-1 monomers) as well as at 596 nm (orange-red emission, JC-1 aggregates). The JC-1 monomers-to-aggregates emission ratio (527/596) was assessed. The greater value of this emission ratio specified larger membrane depolarization. Subsequently, after incubation of SH-SY5Y cells with Aβ40 (10 μM) over time (0-24 h), the cells were incubated with a JC-1-based mitochondrion membrane potential detection kit for 15 min using the manufacturer's supplied protocol at 37 °C in dark. Next, $\Delta\Psi_m$ was evaluated on a FACS instrument (BD Biosciences, Mountain View, CA, USA), and the cytogram analysis was executed by the Cell Quest software (BD Biosciences). After SH-SY5Y cells were incubated with the JC-1 probe, the emission signals were scrutinized in the FITC and PE channels by a 494 nm laser.

Annexin V-FITC/PI Apoptosis Detection Assay after Incubation with Aβ40 Over Time: The extent of apoptosis was quantitatively acquired by the Annexin V-FITC/PI apoptosis assay kit by FACS. Negatively charged phosphatidylserine (PS) usually exists in the inner leaflet of a healthy cell membrane. In the event of early apoptosis, the PS is flipped from the inner to outer membrane and is exposed. FITC-conjugated Annexin V has a great affinity for PS on the apoptotic cell membrane surface and is the most sensitive biomarker to identify early apoptosis. The assay kit also comprises propidium iodide (PI) to stain the cellular DNA in necrotic cells. PI cannot penetrate the healthy or early apoptotic intact cell membrane. PI can infiltrate the late apoptotic and necrotic cell membranes and stain these cells. The cultured SH-SY5Y cells (5×10^4 cells/well) were incubated with Aβ40 (10 μM) at various times (0-24 h). The SH-SY5Y cells were then trypsinized and rinsed with cold 1x PBS twice. Next, the cells were suspended in 1× annexin-binding buffer; subsequently, 100 μL of the solution was taken into a 5 mL culture tube. Maintaining the manufacturer's protocol, the SH-SY5Y cells were incubated with Annexin V-FITC/PI apoptosis detection assay kit solutions for 15 minutes at 25 °C in the dark. 400 μL of 1× Binding Buffer was mixed to each tube. The binding buffer in the apoptosis kit contains $CaCl_2$. After the incubation period, the samples were preserved on ice. The emissions at different time points were recorded on a BD FACSCalibur Flow Cytometer (BD Bioscience). Data were examined, and the percentage of cells that undergo early and late apoptosis was determined by BD CellQuest Pro software (BD Bioscience). A control experiment was performed without the addition of Aβ40.

Constructions and Characterizations of Cou-AIE and Cou-AIE-TPP$^+$ Probes: All the compounds were synthesized in oven-dried flasks using dry solvents in an inert N_2 environment, unless otherwise specified. Analytical TLC was performed using aluminium sheets coated with Silica gel (TLC silica gel 60 F_{254}), and the corresponding spots were then found using a UV light or the human eye, or by developing with I_2. Column chromatography (silica gel, 100-200 mesh) was used to separate the compound from the raw ingredients as well as side products and eluted with solvents specified. The column chromatography solvents were distilled by the

appropriate drying agent before use. A variety of spectroscopic methods were used to characterize each of the molecules.

Synthesis of 7-(diethylamino)-2*H*-chromen-2-one (1): Diethyl malonate (4.16 g, 0.026 mol) and 4-(diethylamino)salicylaldehyde (2.5 g, 0.013 mol) were dissolved in 30 mL of pure EtOH. Next, pyridine (1.29 mL, 0.016 mol) was added and it was refluxed at 90 °C for 6 h. The solvent was then drawn out in a vacuum once the reaction mixture had been cooled to room temperature. The residue was mixed with 20 mL of HCl (37%) and 20 mL of glacial AcOH, and the mixture was again refluxed at 125 °C for an additional 6 h. After being brought to room temperature, the reaction mixture was dissolved in 100 mL of ice-cold distilled H_2O. By adding 40% aqueous NaOH, the pH of the solution was kept at 5, and the combination remained at room temperature for 30 minutes. It was filtered to obtain a yellow precipitate that was then rinsed with distilled H_2O to acquire a pure, solid yellow compound **1**.

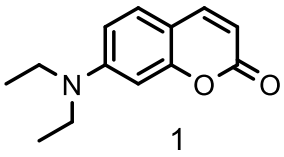

1

Yield: 2.26 g (80%)

^{1}H NMR ($CDCl_3$, 300 MHz, 25 °C): δ = 7.57 (d, J = 9.3 Hz, 1H), 7.28 (d, J = 8.7 Hz, 1H), 6.59 (dd, J = 2.6 Hz, 8.8 Hz, 1H), 6.52 (d, J = 2.5 Hz, 1H), 6.07 (d, J = 9.3 Hz, 1H), 3.45 (q, J = 7.1 Hz, 4H), and 1.24 (t, J = 7.1 Hz, 6H) ppm.

^{13}C NMR ($CDCl_3$, 75 MHz, 25 °C) δ = 162.2, 156.7, 150.6, 143.7, 128.8, 109.2, 108.8, 108.4, 97.6, 44.9, and 12.4 ppm.

HRMS (ESI +ve) *m*/*z*: Observed for $C_{13}H_{16}NO_2^+$ $[M+H]^+$ = 218.1170, $[M+H]^+$ calcd = 218.1176.

Synthesis of 7-(diethylamino)-2-oxo-2*H*-chromene-3-carbaldehyde (2): Anhydrous DMF (10.8 mL, 0.147 mol) was taken into a 25 mL two-neck round bottomed flask under N_2 atmosphere and $POCl_3$ (2 mL, 0.021 mol) was added dropwise, and the mixture was stirred at 0 °C for 30 min. The solution of 1 (1.5 g, 0.007 mol) in anhydrous DMF (7 mL) was added dropwise to the DMF-$POCl_3$ mixture at 0 °C. After being heated at 60 °C for 12 h, the mixture was cooled and put into ice-cold distilled H_2O. With the addition of a 20% aqueous NaOH solution, the resulting solution's pH was kept at 7. The residue was filtered, and rinsed with distilled H_2O for numerous times. The substance was dried using a rotary evaporator to obtain the pure product **2** as an orange solid.

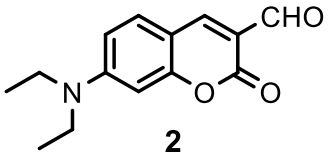

2

Yield: 1.20 g (70%).

^{1}H NMR ($CDCl_3$, 300 MHz, 25 °C): δ = 10.12 (s, 1H), 8.25 (s, 1H), 7.41 (d, J = 9.0 Hz, 1H), 6.63 (dd, J = 2.5 Hz, 9.0 Hz, 1H), 6.48 (d, J = 2.5 Hz, 1H), 3.47 (q, J = 7.1 Hz, 4H), and 1.25 (t, J = 7.1 Hz, 6H) ppm.

^{13}C NMR ($CDCl_3$, 75 MHz, 25 °C) δ = 187.9, 161.9, 158.9, 153.5, 145.4, 132.5, 114.3, 110.2, 108.2, 97.2, 45.3, and 12.5 ppm.

HRMS (ESI +ve) *m/z*: Observed for $C_{14}H_{16}NO_3^+$ $[M+H]^+$ = 246.1132 , $[M+H]^+$ calcd = 246.1125.

2-(4-(Diethylamino)phenyl)acetonitrile (3): To a solution of 2-(4-aminophenyl)acetonitrile (1 g, 0.008 mol) in dry DMF (20 mL), K_2CO_3 (2.1 g, 0.015 mol) was added, and the solution was stirred at 80 °C. Iodoethane (1.2 mL, 0.015 mol) was slowly added to the reaction mixture, and the reaction was continued at 80 °C for 12 h. DCM was used to extract the mixture after it had been cooled down to room temperature. The organic phase was dried over anhydrous Na_2SO_4, filtered, and the solvent evaporated in a vacuum. EtOAc and n-hexane (5:95 v/v, R_f = 0.7) were used in column chromatography to obtain the pure product **3** as a brown colored liquid.

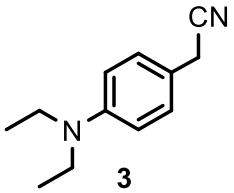

3

Yield: 1.08 g (72%).

^{1}H NMR (300 MHz, $CDCl_3$, 25 °C): δ = 7.16 (d, J = 8.3 Hz, 2H), 6.68 (d, J = 8.3 Hz, 2H), 3.65 (s, 2H), 3.37 (q, J = 7.1 Hz, 4H), and 1.18 (t, J = 7.1 Hz, 6H) ppm.

^{13}C NMR (75 MHz, $CDCl_3$, 25 °C): δ = 147.4, 129.0, 118.8, 115.9, 112.1, 44.4, 22.6, and 12.5 ppm.

HRMS (ESI +ve) *m/z*: Observed for $C_{12}H_{17}N_2^+$ $[M+H]^+$ = 189.1386, $[M+H]^+$ calcd = 189.1386.

(*Z*)-3-(7-(diethylamino)-2-oxo-2*H*-chromen-3-yl)-2-(4-(diethylamino)phenyl)acrylonitrile (Cou-AIE): Compounds 2 (0.49 g, 0.002 mol), 3 (0.38 g, 0.002 mol), and 20 mL *tert*-BuOH were placed in a round-bottomed flask. Then tetrabutylammonium hydroxide (TBAOH, 25% in Methanol, 0.629 mL) was added dropwise into the mixture. The solution was stirred at 80 °C for 24 h under N_2 atmosphere. It was cooled to room temperature, and the crude product was filtered, washed with MeOH, and dried. The crude material was further purified by silica gel column chromatography using DCM:MeOH (20:1 v/v, R_f = 0.6) to acquire the pure product **Cou-AIE** as an red solid.

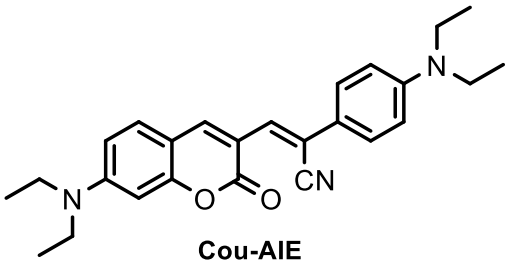

Cou-AIE

Yield: 0.42 g (51%).

^{1}H NMR ($CDCl_3$, 300 MHz, 25 °C): δ = 8.63 (s, 1H), 7.74 (d, J = 8.8 Hz, 1H), 7.65 (s, 1H), 7.57 (d, J = 8.8 Hz, 2H), 6.72–6.64 (m, 3H), 6.51 (d, J = 2.4 Hz, 1H), 3.50–3.41 (m, 8H), and 1.28 (t, J = 7.1 Hz, 12H) ppm.

^{13}C NMR ($CDCl_3$, 75 MHz, 25 °C): δ = 159.5, 140.8, 131.6, 131.3, 130.9, 130.5, 130.3, 128.3, 126.9, 126.7, 126.6, 114.4, 113.6, 111.2, 111.1, 44.5, and 12.6 ppm.

HRMS (ESI +ve) *m/z*: Observed for $C_{26}H_{30}N_3O_2^+$ $[M+H]^+$ = 416.2320, $[M+H]^+$ calcd = 416.2333. Observed for $C_{26}H_{31}N_3O_2^{2+}$ $[M+2H]^+$ = 208.6206, $[M+H]^+$ calcd = 208.6203.

2-(4-(ethylamino)phenyl)acetonitrile (4): To a solution of 2-(4-aminophenyl)acetonitrile (1.06 g, 0.008 mol) in dry DMF (15 mL), K_2CO_3 (0.97 g, 0.007 mol) was mixed, and the solution was stirred at 80 °C. Then iodoethane (0.6 mL, 0.007 mol) was slowly added to the reaction mixture, and the reaction was continued at 80 °C for 12 h. It was cooled to room temperature, and the mixture was extracted with DCM. The organic phase was dried over anhydrous Na_2SO_4, filtered, and the solvent evaporated in a vacuum. The crude product was purified by column chromatography using EtOAc and n-hexane (10:90 v/v, R_f = 0.3) to obtain the pure product **4** as a brown colored liquid.

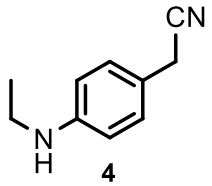

4

Yield: 0.96 g (86%).

^{1}H NMR (300 MHz, $CDCl_3$, 25 °C): δ = 7.13 (d, J = 8.3 Hz, 2H), 6.61 (d, J = 8.6 Hz, 2H), 3.65 (s, 2H), 3.18 (q, J = 7.1 Hz, 2H), and 1.28 (t, J = 7.1 Hz, 3H) ppm.

^{13}C NMR (75 MHz, $CDCl_3$, 25 °C): δ = 148.1, 128.9, 118.7, 117.8, 113.1, 38.5, 22.8, and 14.8 ppm.

HRMS (ESI +ve) *m/z*: Observed for $C_{10}H_{13}N_2^+$ $[M+H]^+$ = 161.1077, $[M+H]^+$ calcd = 161.1073.

***Tert*-butyl *N*-(4-(cyanomethyl)phenyl)-*N*-ethylglycinate (5)**: A mixture of 2-(4-(ethylamino)phenyl)acetonitrile (0.96 g, 0.006 mol), *tert*-butyl bromoacetate (1.37 mL, 0.009 mol), K_2CO_3 (2.49 g, 0.018 mol), and KI (0.15 g, 0.0009 mol) in CH_3CN (20 mL) was heated to reflux for 12 h. The solvent was evaporated off, after which DCM (50 mL) and H_2O (50 mL) were added, and the organic layer was extracted. The DCM layer was dried with anhydrous Na_2SO_4. After removal of the solvents using a rotary evaporator, the crude product was purified over silica gel using n-Hexane:EtOAc (95:5, R_f = 0.7) as the eluent to yield the pure compound **5** as a brown liquid.

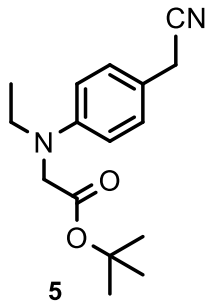

5

Yield: 1.51 g (92%).

^{1}H NMR (300 MHz, $CDCl_3$, 25 °C): δ = 7.16 (d, J = 8.6 Hz, 2H), 6.63 (d, J = 8.6 Hz, 2H), 3.93 (s, 2H), 3.64 (s, 2H), 3.47 (q, J = 7.1 Hz, 2H), 1.47 (s, 9H), and 1.22 (t, J = 6.8 Hz, 3H) ppm.

^{13}C NMR (75 MHz, $CDCl_3$, 25 °C): δ = 170.3, 147.6, 128.9, 118.7, 117.2, 112.2, 81.6, 53.1, 46.3, 28.1, 22.6, and 12.5 ppm.

HRMS (ESI +ve) *m/z*: Observed for $C_{16}H_{22}N_2O_2Na^+$ $[M+Na]^+$ = 297.1570, $[M+Na]^+$ calcd = 297.1573.

***Tert*-butyl (*Z*)-*N*-(4-(1-cyano-2-(7-(diethylamino)-2-oxo-2*H*-chromen-3-yl)vinyl)phenyl)-*N*-ethylglycinate (6)**: Compounds 2 (0.49 g, 0.002 mol), 5 (0.55 g, 0.002 mol), and ^{t}BuOH (20 mL) were placed in a round-bottomed flask. Then tetrabutylammonium hydroxide (TBAOH, 25% in Methanol, 0.629 mL) was added dropwise into the mixture. Next, the solution was reflux for 24 h under N_2 atmosphere. The solution was cooled to room temperature, and the crude product was filtered. The residue was washed with MeOH and then dried. The crude residue

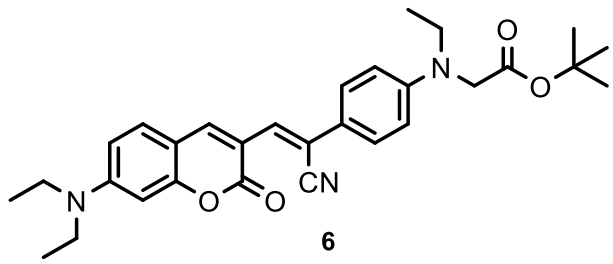

6

was further purified by column chromatography utilizing Hexane/EtOAc (5:1, R_f = 0.6) as the eluent to acquire the pure material **6** as a red solid.

Yield: 0.4 g (40%).

^{1}H NMR ($CDCl_3$, 400 MHz, 25 °C): δ = 8.63 (s, 1H), 7.67 (s, 1H), 7.57 (d, J = 9.0 Hz, 2H), 7.40 (d, J = 9.0 Hz, 1H), 6.67–6.62 (m, 3H), 6.51 (d, J = 2.5 Hz, 1H), 3.97 (s, 2H), 3.54–3.42 (m, 6H), 1.48 (s, 9H), and 1.25 (t, J = 7.3 Hz, 9H) ppm.

^{13}C NMR (101 MHz, $CDCl_3$, 25 °C): δ = 169.9, 162.1, 156.3, 151.5, 148.5, 139.5, 130.3, 129.9, 127.1, 122.5, 118.7, 114.7, 111.9, 110.1, 109.6, 108.7, 97.2, 81.9, 53.1, 46.4, 45.0, 29.7, 28.1, and 12.5 ppm.

HRMS (ESI +ve) *m*/*z*: Observed for $C_{30}H_{35}N_3O_4Na^+$ $[M+Na]^+$ = 524.2524, $[M+Na]^+$ calcd = 524.2520.

(*Z*)-*N*-(4-(1-cyano-2-(7-(diethylamino)-2-oxo-2*H*-chromen-3-yl)vinyl)phenyl)-*N*-ethylglycine (7): To a solution of **6** (0.5 g, 0.001 mol) in EtOH (10 mL), 10 mL of 10% NaOH was mixed, and the solution was heated to reflux for 15 min. The solution was acidified to pH 2 using conc. HCl and cooled to 0 °C, giving a large amount of precipitate. The product was filtered and thoroughly washed with water, dried, and recrystallized in absolute EtOH to give **7** as a reddish solid.

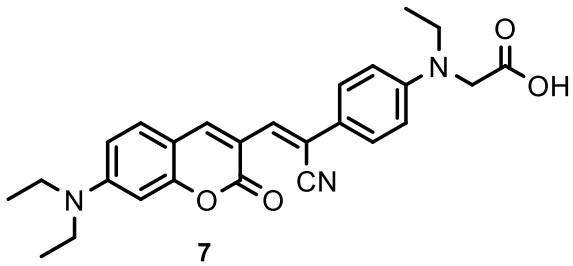

7

Yield: 0.31 g (70%).

^{1}H NMR (400 MHz, $CDCl_3$, 25 °C): δ = 10.15 (s, 1H), 8.64 (s, 1H), 7.67 (s, 1H), 7.57 (d, J = 7.8 Hz, 2H), 7.44 (d, J = 9.2 Hz, 1H), 6.67–6.65 (m, 3H), 6.52 (d, J = 2.4 Hz, 1H), 3.97 (s, 2H), 3.53–3.46 (m, 6H), and 1.28 (t, J = 7.5 Hz, 9H) ppm.

^{13}C NMR (101 MHz, $CDCl_3$, 25 °C) δ = 190.3, 176.8, 165.9, 159.7, 158.1, 149.9, 145.4, 141.8, 127.2, 118.9, 118.5, 117.8, 111.9, 110.2, 98.7, 61.5, 45.3, 45.0, 12.6, and 12.5 ppm.

HRMS (ESI +ve) m/z: Observed for $C_{26}H_{27}N_3O_4$ $[M]^+$ = 445.2008, $[M]^+$ calcd = 445.2002.

(2-Aminoethyl)triphenylphosphonium bromide (8): 2-Bromoethylamine hydrobromide (2.05 g, 0.01 mol) and PPh_3 (2.62 g, 0.01 mol) was stirred in CH_3CN (15 mL) at 80 °C for 24 h in a N_2 atmosphere. A white precipitate was obtained, and it was filtered. The residue was dissolved in water, and K_2CO_3 was added until the pH of the solution reached 10-11. DCM was mixed, and the extracted organic layer was rinsed with brine (3×). The organic portion was dried with anhydrous Na_2SO_4, filtered, and evaporated using a rotary evaporator to achieve a white residue. The residue was rinsed with Et_2O (3×) to acquire a white solid pure product (2-aminoethyl)triphenylphosphonium bromide.

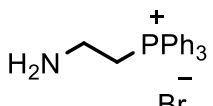

8

Yield: 3.67 g (95%).

^{1}H NMR (300 MHz, $CDCl_3$, 25 °C): δ = 7.83–7.64 (m, 15H), 3.84–3.75 (m, 2H), 3.15–3.07 (m, 2H), and 2.81 (br, 2H) ppm.

^{13}C NMR (75 MHz, $CDCl_3$, 25 °C): δ = 134.7, 133.8, 130.5, 119.0, 117.9, 41.7, and 23.9 ppm.

ESI-HRMS (+ve) *m/z*: Observed for $C_{20}H_{21}NP^+$ $[M]^+$ = 306.1407, $[M]^+$ calcd = 306.1406.

(*Z*)-(2-(2-((4-(1-cyano-2-(7-(diethylamino)-2-oxo-2*H*-chromen-3-yl)vinyl)phenyl)(ethyl)amino)acetamido) ethyl)triphenylphosphonium bromide (Cou-AIE-TPP$^+$): (*Z*)-*N*-(4-(1-cyano-2-(7-(diethylamino)-2-oxo-2*H*-chromen-3-yl)vinyl)phenyl)-*N*-ethylglycine (Compound 7, 0.16 g, 0.35 mmol), DIPEA (60 µL, 0.35 mmol), and HATU (0.13 g, 0.35 mmol) were dissolved in 5 mL of DMF under N_2 atmosphere and stirred for 30 m at 25 °C. The synthesized compound (2-aminoethyl)triphenylphosphonium bromide (Compound 8, 0.16 g, 0.42 mmol) was mixed to this solution and stirred for 24 h. The resultant solution was evaporated under reduced pressure. Cold Et_2O was mixed to obtain a red colored crude product, which was collected by filtration. This crude compound was purified via column chromatography utilizing CH_2Cl_2:CH_3OH (95:5, R_f = 0.65) to get the red colored solid pure product **Cou-AIE-TPP$^+$**.

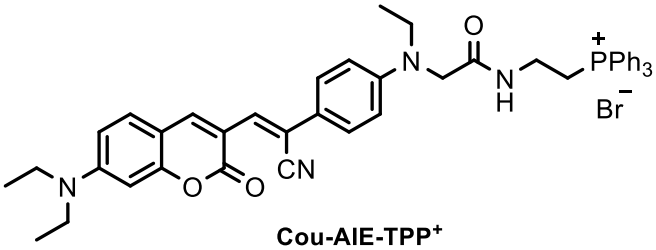

Cou-AIE-TPP$^+$

Yield: 0.19 g (67%).

^{1}H NMR (300 MHz, $CDCl_3$, 25 °C): δ = 8.62 (s, 1H), 7.91–7.64 (m, 16H), 7.55 (d, *J* = 8.9 Hz, 2H), 7.40 (d, *J* = 8.9 Hz, 1H), 6.66–6.60 (m, 3H), 6.50 (d, *J* = 2.4 Hz, 1H), 3.97 (2H, s), 3.86–3.75 (2H, m), 3.52–3.39 (6H, m), 3.17–3.12 (2H, m), and 1.29 (9H, t, *J* = 6.1 Hz) ppm.

^{13}C NMR (101 MHz, $CDCl_3$, 25 °C): δ = 169.9, 162.1, 156.3, 151.5, 148.5, 139.5, 134.6, 134.0, 133.9, 130.5, 130.4, 130.3, 130.0, 128.9, 128.8, 127.1, 122.5, 119.0, 118.2, 114.7, 112.2, 111.9, 109.6, 108.7, 97.2, 53.1, 46.4, 46.3, 45.0, 29.7, and 12.5 ppm.

DEPT-135 (101 MHz, $CDCl_3$, 25 °C): δ = 169.9 (disappear), 162.1 (disappear), 156.3 (disappear), 151.5 (disappear), 148.5 (disappear), 139.5 (positive), 134.6 (positive), 134.0 (positive), 133.9 (positive), 130.5 (positive), 130.4 (positive), 130.3 (positive), 130.0 (positive), 128.9 (positive), 128.8 (positive), 127.1 (positive), 122.5 (disappear),, 119.0 (disappear), 118.2 (disappear), 114.7 (disappear), 112.2 (positive), 111.9 (positive), 109.6 (positive), 108.7 (disappear), 97.2 (positive), 53.1 (negative), 46.4 (negative), 46.3 (negative), 45.0 (negative), 29.7 (negative), and 12.5 (negative) ppm.

^{31}P NMR (121 MHz, $CDCl_3$, 25 °C): δ = 23.9 (s) ppm.

2D NMR: ^{1}H–^{1}H COSY (Correlation Spectroscopy) NMR (300 MHz, $CDCl_3$, 25 °C) spectrum of Cou-AIE-TPP$^+$ probe confirmed the coupling connectivity.

HRMS (ESI +ve) *m/z*: Observed for $C_{46}H_{47}N_4O_3P^{2+}$ $[M+H]^{2+}$ = 367.1695, $[M+H]^{2+}$ calcd = 367.1687.

Photophysical properties of Cou-AIE-TPP$^+$ in PBS: λ_{abs}= 480 nm, λ_{em}= 604 nm, Stokes shift ($\Delta\lambda$) = 124 nm, ε = 1.68 ×10^4 M^{-1}cm^{-1}, Φ_f = 0.45 in PBS [Φ_f of Rhodamine-B (reference) in EtOH = 0.49]. Fluorescence lifetime (τ) = 2.168 ± 0.126 ns in PBS.

Synthesis of the Aβ40 peptide:

Manual MW Assisted Solid-Phase Peptide Synthesis (SPPS)

Aβ40 peptide was synthesized by a manual microwave (MW)-assisted Fmoc-SPPS procedure on a MW peptide synthesizer (*CEM, Discover Bio*) and stored at –20 °C prior to use. Wang resin (LL, 0.60 mmol/g loading density) was used to synthesize Aβ40 peptide from the C-termini to the N-termini. Fmoc-amino acid building blocks Fmoc-Gly-OH, Fmoc-Ser(tBu)-OH, Fmoc-Asn(Trt)-OH, Fmoc-Lys(Boc)-OH, Fmoc-Glu(OtBu)-OH, Fmoc-Ala-OH, Fmoc-Ile-OH, Fmoc-Leu-OH, Fmoc-Met-OH, Fmoc-Val-OH, Fmoc-Tyr(tBu)-OH, Fmoc-His(Trt)-OH, Fmoc-Gln(Trt)-OH, Fmoc-Asp(tBu)-OH, Fmoc-Arg(Pbf)-OH, and Fmoc-Phe-OH were used.

Handling of Wang Resin and Fmoc Amino Acid Building Blocks: Fmoc amino acid building blocks were stored at –20 ºC. Wang resin was stored at 4 ºC. Before opening, all the Fmoc amino acid building blocks and resins were warmed to room temperature for 20 min.

First Amino Acid Loading on Wang Resin: For the synthesis of Aβ40 peptide, the first amino acid Fmoc-Val-OH loading on Wang resin (LL, 0.60 mmol/g loading density) was achieved in a SPE cartridge with frit. The Wang resin (0.1 mmol) was swollen in DMF (2 mL) for 60 m. Next, drain the solvent off and wash with DMF (2×). Fmoc-Val-OH (5 eq), HBTU (4.9 eq.), and HOBt (5 eq.) were dissolved in 1:1 DCM/DMF (2 mL); subsequently, DIPEA (10 eq.) was mixed, and the solution was transferred in a SPE cartridge comprising the Wang resin and shaken for 3 h under N_2 bubbling. Drain the solvent, and the resin was successively rinsed with DMF (2×), DCM (2×), and MeOH (2×). Afterward Fmoc-Val-OH loading on Wang resin, the loading density was measured by UV/vis assay of the Fmoc-dibenzofulvene deprotection product.

Estimation of the Loading Density of First Amino Acid Fmoc-Val-OH on Wang resin: The Fmoc-Val-Wang resin (5 mg) and DBU in NMP (2 mL, 2 % in NMP) were taken in a volumetric flask (10 mL). It was shaken for 30 min in a shaker, and the volumetric flask (10 mL) was filled up to the mark with CH_3CN. The solution was diluted with CH_3CN (1/12.5) and taken in an UV cuvette. The cleaved dibenzofulvene was monitored at 304 nm (ε_{304} = 7624 L mol^{-1} cm^{-1}) and contrasted with reference. The first amino acid Fmoc-Val-OH loading on the Wang resin was determined based on Lambert-Beer's law.

ρ(mmol/g) = 163.96×(A – A_0)/m

ρ : loading density of the resin

A : absorption of a sample

A_0 : absorption of reference

m : mass of the analyzed resin in mg.

Microwave-assisted SPPS: Synthesis of Aβ40 peptide was achieved on a MW-assisted solid-phase peptide synthesizer at a 0.1 mmol scale by the Fmoc-SPPS protocol. After the final coupling, Fmoc-deprotection was executed to acquire an *N*-terminus free Aβ40 peptide, and it was stored at –20 °C prior to use.

Protocols for MW-Assisted SPPS:

1. Bubbling during the MW-assisted synthesis for all steps: on 3 sec; off 7 sec.

2. **Fmoc deprotection**: 20% piperidine/DMF; time 180 sec, power 20 W, temperature 75 ºC, delta temperature 5 ºC.

To circumvent aspartimide formation in the Fmoc deprotection step of Asp comprising sequence, 0.1 M HOBt monohydrate in the Fmoc deprotection solution (20% piperidine/0.1 M HOBt/DMF) was utilized to diminish aspartimide development.

Washing after Fmoc-deprotection: DMF (4×), DCM (4×), and DMF (4×) to remove dibenzofulvene by-product.

3. **Coupling**: 0.5 M HBTU/0.5 M HOBt/2 M DIPEA/DMF;

General protocol: time 300 sec, power 20 W, temperature: 75 ºC, delta temperature: 5 ºC.

Double coupling was performed.

Arg (R) is vulnerable to δ-lactam formation, which considerably reduces the coupling output. Special care was taken in the case of the Arg coupling to reduce the side reactions. A modified double coupling was executed for Arg. 1st coupling: 25 min at 25 °C (MW Power 0 W), next 2 min at 75 °C (MW Power 30 W); 2nd coupling: 5 min at 75 °C (MW Power 30 W).

Special care for His coupling: the MW temperature was reduced to 50 °C to suppress epimerization.

Washing after coupling: DMF (3×), DCM (3×), DMF (3×)

After the final step, the resin was taken in a SPE cartridge with frit and rinsed with DMF (5×), DCM (5×), MTBE (5×), and lastly with MeOH (5×). The resins were dried in a vacuum and stored at –20 °C.

Test Cleavage from Wang Resin: To a pinch of the resin, a mixture of TFA/TIPS/EDT/H_2O (92.5/2.5/2.5/2.5 *v*/*v*) solution (2 mL) was added, and the cleavage reaction was executed by shaking the resin for 2 h at 25 °C. Next, the resin beads were filtered off, and the solvent was vaporized using N_2 stream. The Aβ40 peptide was precipitated by using cold MTBE. The MTBE suspension was centrifuged at –5°C. The supernatant was rejected,

and the residue was washed with cold MTBE (3×) and dried to acquire the desired Aβ40 peptide, and it was stored at –20 °C prior to use.

MW Assisted Fmoc-SPPS Protocol for Aβ40 Peptide Synthesis

Working Step	Resin	Reagents	Reaction condition
Coupling	Wang	HBTU/HOBt/DIPEA/DMF	300 sec/75 °C/20 W Double coupling was performed **Special care for the Arg coupling:** **1) 25 min/25 °C/0 W, then** **2 min/75 °C/30 W** **2) 5 min/75 °C/30 W** **Special care for the His coupling:** **The MW temperature was reduced to 50 °C**
Washing after coupling	Wang	DMF(5×), DCM(5×), DMF(5×)	
Fmoc deprotection	Wang	20% piperidine/DMF **Special care for Asp Fmoc-deprotection step: 20% piperidine/DMF with 0.1 M HOBt monohydrate**	180 sec/75 ºC/20 W
Washing after deprotection	Wang	DMF (4×), DCM (4×), DMF (4×)	
Washing after the final coupling	Wang	DMF(5×), DCM(5×), MTBE(5×), MeOH(5×)	
Final Cleavage	Wang	TFA/TIPS/EDT/H_2O (92.5/2.5/2.5/2.5 *v*/*v*)	2 h/25 °C

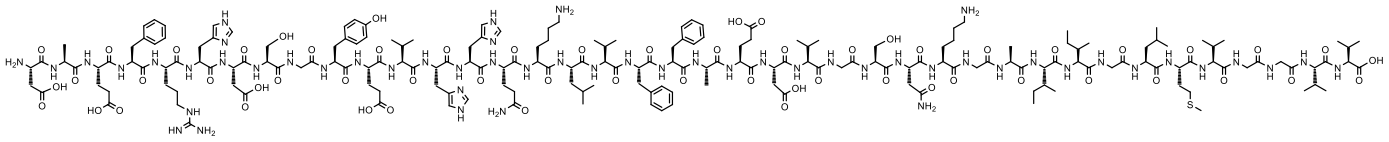

Aβ40 DAEFRHDSGYEVHHQKLVFFAEDVGSNKGAIIGLMVGGVV

The Aβ40 peptide is dissolved in ACN/H_2O and purified on a C8 column using reversed-phase HPLC. CH_3CN and H_2O gradient system containing 0.1% TFA were used to purify the peptide.

FTIR:

Aβ40 monomer: 3281 cm^{-1} (amide A region, N–H stretching), a sharp peak at 1650 cm^{-1} (amide I region, amide CO stretching), 1536 cm^{-1} (amide II region, NH bending).

Aβ40 fibril: 3290 cm^{-1} (amide A region, N–H stretching), a sharp peak at 1624 cm^{-1} (amide I region, amide CO stretching), and 1513 cm^{-1} (amide II region, NH bending).

MALDI *m/z*: Observed for $C_{194}H_{295}N_{53}O_{58}S^+$ $[M]^+$ = 4329.1560, $[M]^+$ calcd = 4329.1551

CD: The CD spectrum of Aβ40 monomer (10 μM) in deionized H2O with 1% TFE characteristically exhibits a curve with a negative peak at 198 nm that corresponds to a random coil that is transformed to a shorter wavelength positive band at 195 nm and the longer wavelength negative maxima at 217 nm after 7 days of incubation, which is characteristic for β-sheet secondary structure.

X-Ray fiber Diffraction: 4.5 Å (meridional reflection) and 10.6 Å (equatorial reflection).

References

(S1) M. J. Frisch, G. W. Trucks, H. B. Schlegel, G. E. Scuseria, M. A. Robb, J. R. Cheeseman, G. Scalmani, V. Barone, B. Mennucci, G. A. Petersson, et al. Gaussian 09W Revision D.01, Gaussian, Inc., Wallingford CT, USA, 2009.

(S2) G. M. Morris, D. S. Goodsell, M. E. Pique, W. L. Lindstrom, R. Huey, S. Forli, W. E. Hart, S. Halliday, R. Belew, A. J. Olson, User Guide, AutoDock Version 4.2, Scripps Research, 2012.

Cartesian coordinates and total energies (Hartrees) of B3LYP/6-31+G* energy minimized structure of Cou-AIE-TPP^{+}

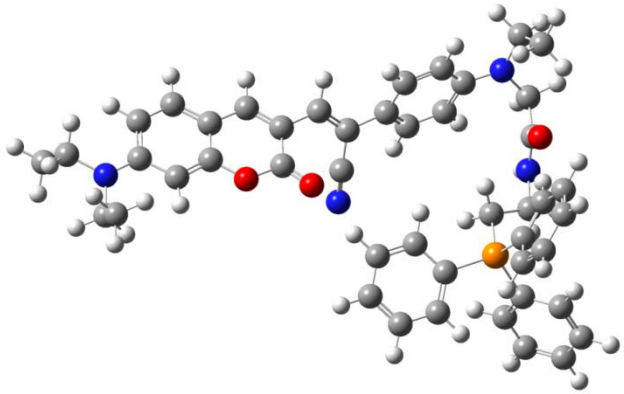

Charge = 1 Multiplicity = 1

C	-6.5614	-4.8343	0.
C	-6.6116	-6.1736	-0.0001
C	-5.2432	-6.8535	-0.0001
C	-4.0689	-6.1875	0.
C	-4.0192	-4.7574	0.0001
C	-5.1989	-4.095	0.0001
N	-8.0025	-6.9213	0.
C	-9.2735	-6.1251	-0.0002
C	-8.2119	-8.4109	0.0002
C	-6.9944	-9.3502	0.001
C	-10.5753	-7.0365	0.0009
O	-2.8997	-6.8732	-0.0001
C	-1.6441	-6.2762	-0.0001
C	-1.4289	-4.7728	0.0002
C	-2.5908	-4.0437	0.0003
O	-0.7009	-7.0451	-0.0004
C	0.1194	-4.0448	0.

C	1.3949	-4.6296	-0.001
C	2.8106	-3.8091	-0.0015
C	4.0157	-4.437	-0.0081
C	5.3674	-3.6498	-0.0056
C	5.361	-2.3056	0.0092
C	4.0277	-1.7001	0.0181
C	2.8603	-2.3649	0.0087
N	6.6669	-1.4597	0.0351
C	7.9773	-2.2217	-0.005
C	6.765	0.1212	0.1802
C	5.5546	1.1851	-0.0037
N	5.8978	2.5457	-0.1437
C	5.0461	3.7995	-0.675
C	4.1617	4.9516	0.3502
O	4.4069	0.7935	-0.1915
C	9.2715	-1.322	0.0041
C	1.527	-6.0436	-0.0005
N	1.6382	-7.1914	-0.0001
P	2.6791	5.6398	-0.5092
C	3.781	7.2454	-0.0576
C	3.3859	8.5503	-0.099
C	4.0236	9.7573	0.0543
C	5.3085	9.6901	0.1441
C	5.9159	8.3491	0.1027
C	5.2046	7.2068	0.0329
C	0.9683	6.5505	-0.227
C	-0.3034	6.1764	-0.4911
C	-1.4561	6.9178	-0.2059

C	-1.3429	8.1699	0.1311
C	-0.1016	8.6556	0.2017
C	0.8941	7.8352	0.0738
C	1.9672	4.0138	0.1419
C	2.5473	2.8414	0.2763
C	1.7949	1.6025	0.3091
C	0.4927	1.6254	0.1446
C	-0.0796	2.8259	0.1816
C	0.6804	3.8695	0.2297
H	7.04659	0.25179	1.20419
H	7.44463	0.39272	-0.60036
H	-7.47048	-4.26996	0.00001
H	-5.2139	-7.9231	-0.00018
H	-5.19115	-3.02503	0.00017
H	-9.28689	-5.58958	0.92605
H	-9.28748	-5.59098	-0.92725
H	-8.7078	-8.61263	0.92664
H	-8.70687	-8.61301	-0.92665
H	-6.09579	-8.76934	0.00133
H	-7.02055	-9.96725	0.87476
H	-7.01968	-9.96761	-0.87254
H	-10.28891	-8.06746	0.00159
H	-11.15649	-6.82719	0.87458
H	-11.15704	-6.82851	-0.87272
H	-2.53891	-2.97496	0.00052
H	0.11425	-2.97481	0.00076
H	4.04085	-5.50668	-0.01525
H	6.29631	-4.18077	-0.01566

H	3.97883	-0.63133	0.03348
H	1.94463	-1.81132	0.00877
H	8.01122	-2.78333	0.90512
H	7.98629	-2.72873	-0.9472
H	6.08722	2.80985	0.802
H	5.7822	4.41133	-1.15325
H	4.27175	3.34225	-1.25483
H	3.79181	4.38966	1.18225
H	4.82326	5.77657	0.51346
H	8.98866	-0.29063	0.03831
H	9.86395	-1.55805	0.86328
H	9.84044	-1.50657	-0.88311
H	2.33977	8.65852	-0.29598
H	3.49305	10.68556	0.09616
H	5.90755	10.571	0.24439
H	6.98318	8.2778	0.12959
H	5.71077	6.26418	0.04542
H	-0.44189	5.2255	-0.96175
H	-2.42119	6.45945	-0.2644
H	-2.19872	8.77712	0.34026
H	0.0681	9.70005	0.36051
H	1.84731	8.28958	0.24649
H	3.61285	2.80024	0.36463
H	2.29953	0.67226	0.46692
H	-0.07479	0.73157	-0.01007
H	-1.14498	2.92478	0.17174
H	0.14887	4.78779	0.36796

Total Energy = –2536.433839

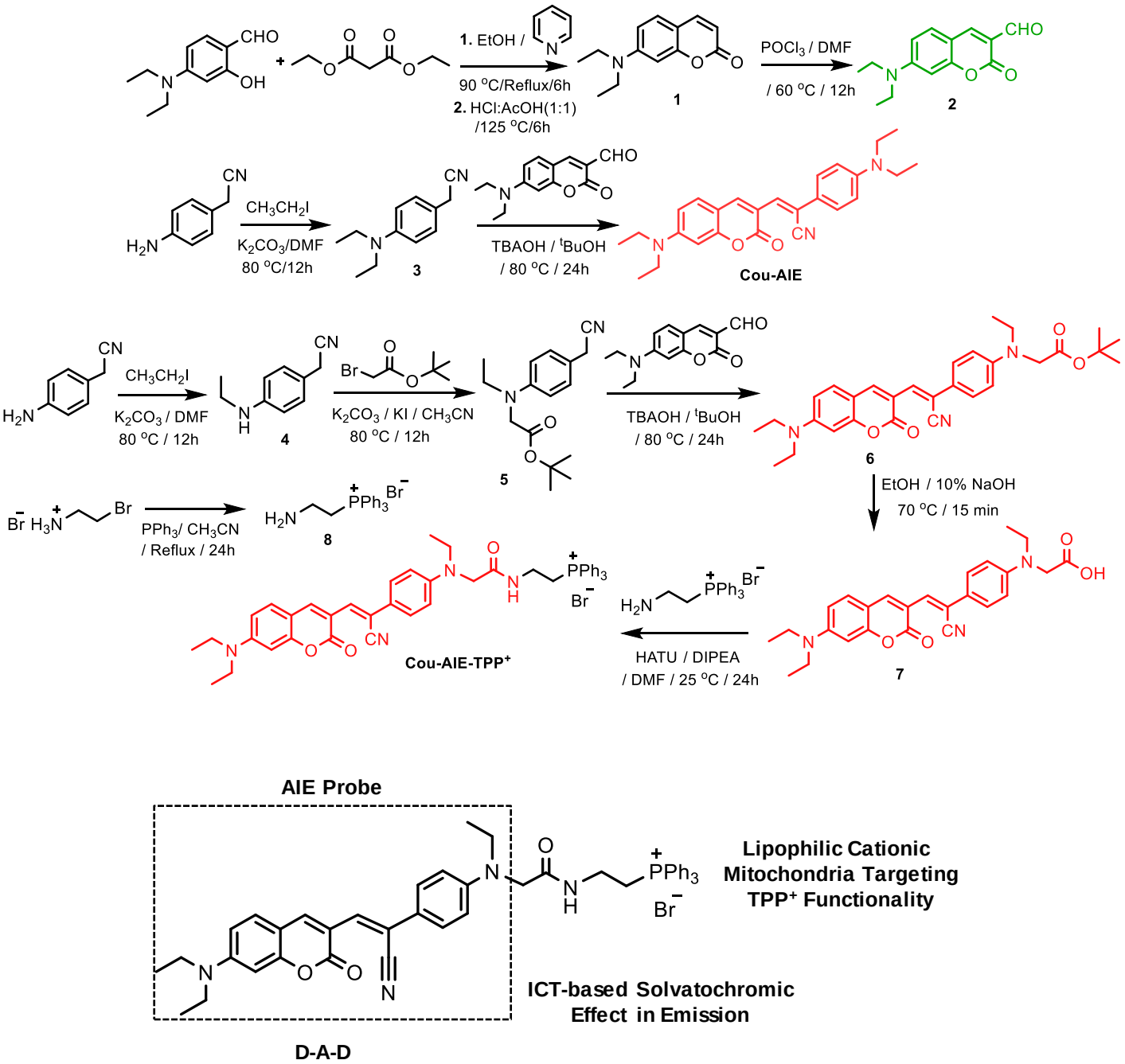

Fig. S1 Synthetic schemes of Cou-AIE-TPP$^+$ and a control compound. Cou-AIE, lacking the lipophilic cationic TPP$^+$ functionality

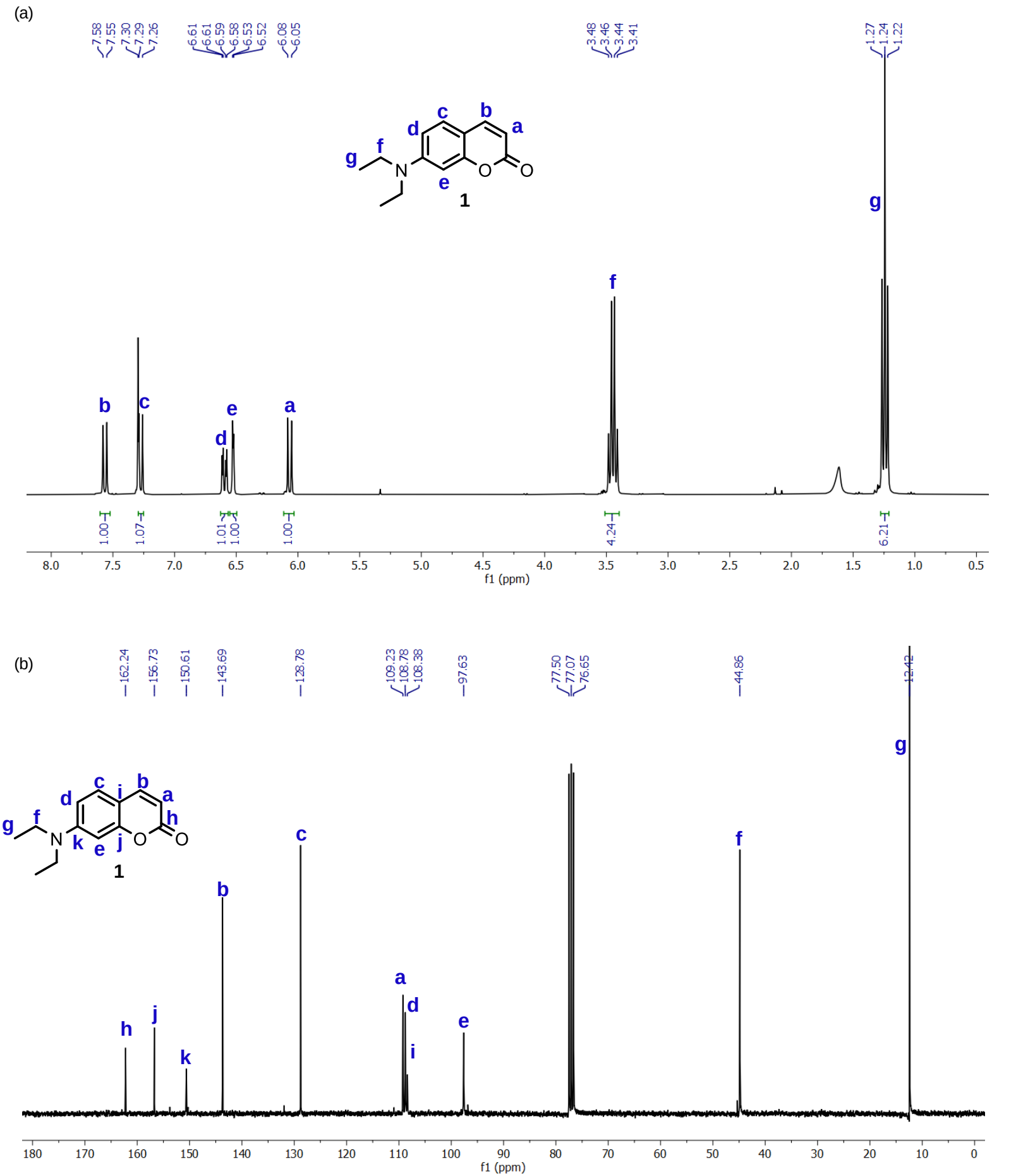

Fig. S2 (a) ^{1}H NMR (300 MHz, $CDCl_3$, 25 °C) spectrum and (b) ^{13}C NMR (75 MHz, $CDCl_3$, 25 °C) spectrum of **1**.

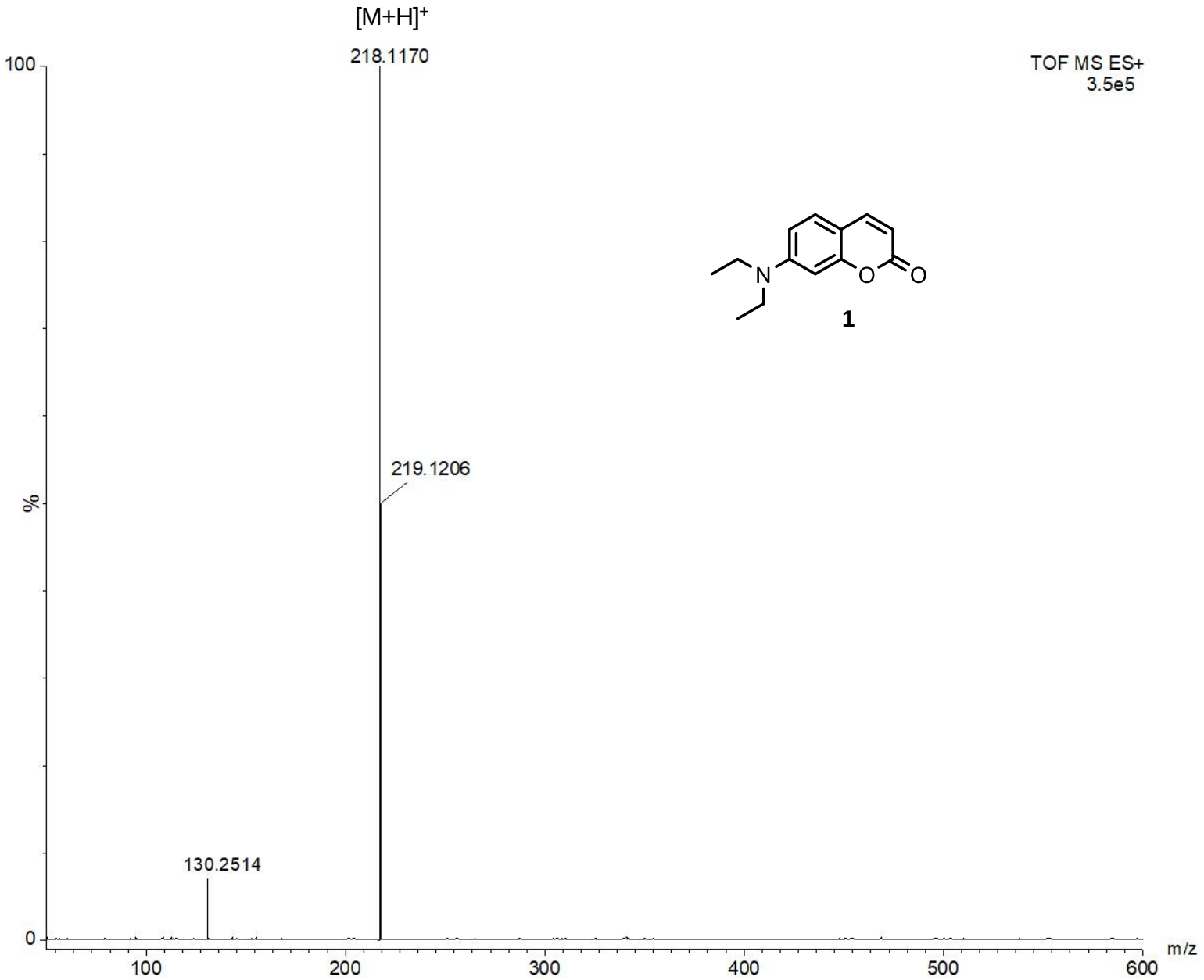

Fig. S3 HRMS (ESI +ve) spectrum of compound **1**.

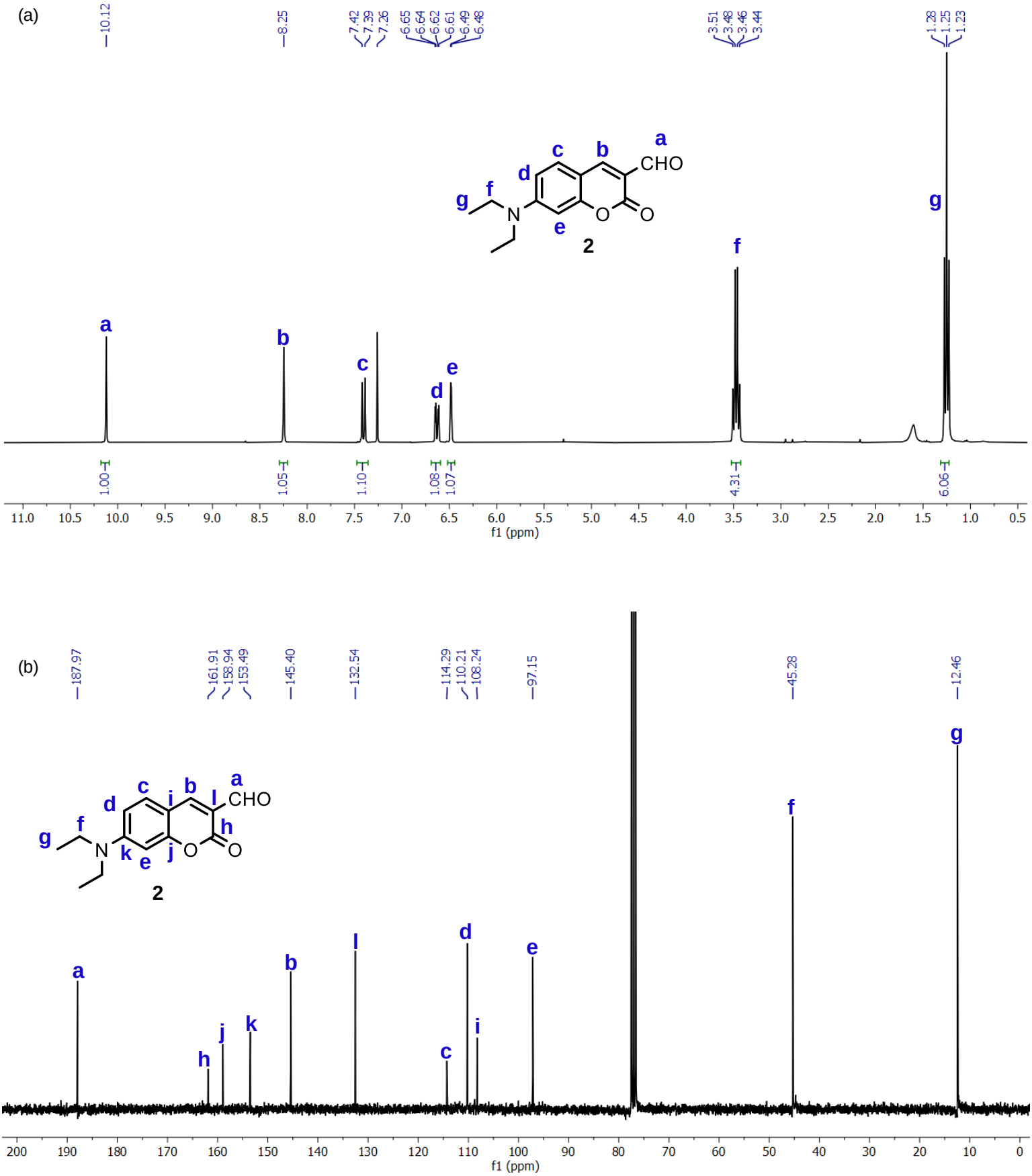

Fig. S4 (a) ^{1}H NMR (300 MHz, $CDCl_3$, 25 °C) spectrum and (b) ^{13}C NMR (75 MHz, $CDCl_3$, 25 °C) spectrum of **2**.

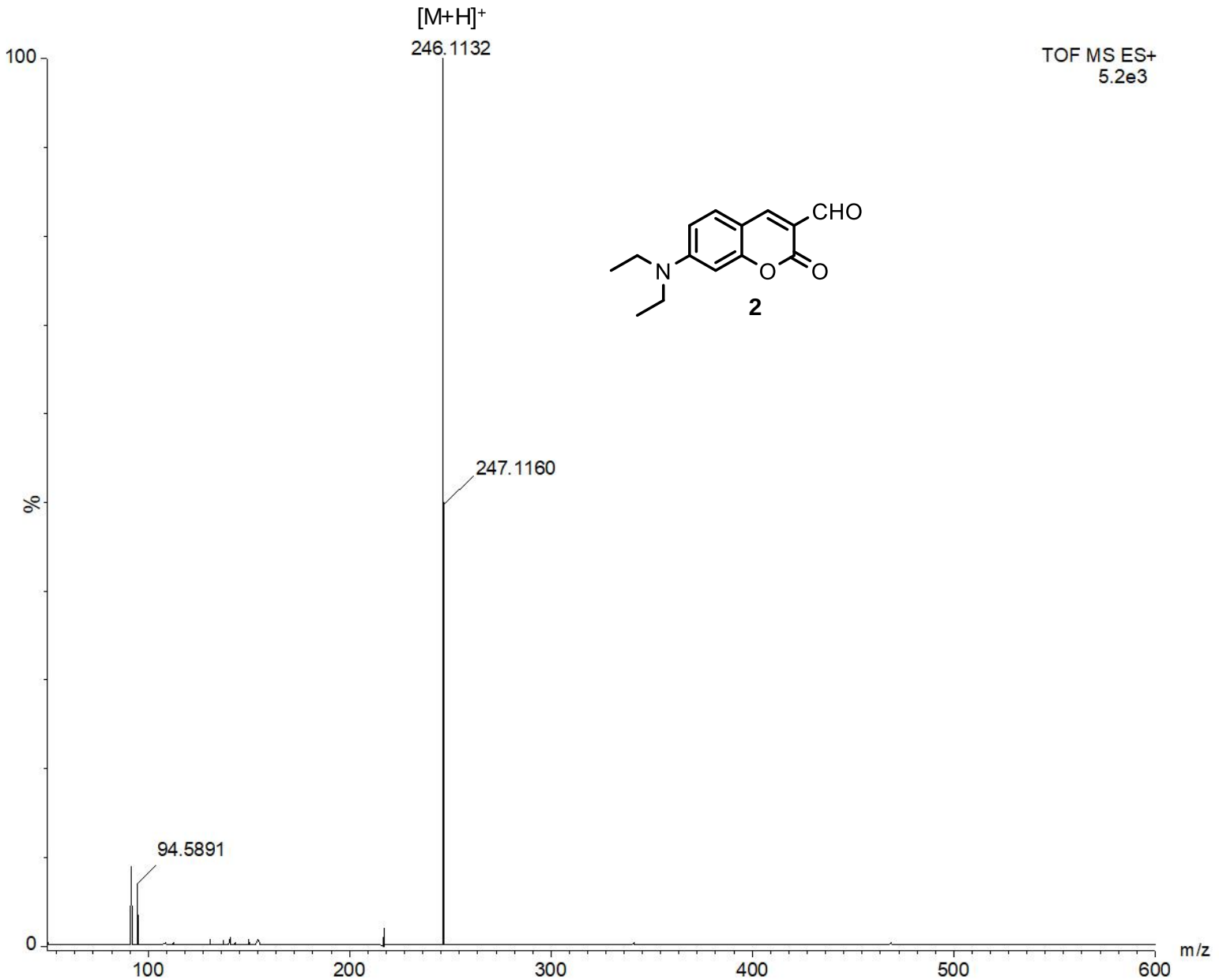

Fig. S5 HRMS (ESI +ve) spectrum of compound **2**.

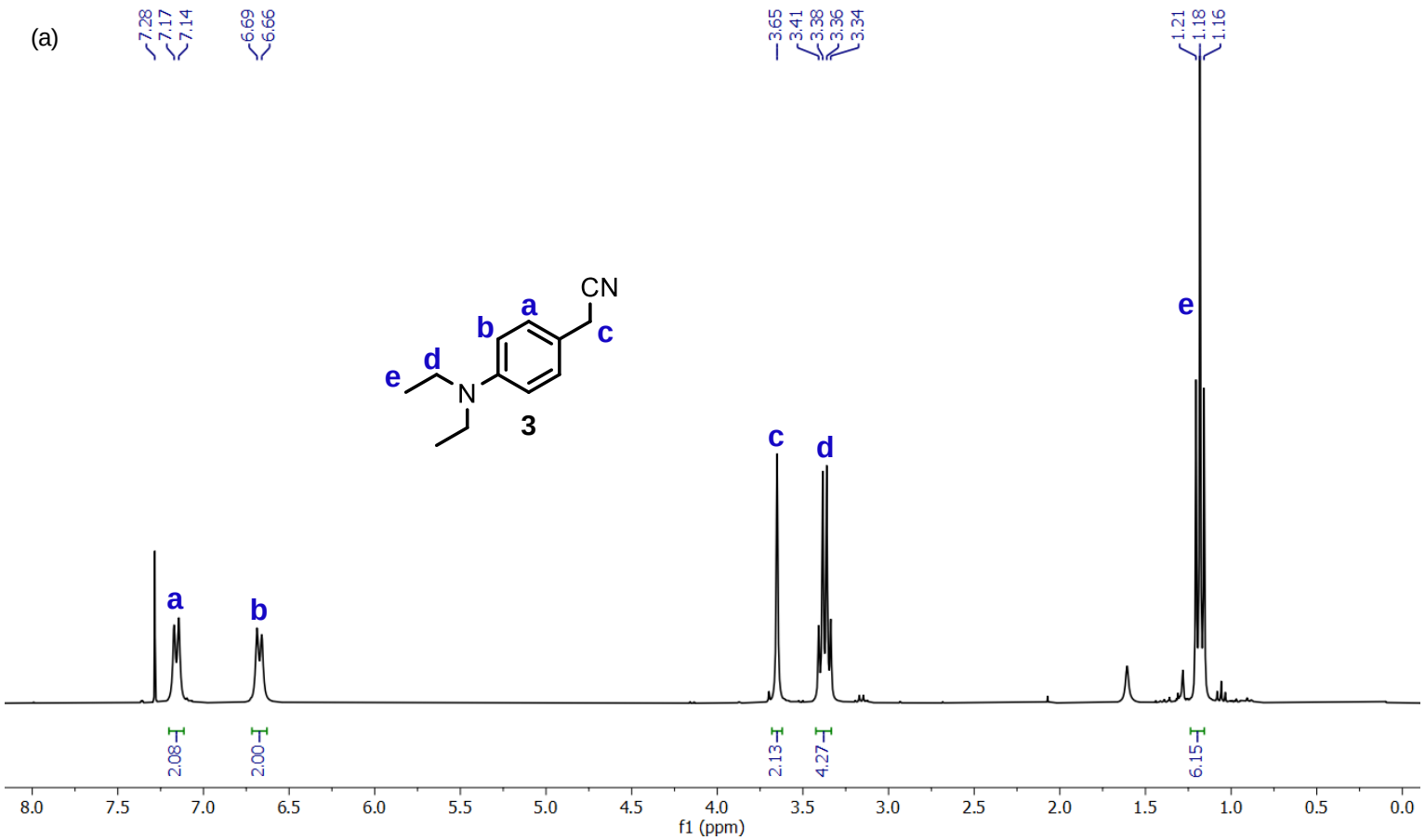

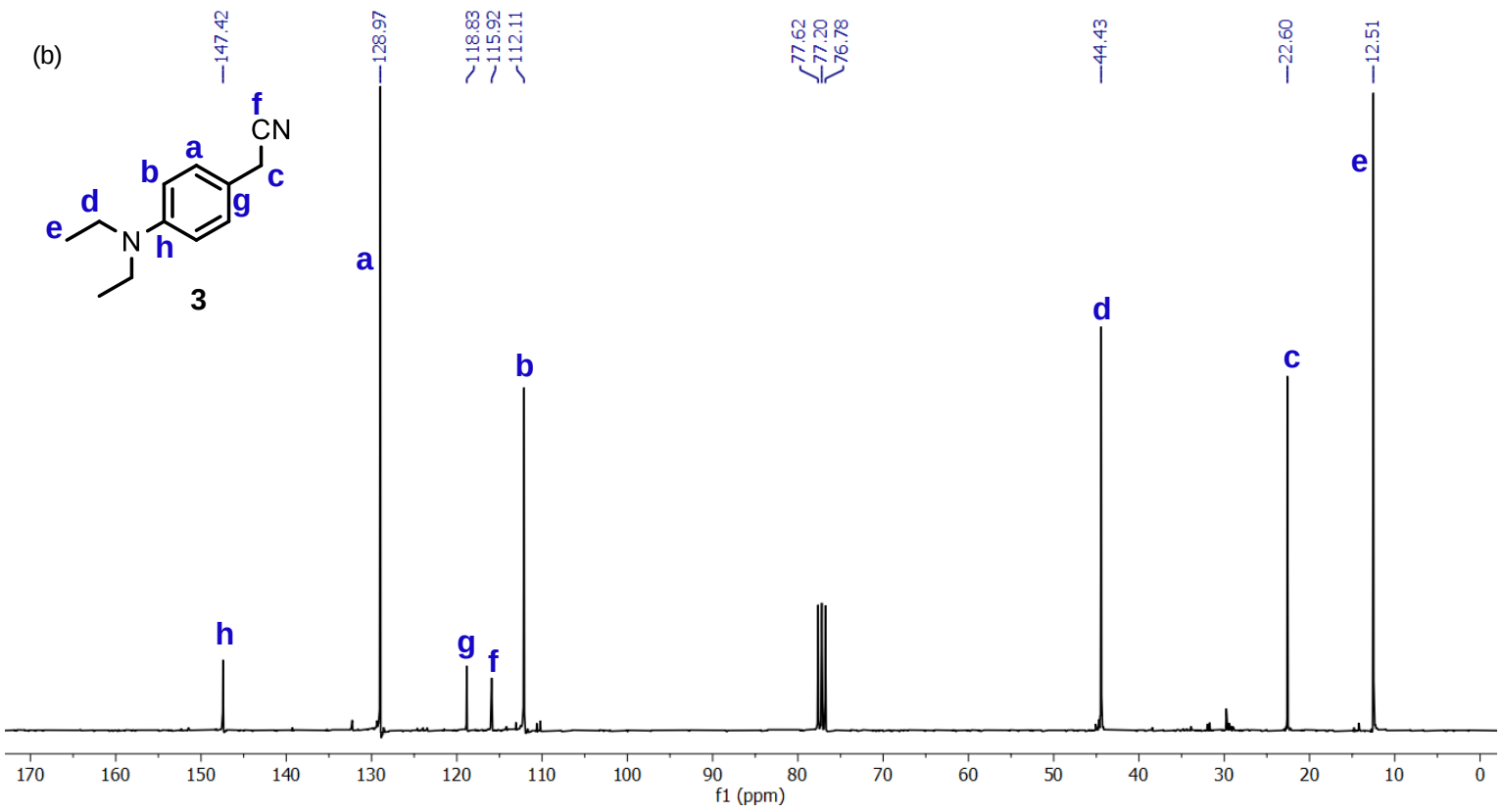

Fig. S6 (a) ^{1}H NMR (300 MHz, $CDCl_3$, 25 °C) spectrum and (b) ^{13}C NMR (75 MHz, $CDCl_3$, 25 °C) spectrum of **3**.

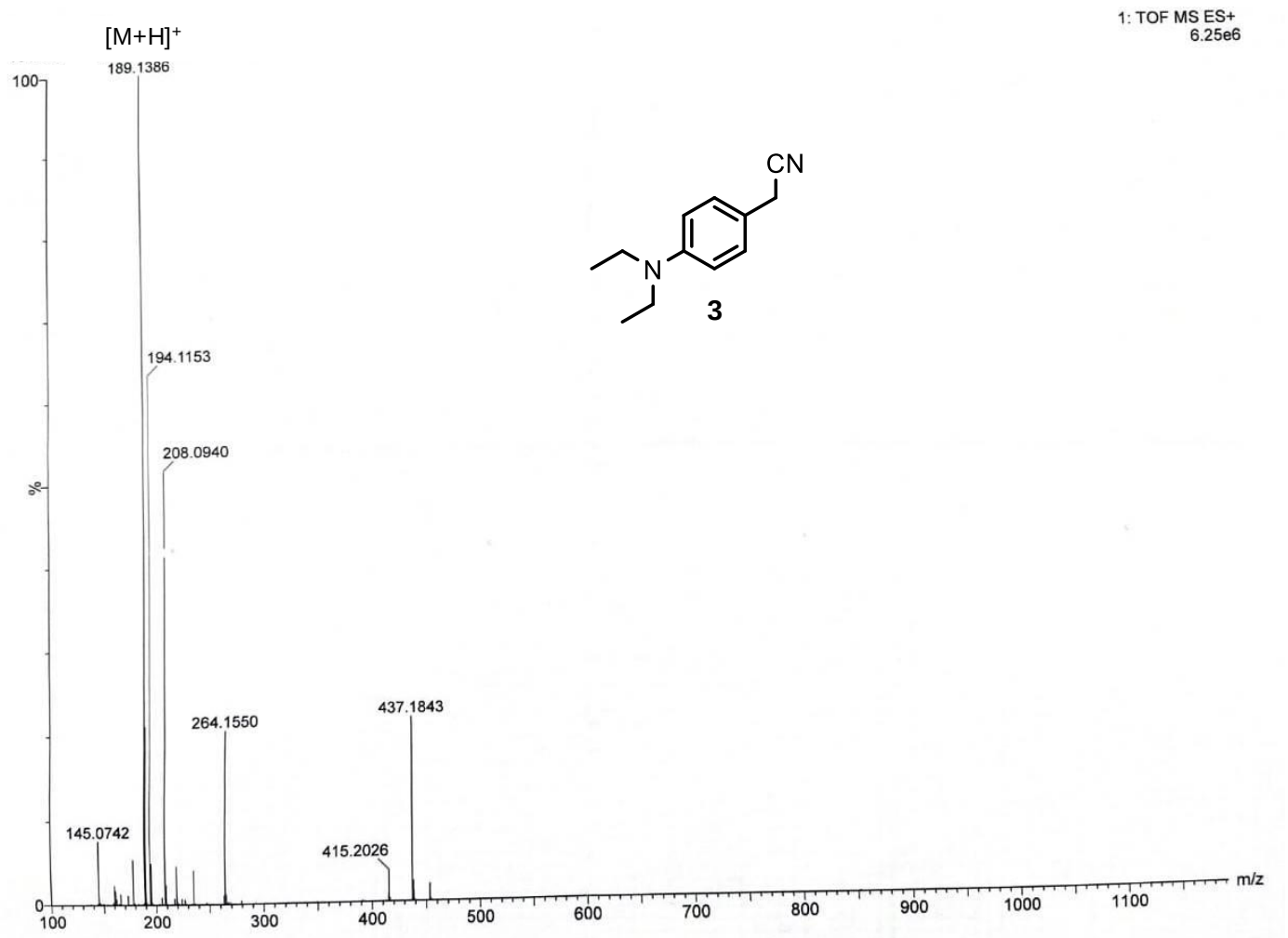

Fig. S7 HRMS (ESI +ve) spectrum of compound **3**.

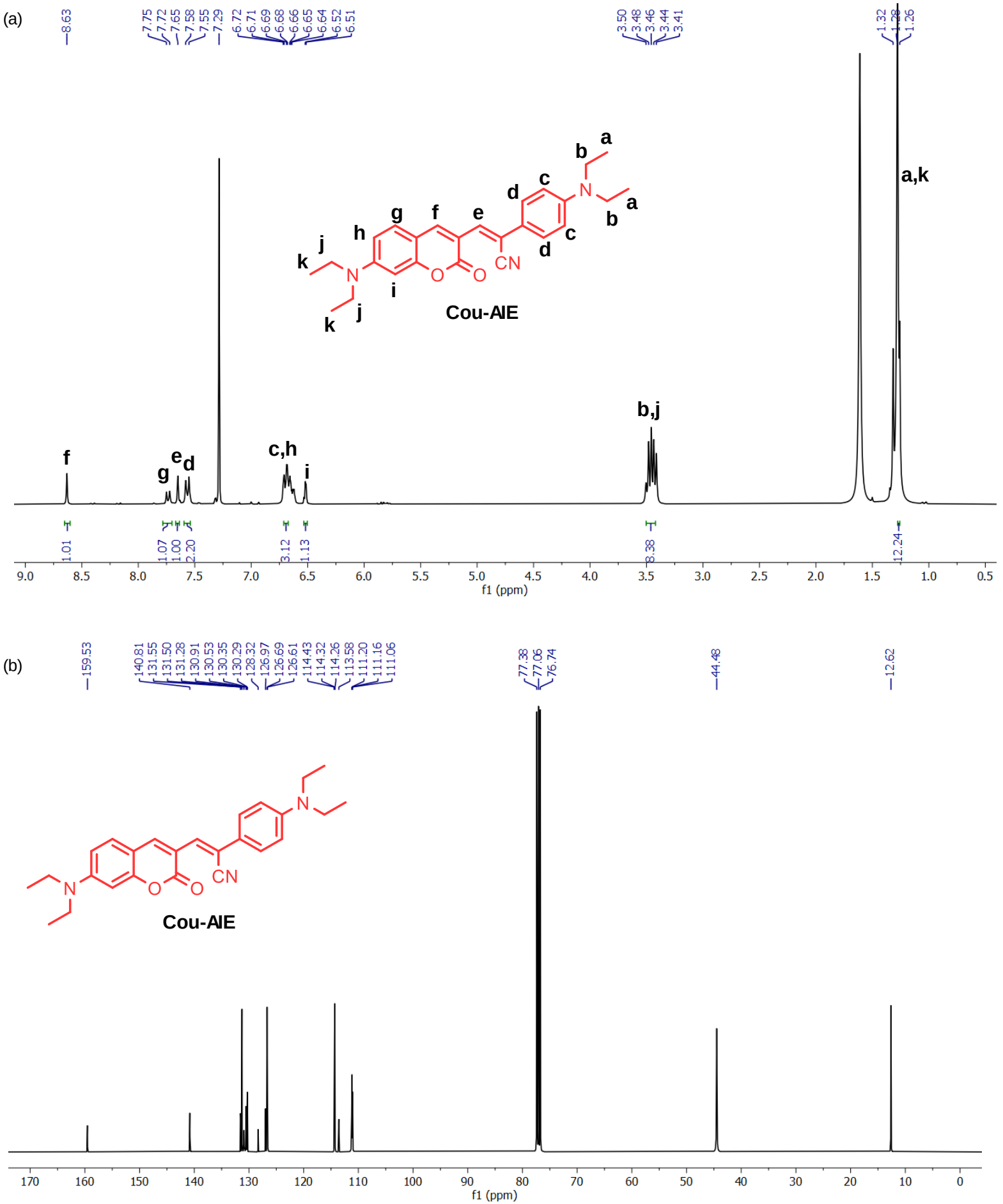

Fig. S8 (a) ^{1}H NMR (300 MHz, $CDCl_3$, 25 °C) spectrum and (b) ^{13}C NMR (75 MHz, $CDCl_3$, 25 °C) spectrum of **Cou-AIE**.

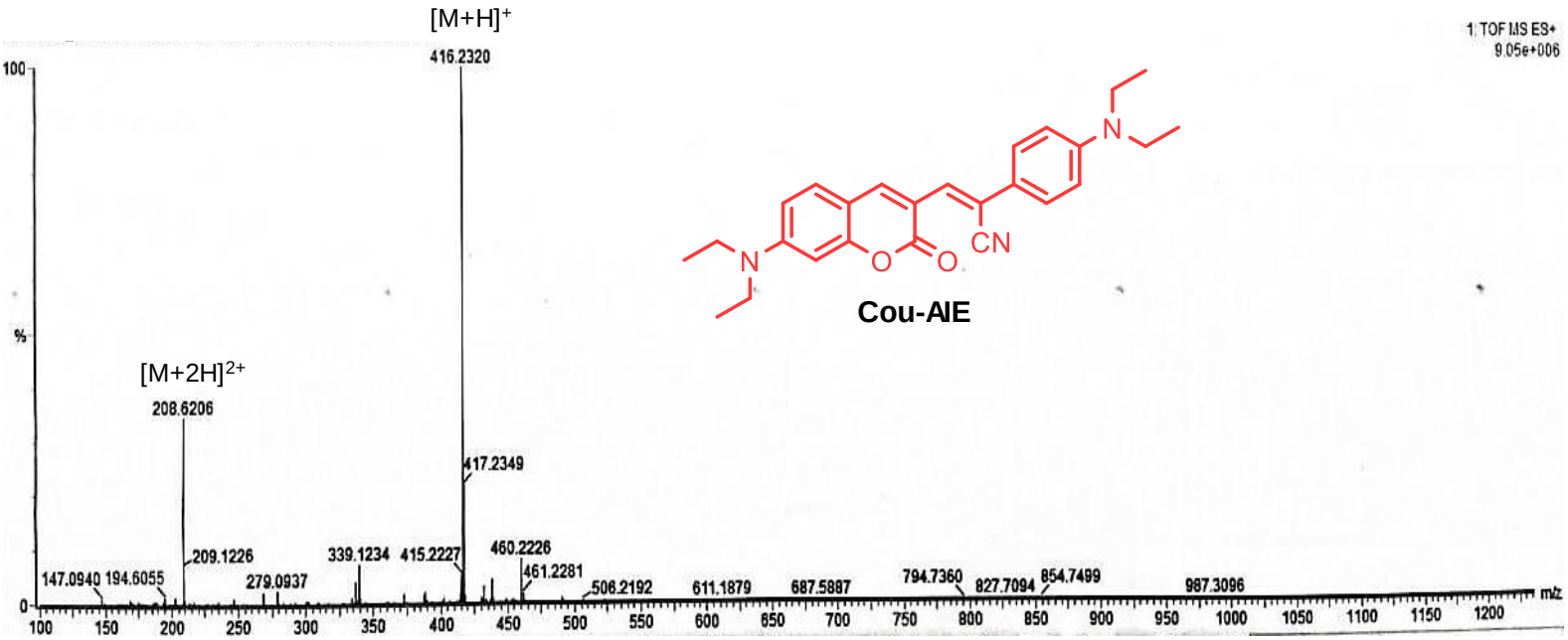

Fig. S9 HRMS (ESI +ve) spectrum of Compound **Cou-AIE**.

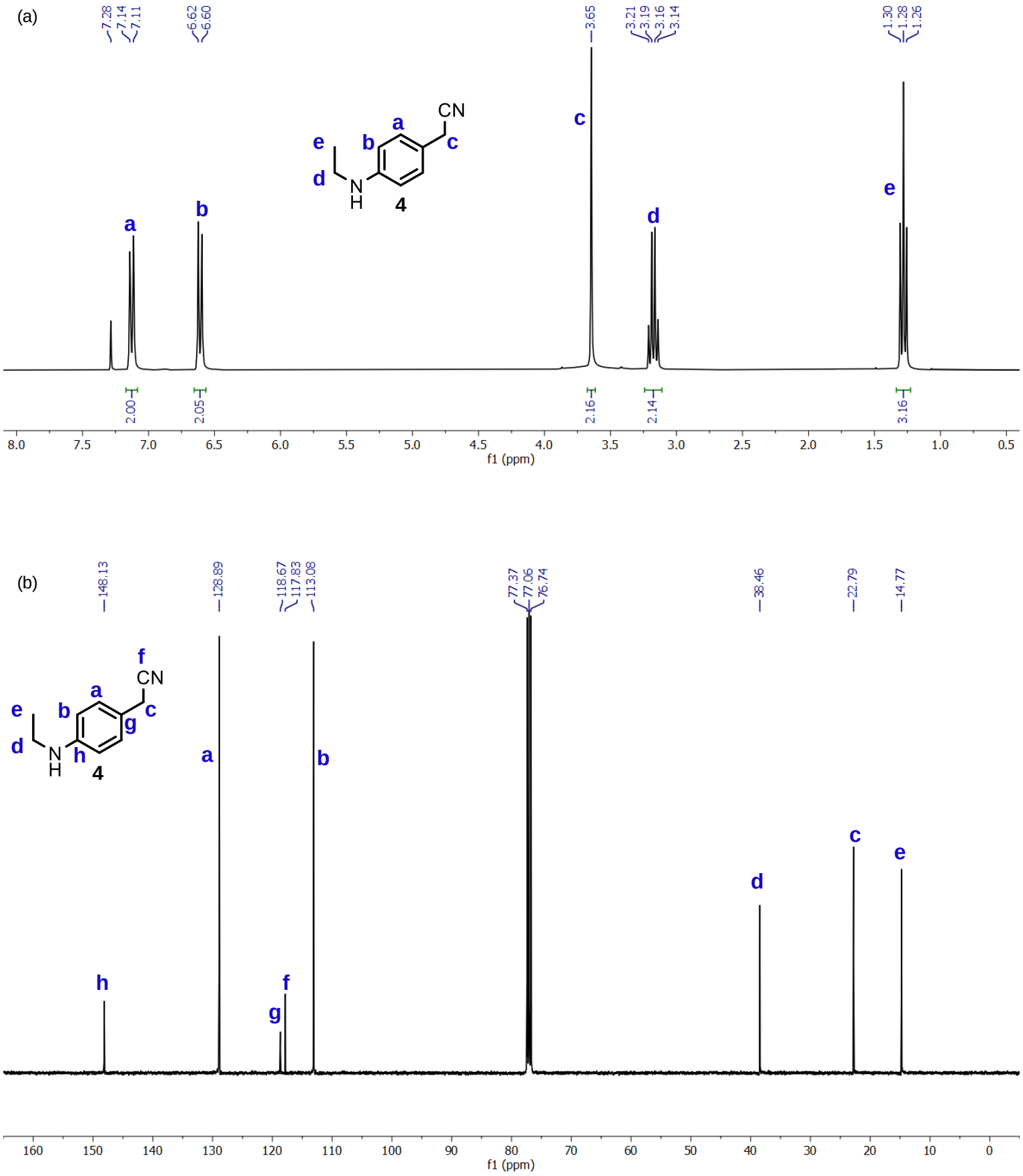

Fig. S10 (a) ^{1}H NMR (300 MHz, $CDCl_3$, 25 °C) spectrum and (b) ^{13}C NMR (75 MHz, $CDCl_3$, 25 °C) spectrum of **4**.

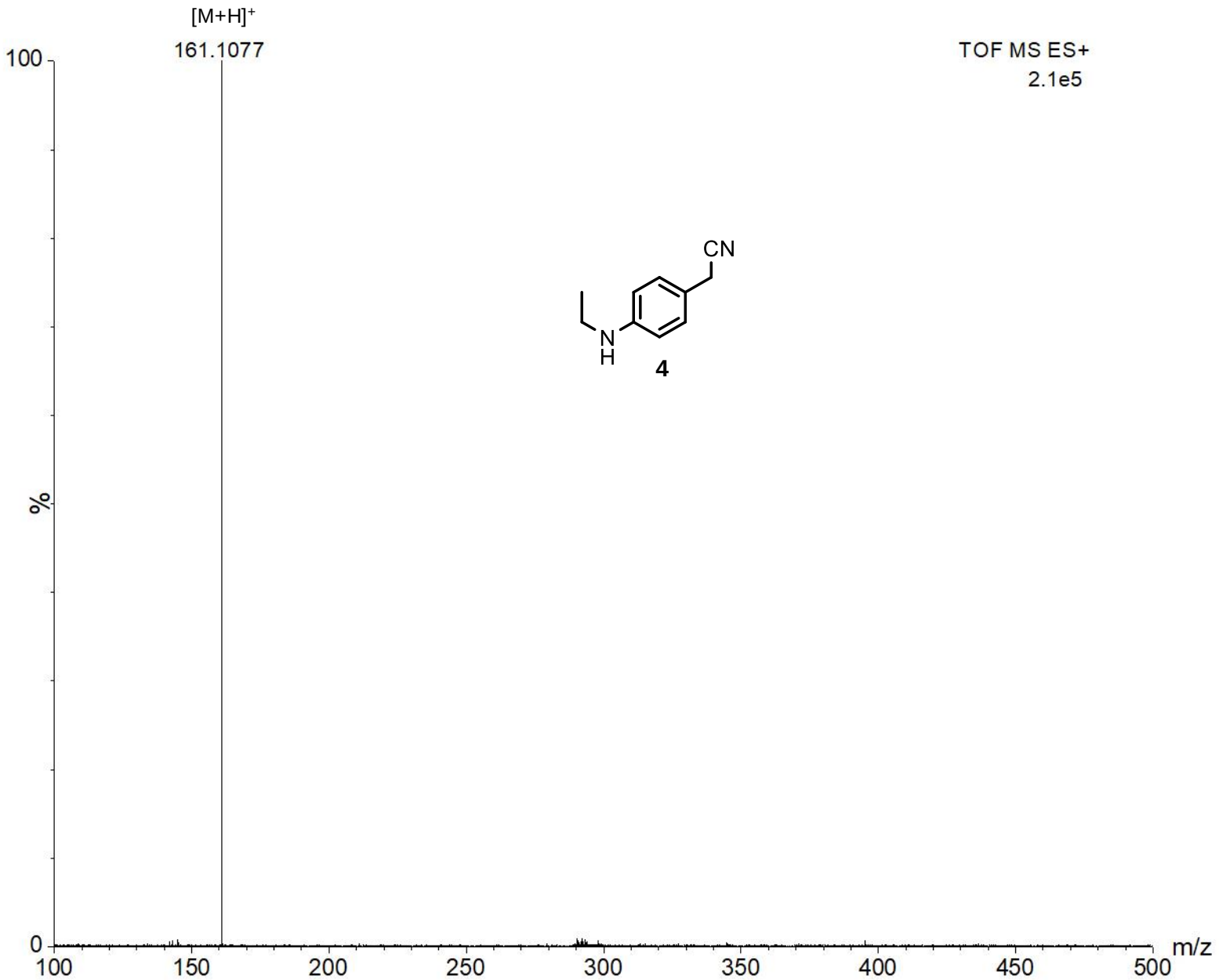

Fig. S11 HRMS (ESI +ve) spectrum of compound **4**.

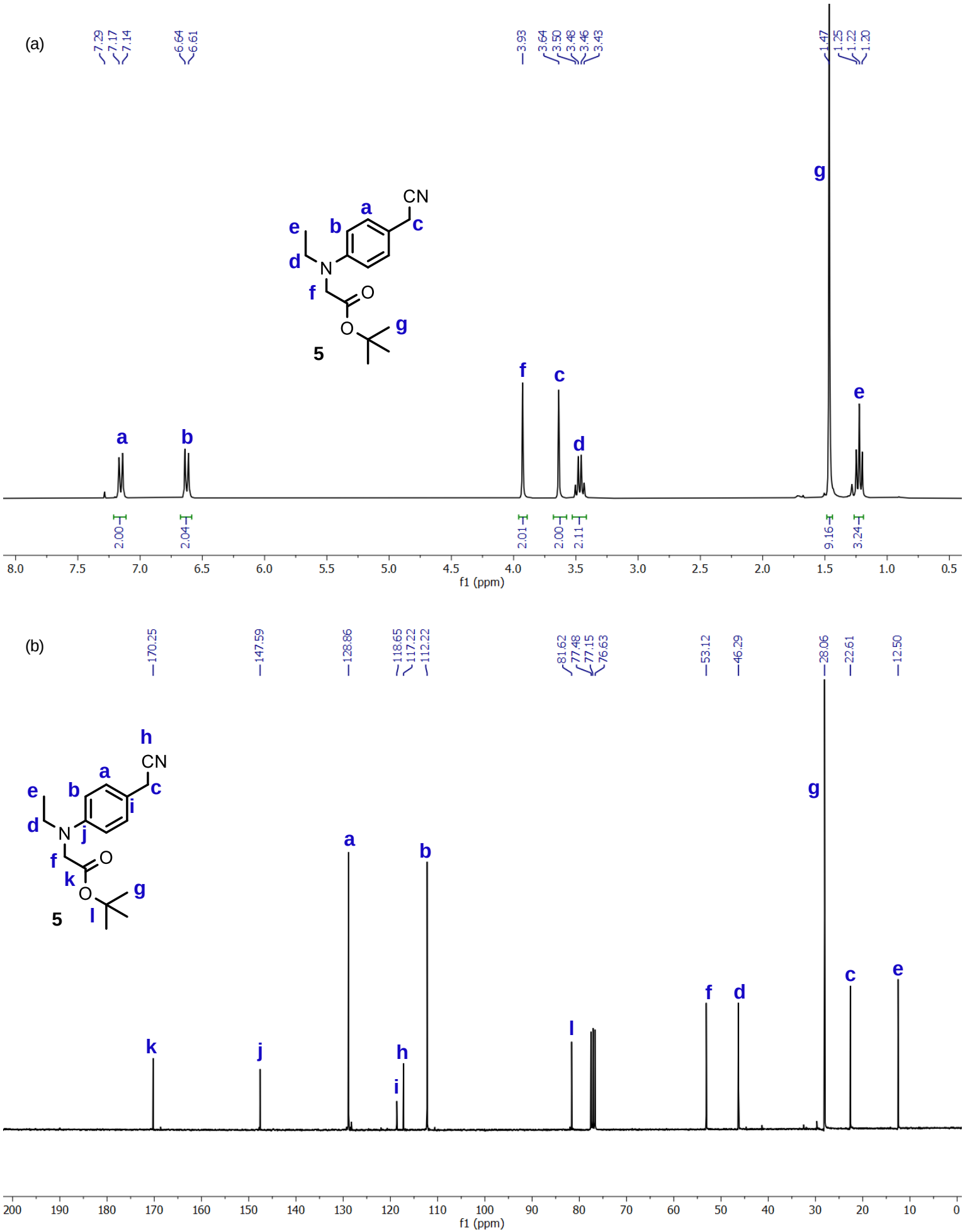

Fig. S12 (a) ^{1}H NMR (300 MHz, $CDCl_3$, 25 °C) spectrum and (b) ^{13}C NMR (75 MHz, $CDCl_3$, 25 °C) spectrum of **5**.

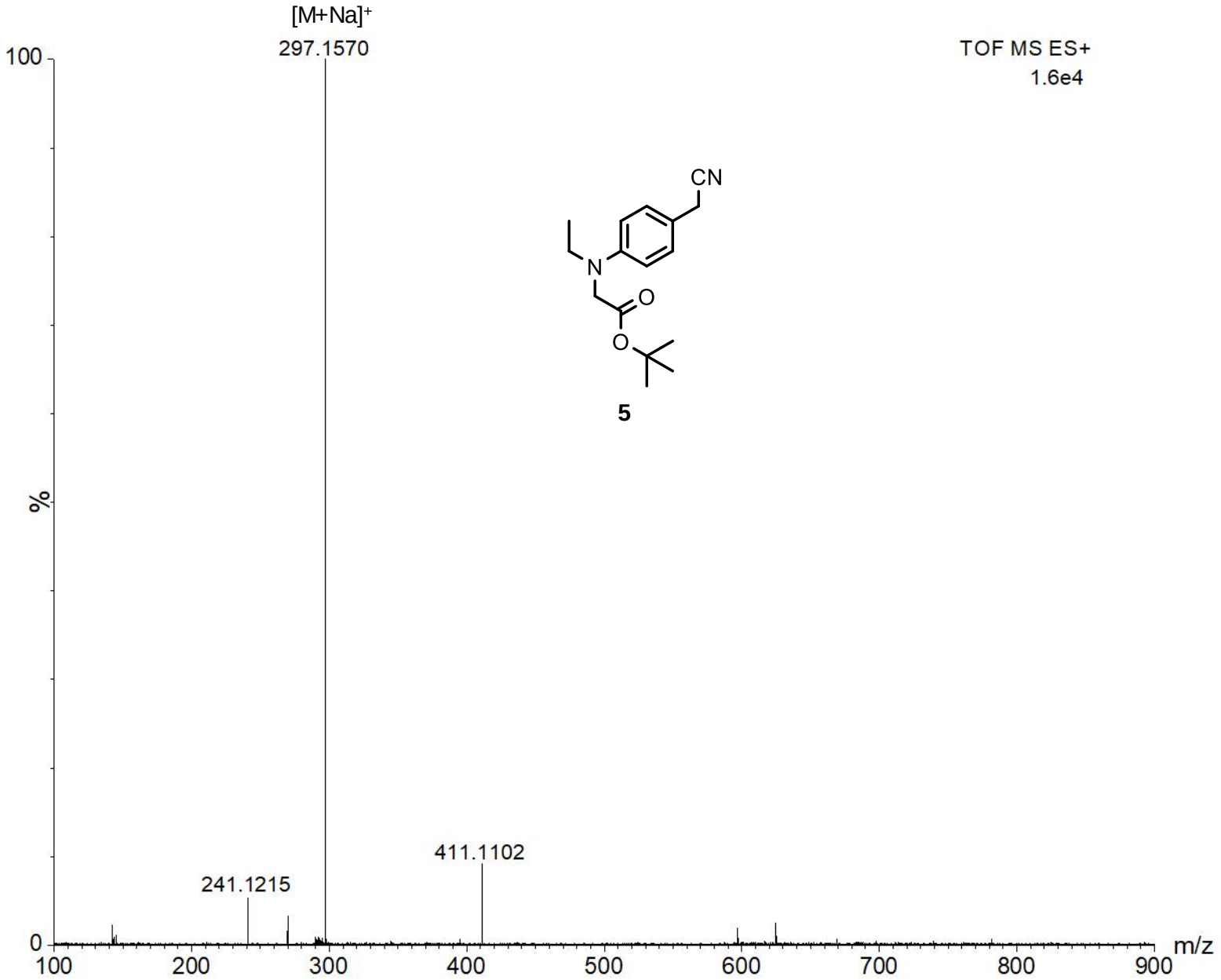

Fig. S13 HRMS (ESI +ve) spectrum of compound **5**.

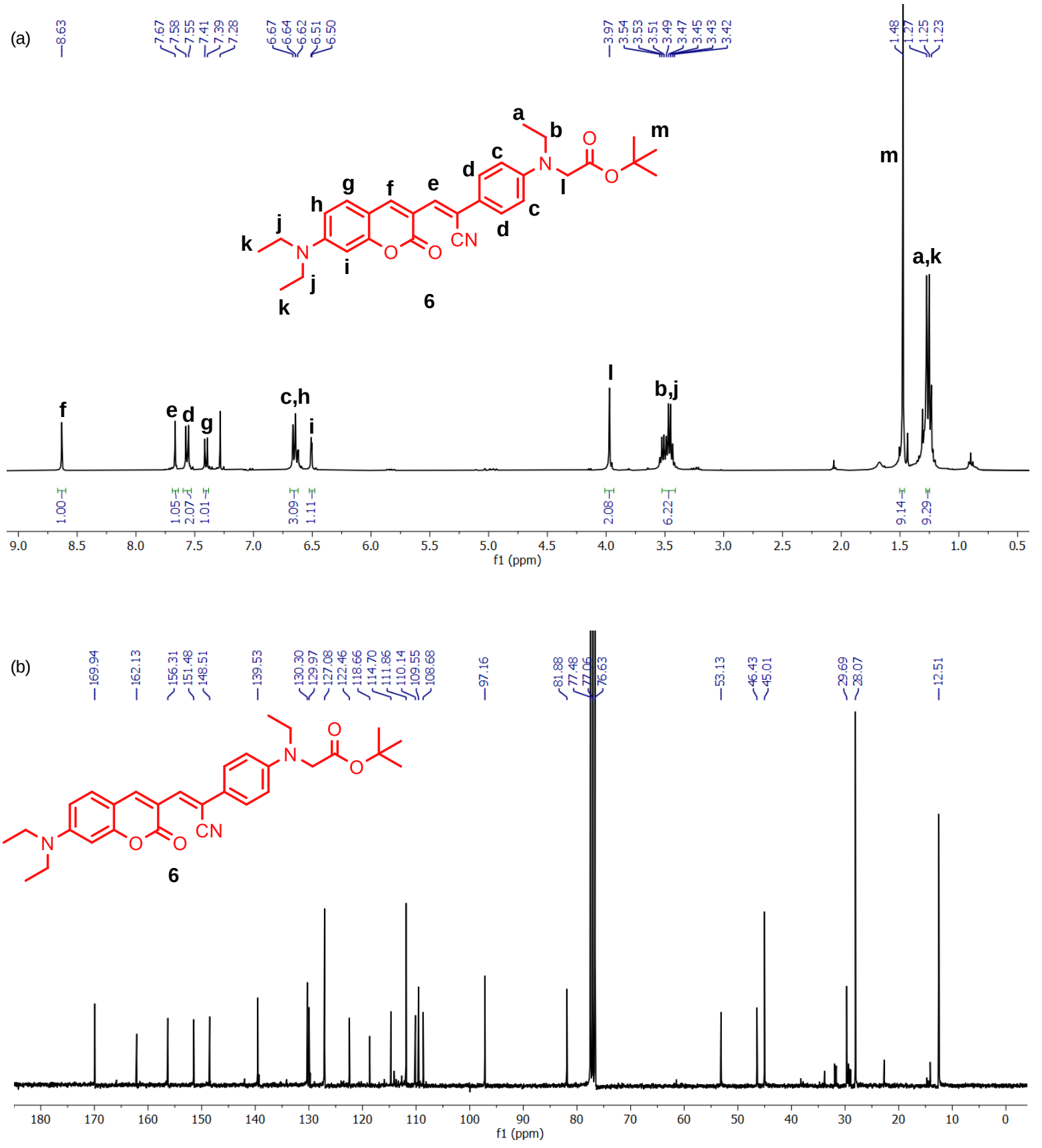

Fig. S14 (a) ^{1}H NMR (400 MHz, $CDCl_3$, 25 °C) spectrum and (b) ^{13}C NMR (101 MHz, $CDCl_3$, 25 °C) spectrum of **6**.

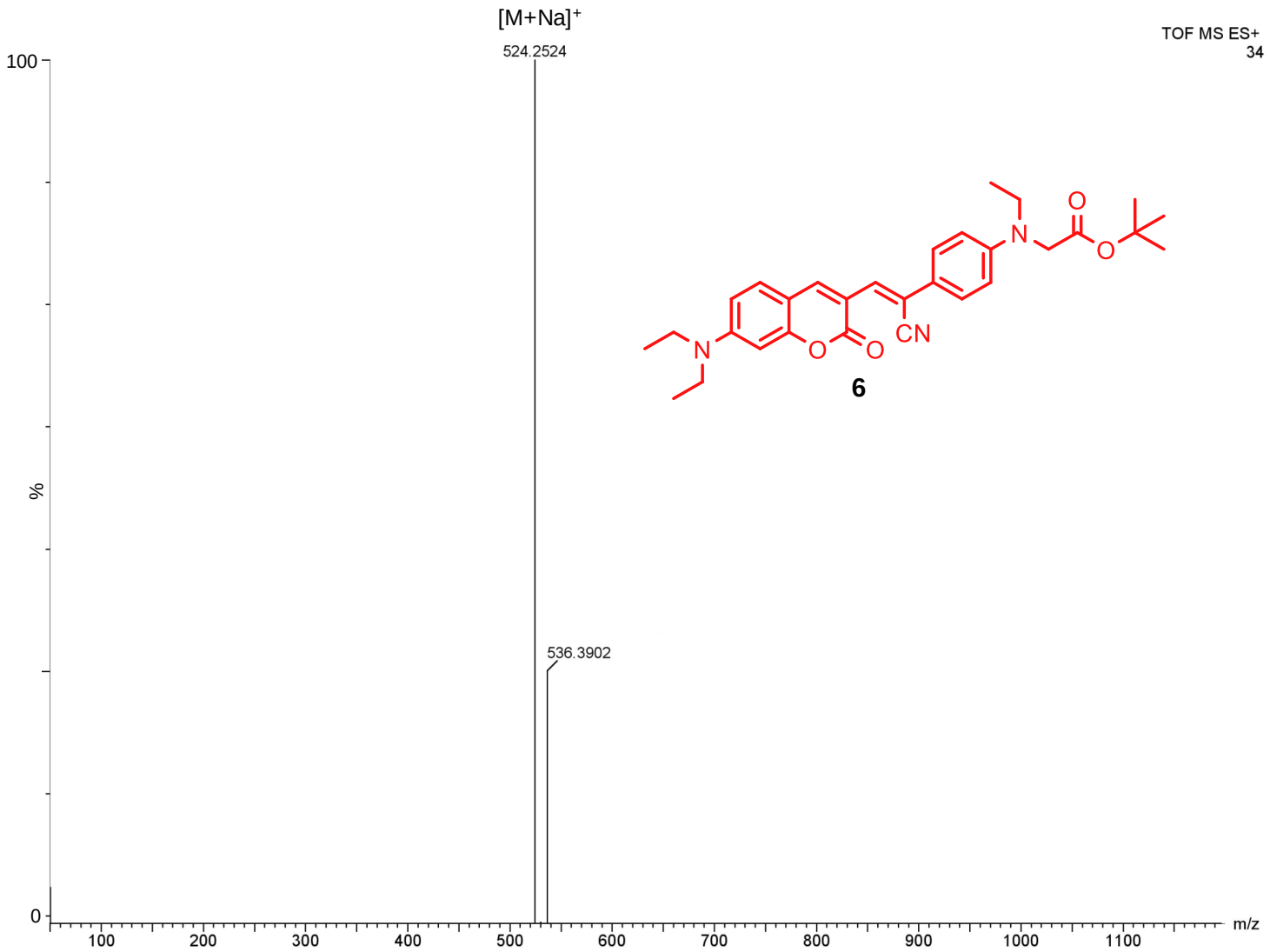

Fig. S15 HRMS (ESI +ve) spectrum of compound **6**.

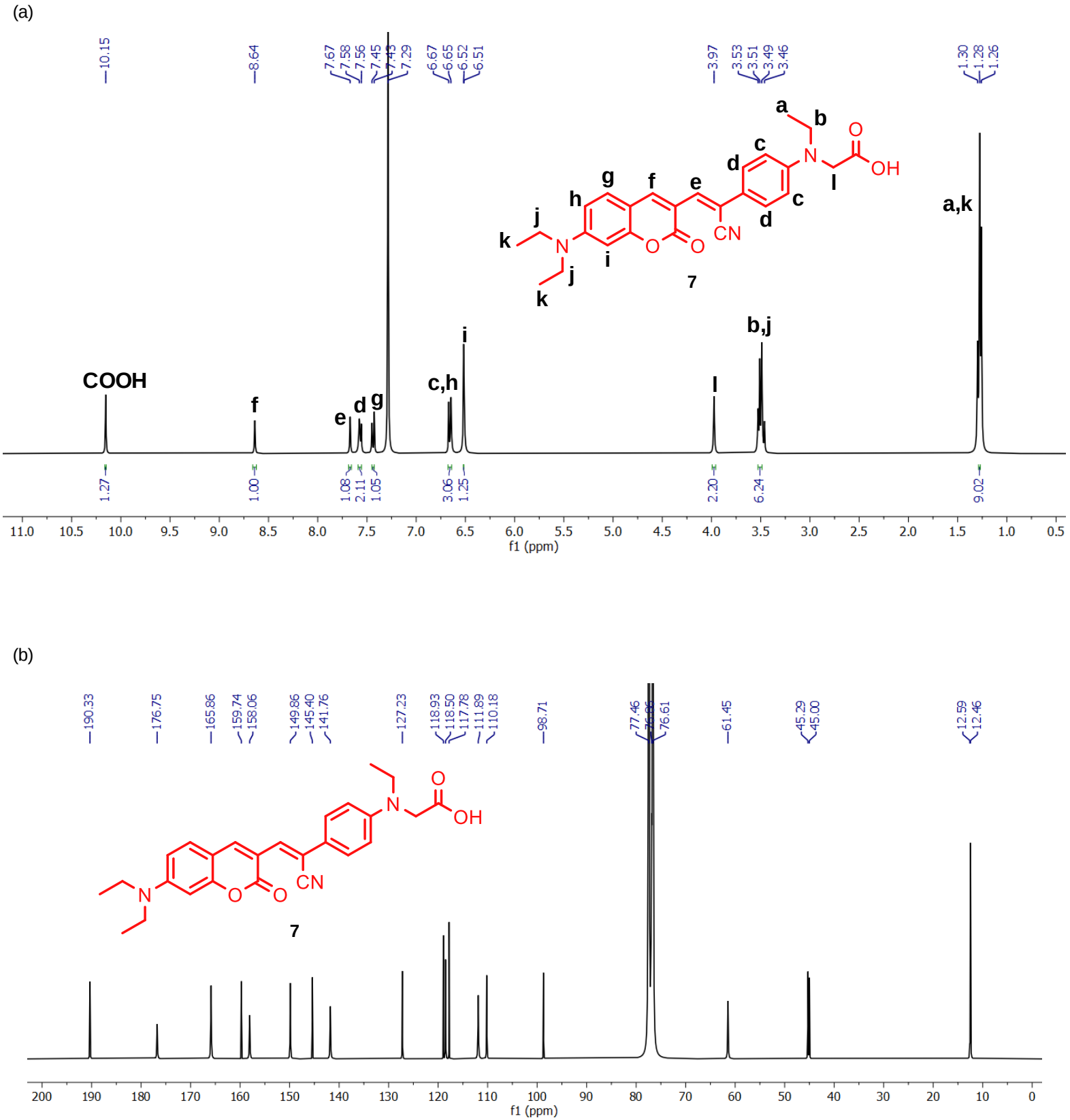

Fig. S16 (a) ^{1}H NMR (400 MHz, $CDCl_3$, 25 °C) spectrum and (b) ^{13}C NMR (101 MHz, $CDCl_3$, 25 °C) spectrum of **7**.

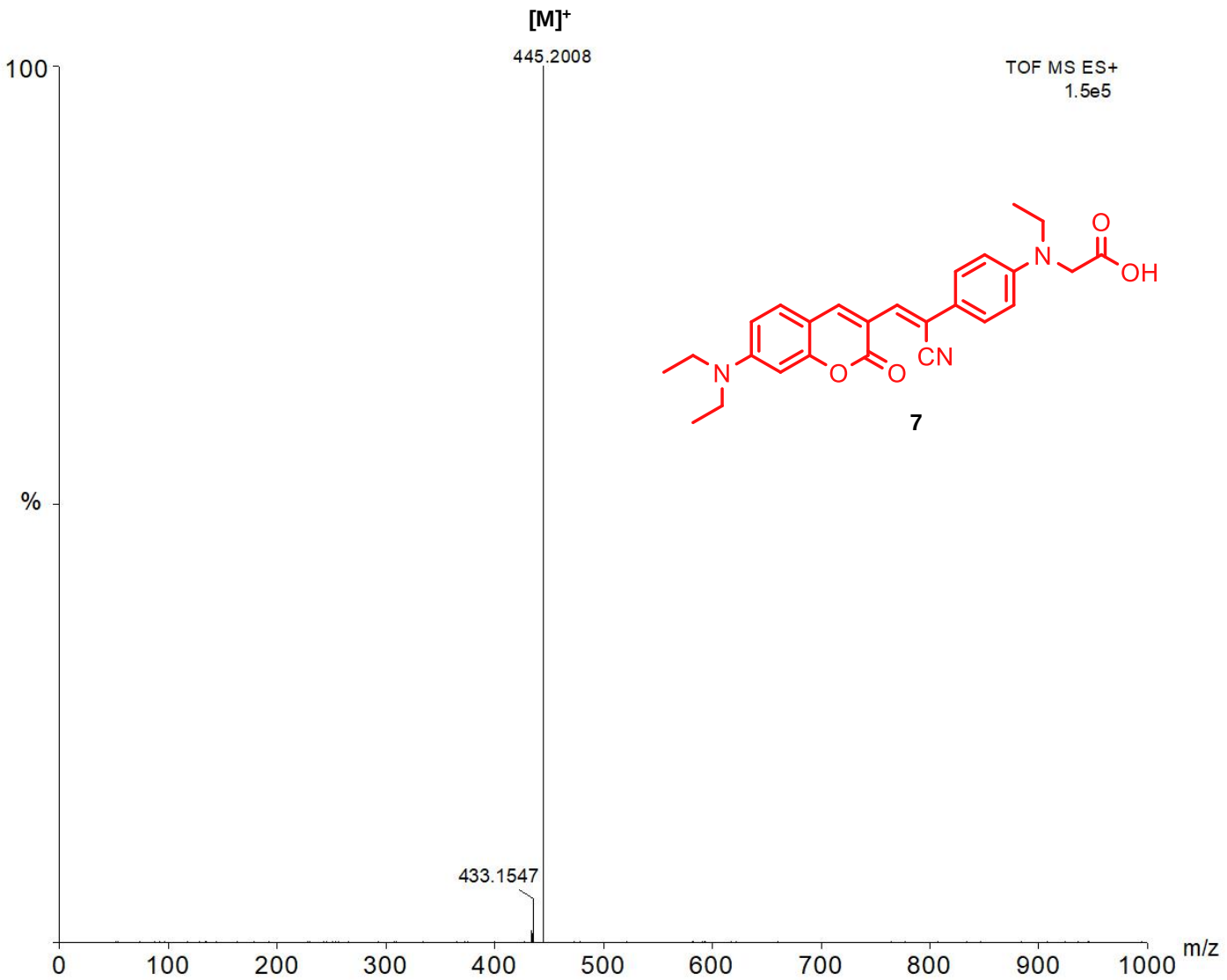

Fig. S17 HRMS (ESI +ve) spectrum of compound **7**.

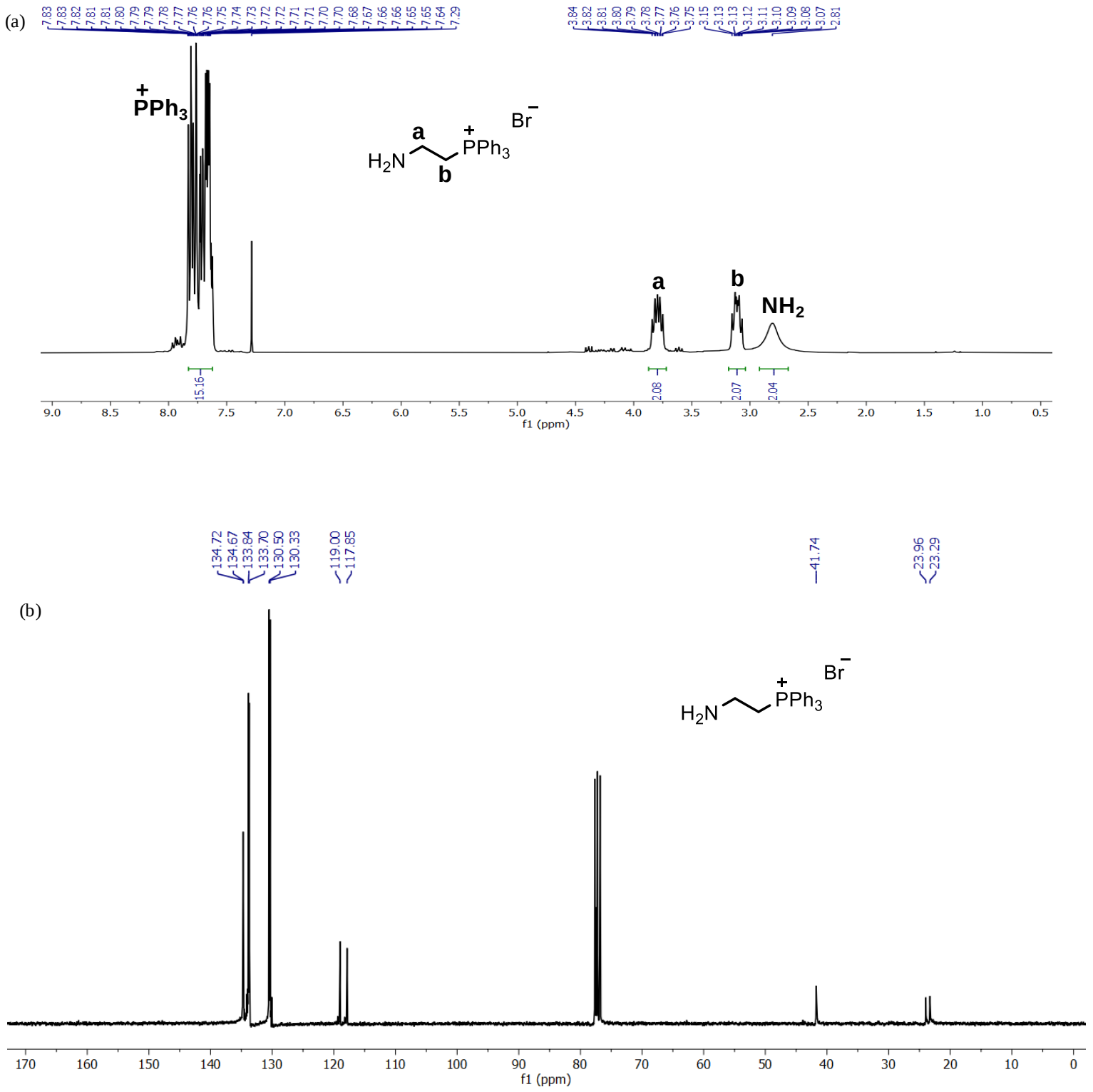

Fig. S18 (a) ^{1}H NMR (300 MHz, $CDCl_3$, 25 °C) spectrum and (b) ^{13}C NMR (75 MHz, $CDCl_3$, 25 °C) spectrum of (2-aminoethyl)triphenylphosphonium bromide.

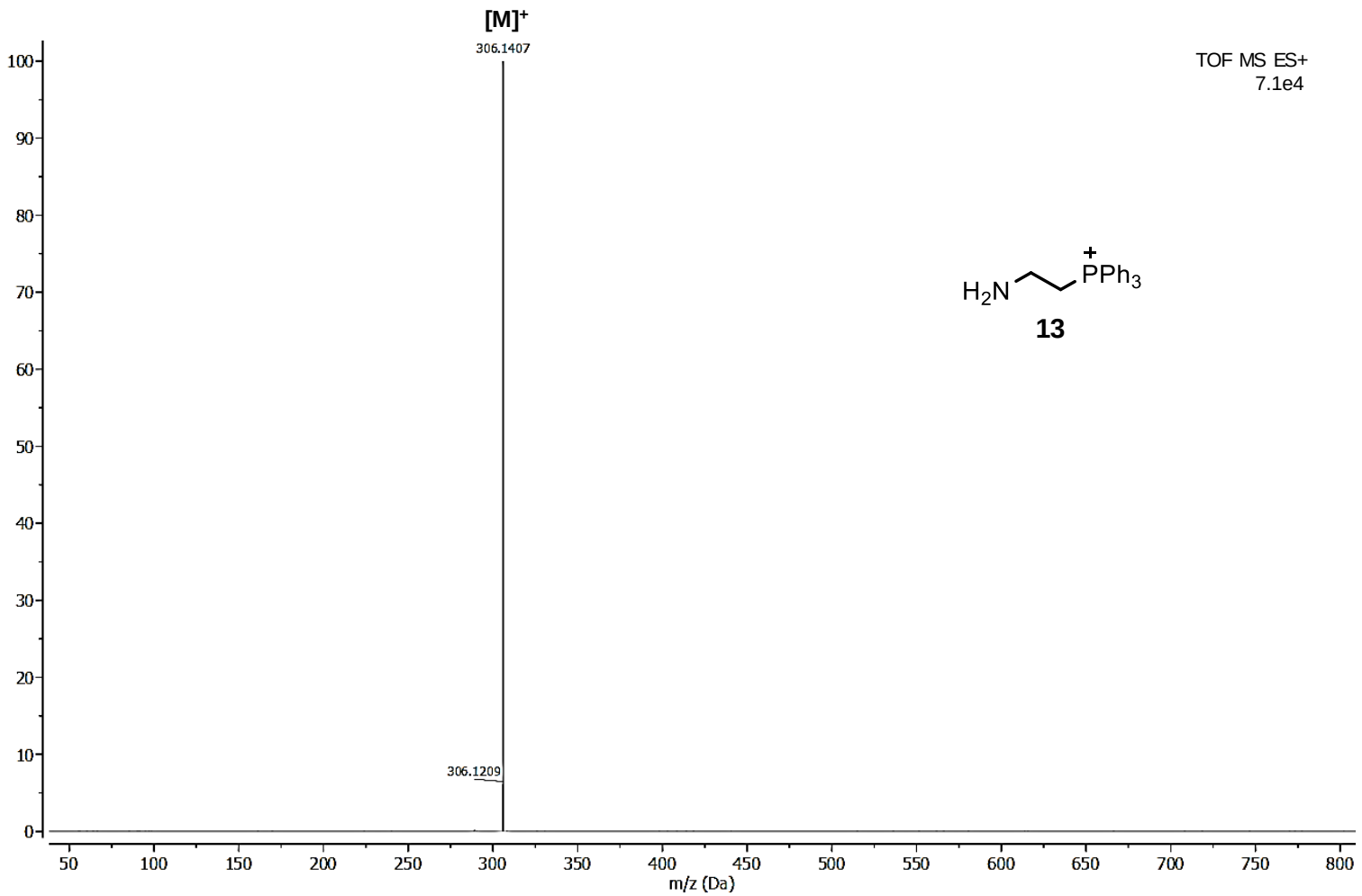

Fig. S19 HRMS (ESI +ve) spectrum of compound (2-aminoethyl)triphenylphosphonium bromide.

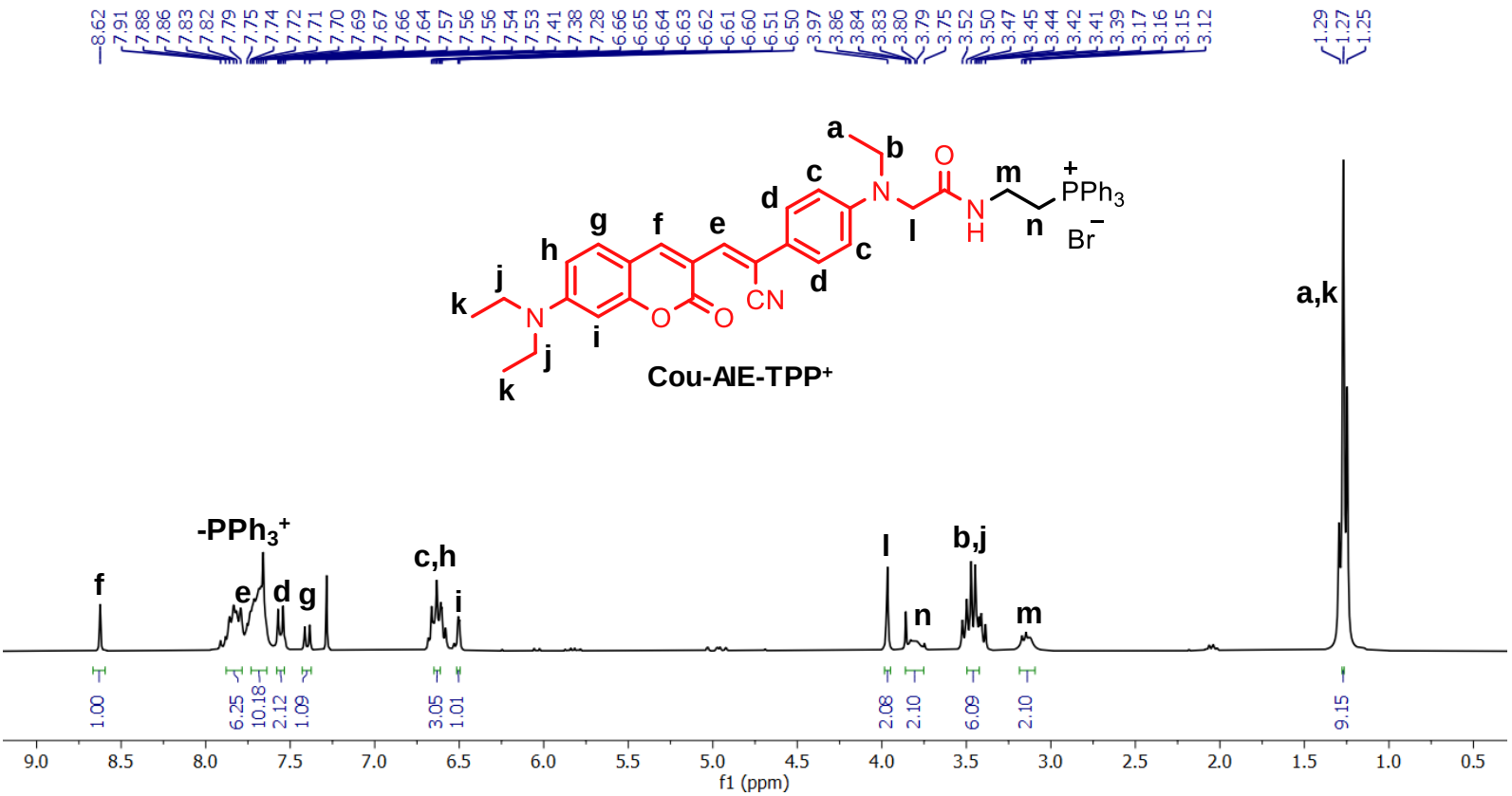

Fig. S20 ^{1}H NMR (300 MHz, $CDCl_3$, 25 °C) spectrum of compound **Cou-AIE-TPP^{+}**.

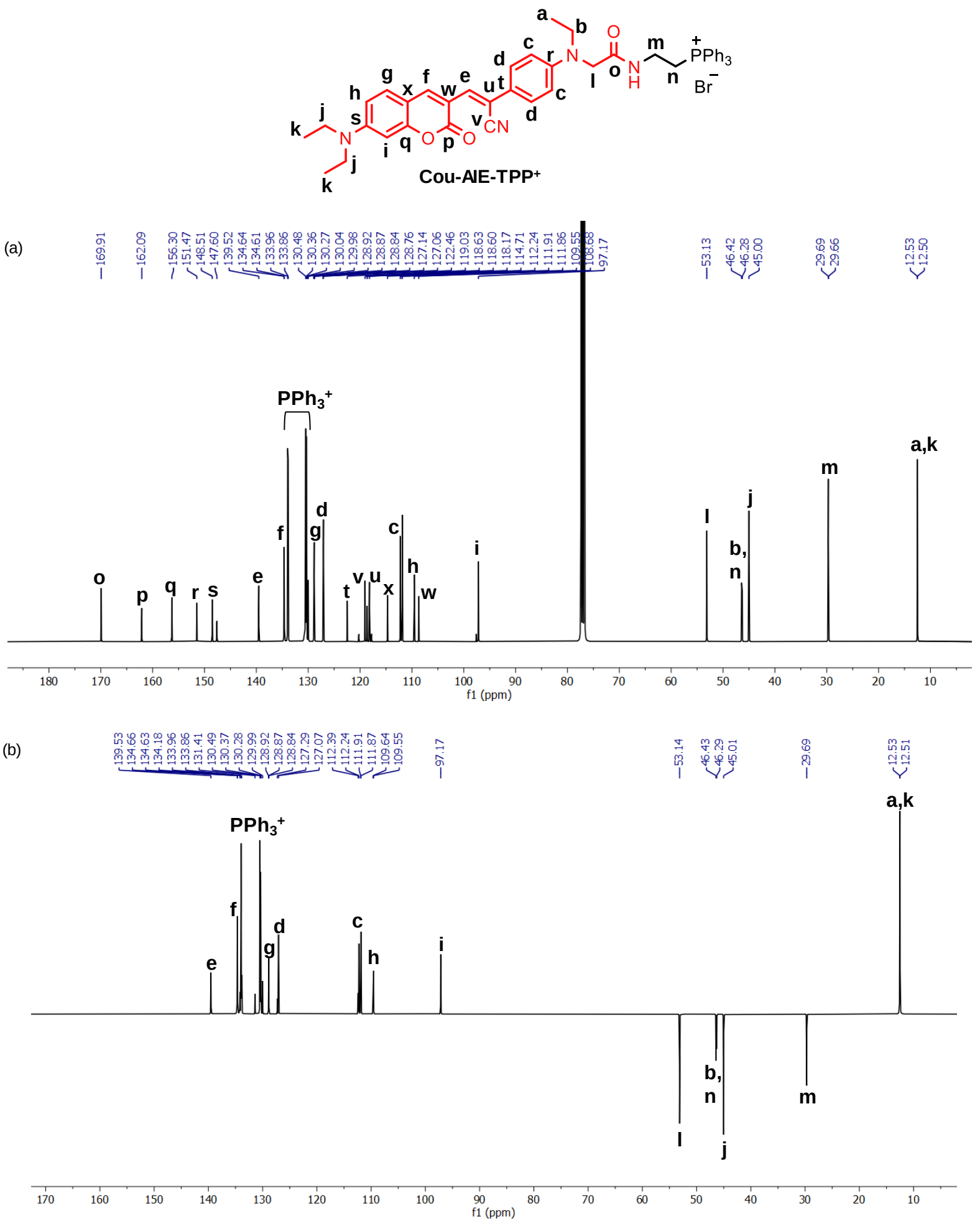

Fig. S21 (a) ^{13}C NMR (101 MHz, $CDCl_3$, 25 °C) spectrum and (b) DEPT-135 (101 MHz, $CDCl_3$, 25 °C) spectrum of compound **Cou-AIE-TPP$^+$**.

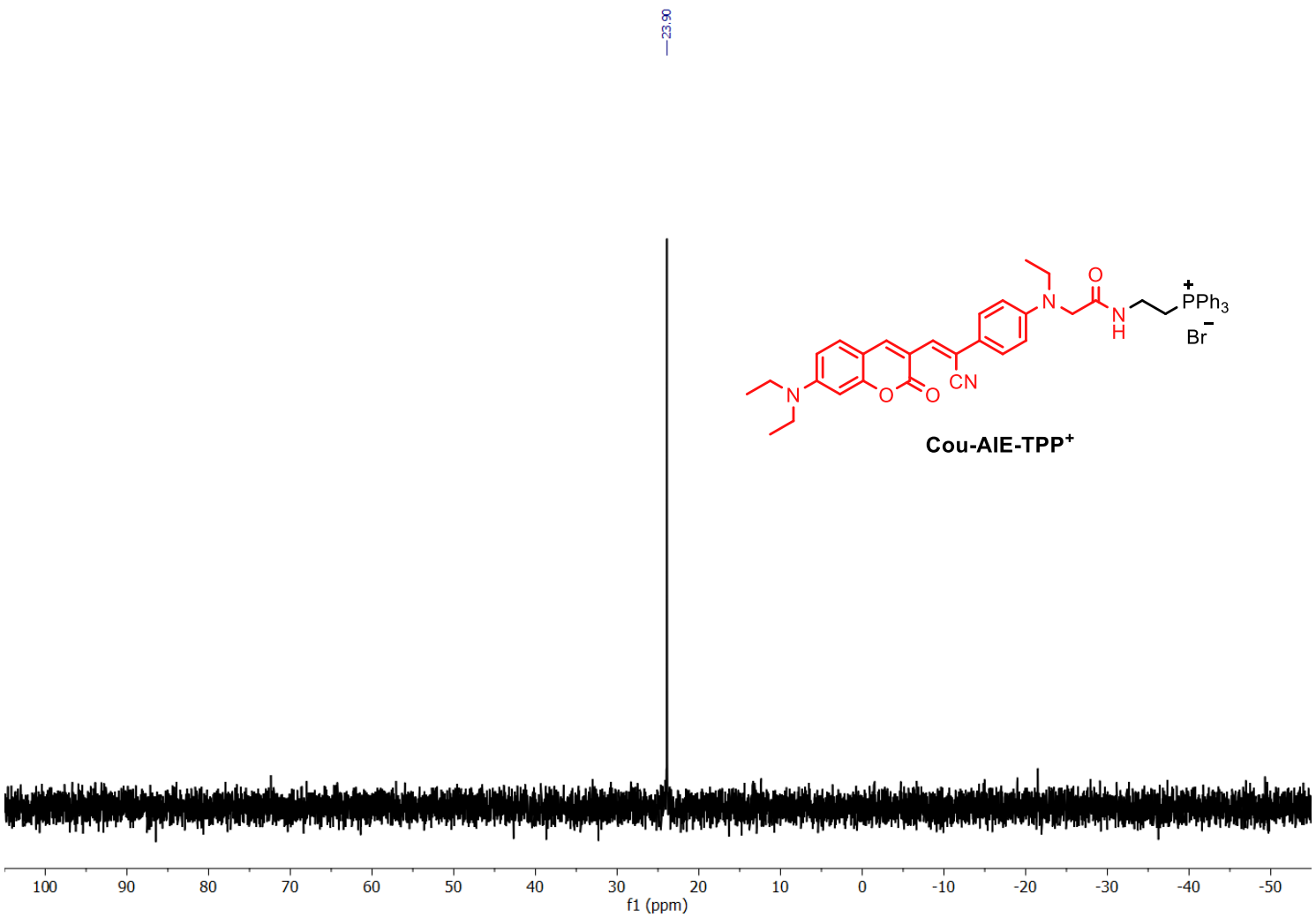

Fig. S22 ^{31}P NMR (121 MHz, $CDCl_3$, 25 °C) spectrum of **Cou-AIE-TPP$^+$** probe.

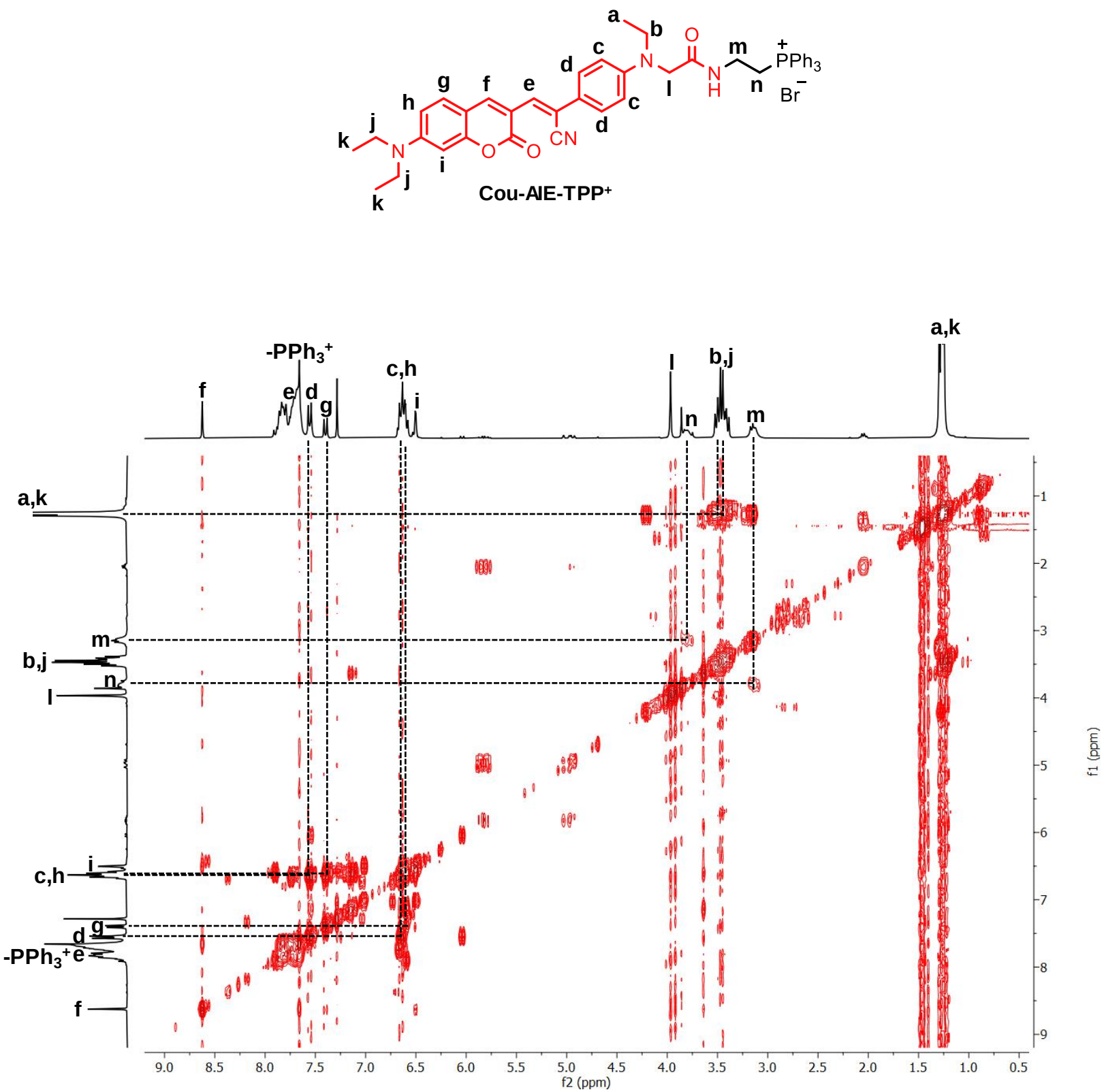

Fig. S23 ^{1}H-^{1}H COSY (Correlation Spectroscopy) NMR (300 MHz, $CDCl_3$, 25 °C) spectrum of the probe **Cou-AIE-TPP^{+}**.

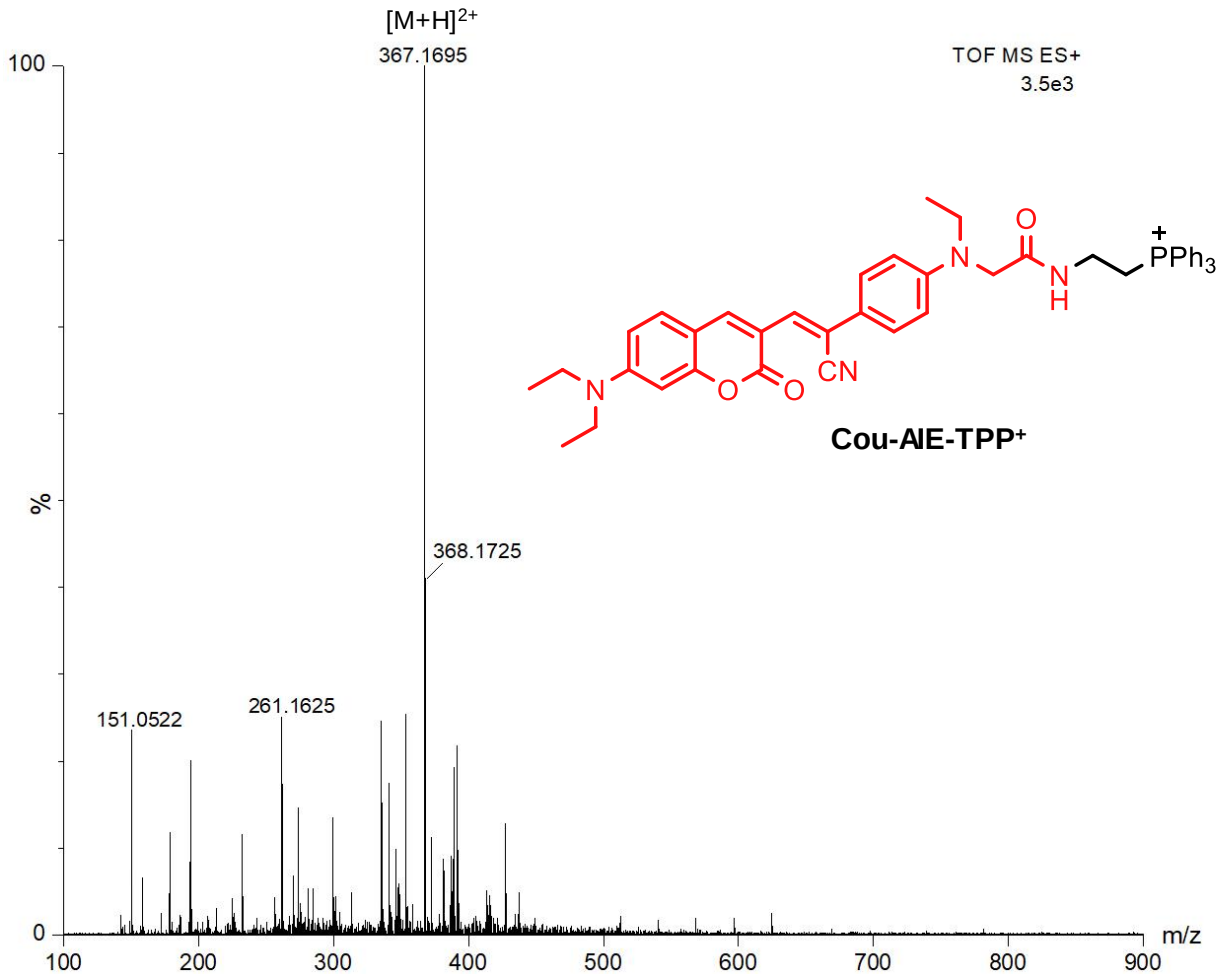

Fig. S24 HRMS (ESI +ve) spectrum of compound **Cou-AIE-TPP**$^{+}$.

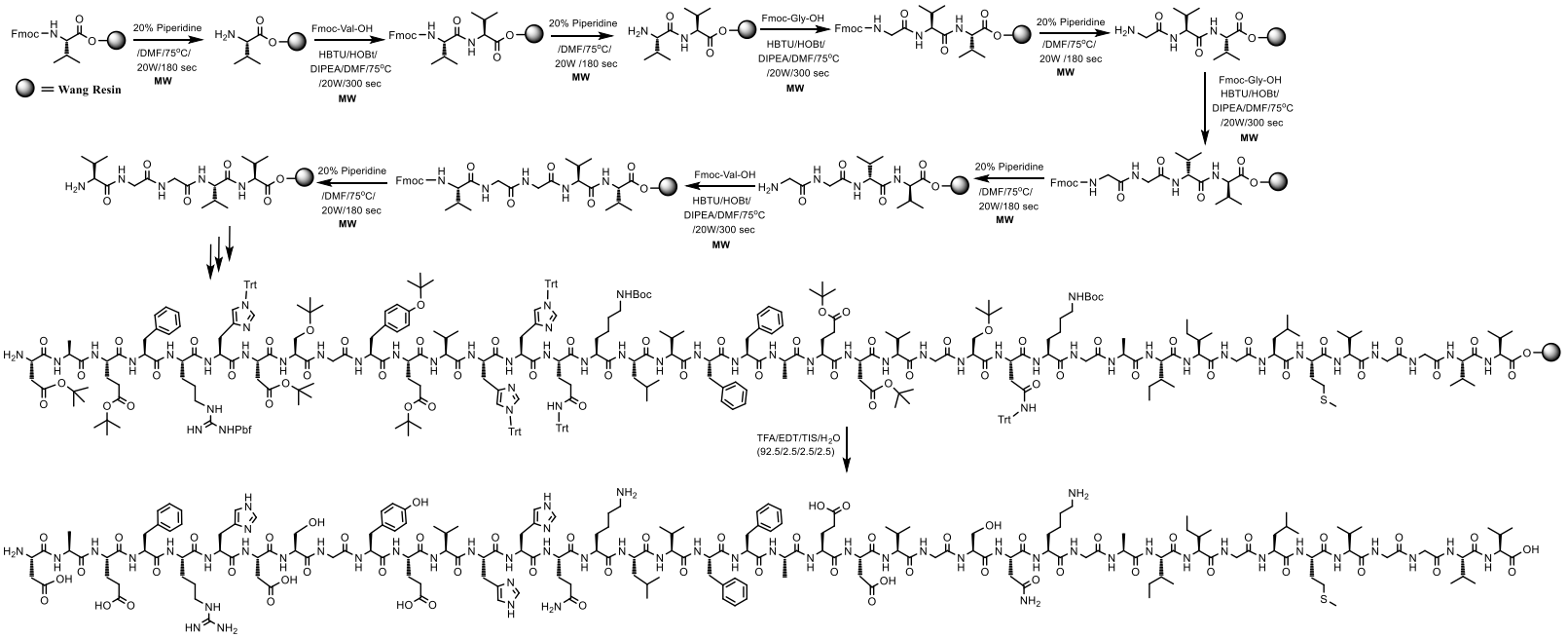

Aβ $^{1-40}$ **DAEFRHDSGYEVHHQKLVFFAEDVGSNKGAIIGLMVGGVV**

Fig. S25 Microwave-assisted Fmoc-SPPS of Aβ40 on Wang resin.

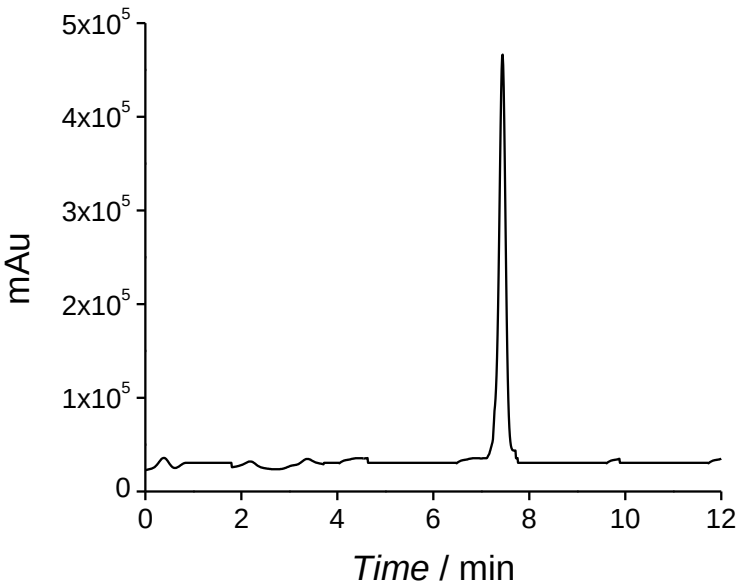

Fig. S26 Analytical HPLC profile of Aβ40 peptide.

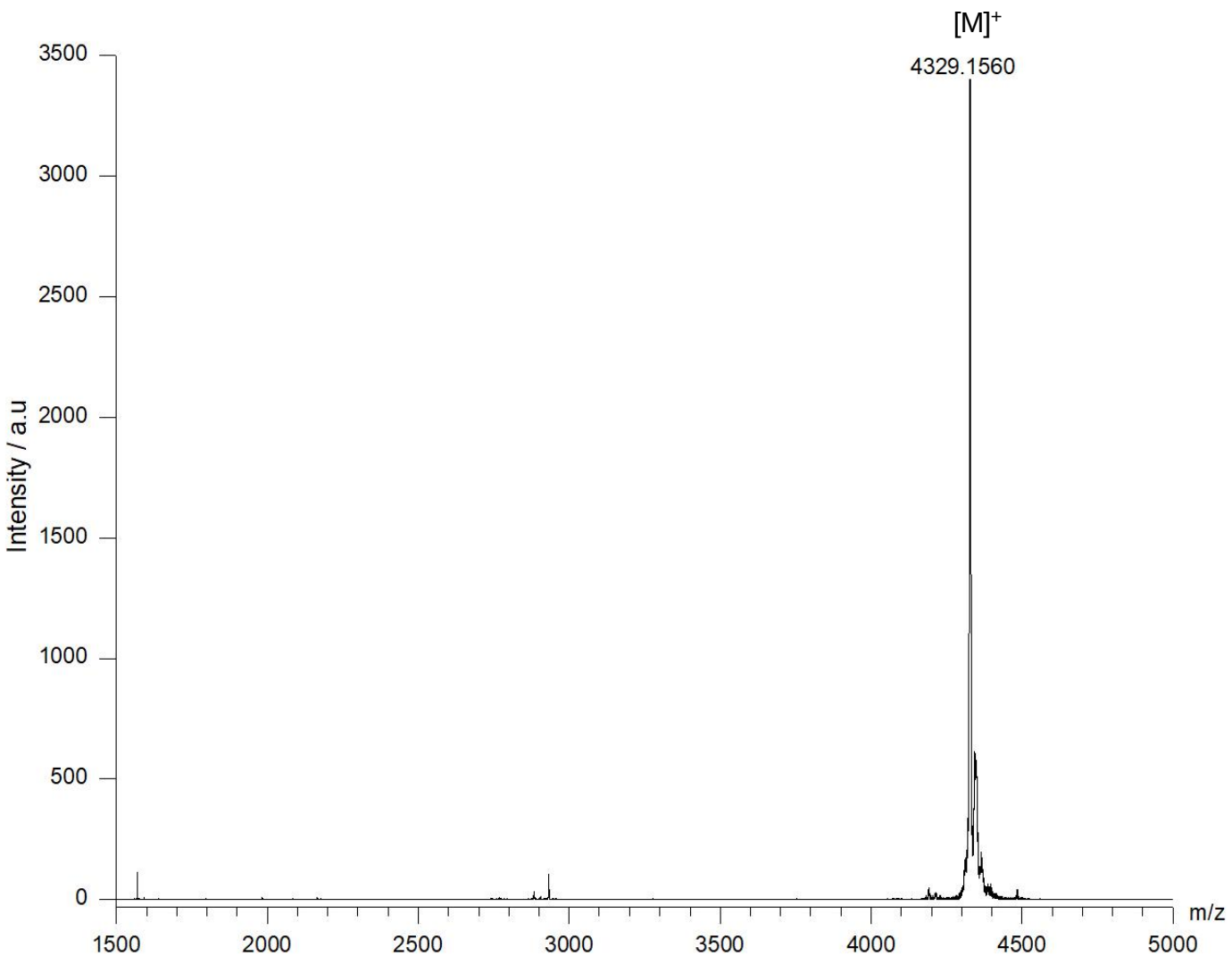

Fig. S27 MALDI mass spectrum of **A*β*40** peptide.

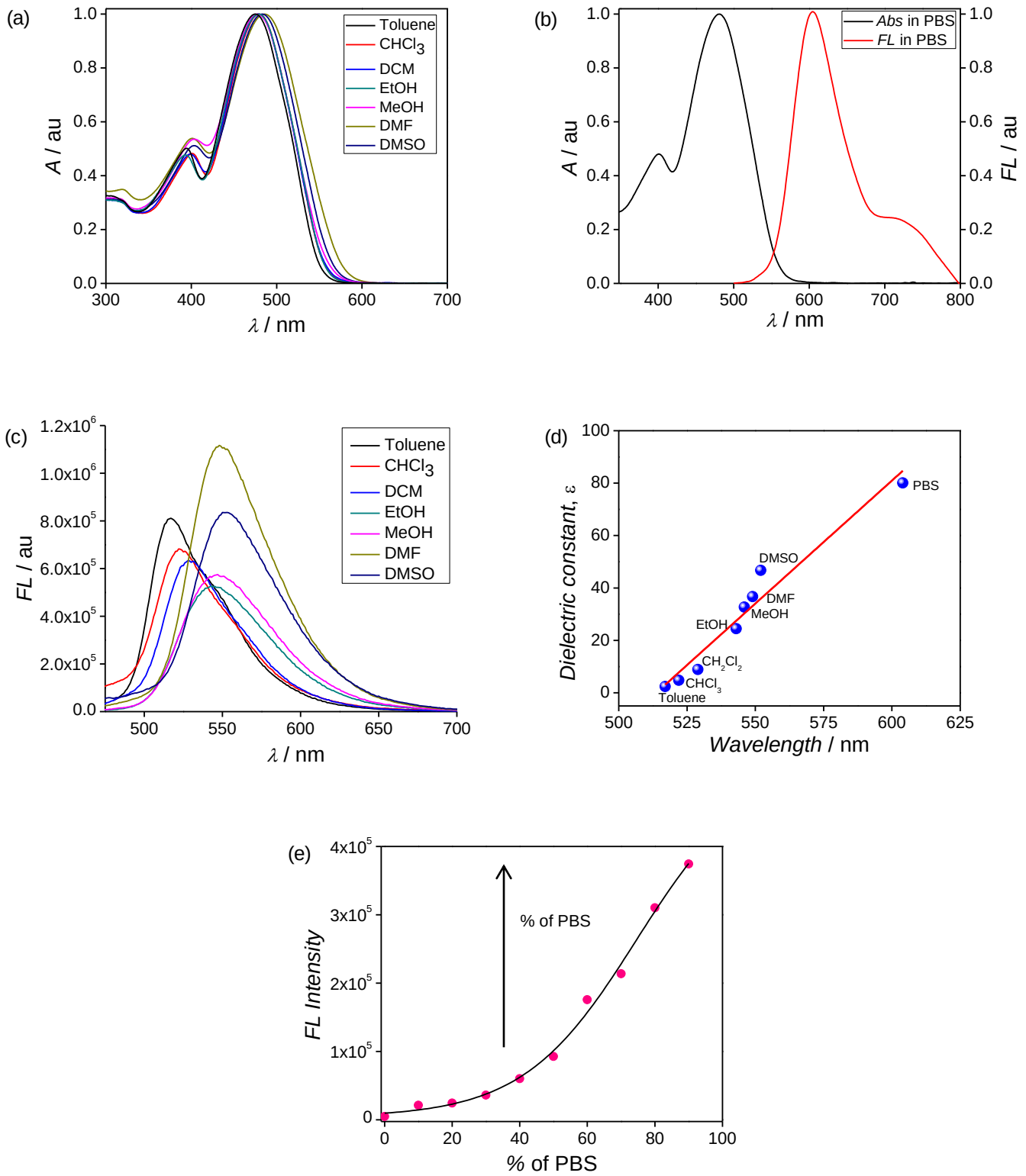

Fig. S28 (a) Normalized absorption spectra of Cou-AIE-TPP$^+$ in different solvents. (b) Normalized absorption and emission spectra of Cou-AIE in PBS exhibits 124 nm Stokes shift. (c) Fluorescence emission spectra of Cou-AIE-TPP$^+$ in different solvents at λ_{ex} 480 nm. (d) The correlation between the λ_{em} and the dielectric constant of the solvents. (e) Fluorescence emission intensity augmentation and AIE effect of Cou-AIE-TPP$^+$ in THF/PBS mixture with different volume percentage (vol%) of PBS fractions.

Table S1. The photophysical properties of Cou-AIE-TPP$^+$ in various solvents.

Solvents	Dielectric constant (ε) of Solvent at 20 °C	Viscosity η (cP at 20 °C)	λ_{abs} (nm)	λ_{em} (nm)	Molar extinction coefficient (ε) $M^{-1}cm^{-1}$	Stokes shift ($\Delta\lambda$, nm)
Toluene	2.4	0.59	475	517	1.01×10^5	42
$CHCl_3$	4.81	0.58	479	522	1.78×10^4	43
CH_2Cl_2	9.08	0.45	478	529	1.80×10^4	51
EtOH	24.55	1.1	479	543	1.36×10^4	64
MeOH	32.6	0.55	477	546	1.87×10^4	69
DMF	36.7	0.92	486	549	1.42×10^4	63
DMSO	46.7	2.24	482	552	1.26×10^4	70
PBS	78.54	1	480	604	1.68×10^4	124

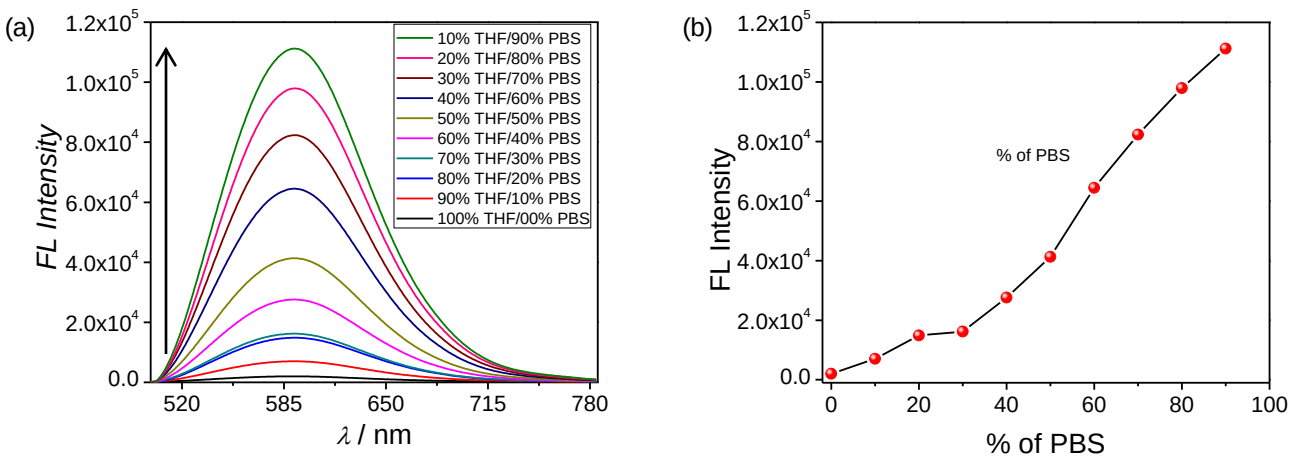

Fig. S29 (a) Fluorescence spectra of the control compound Cou-AIE in THF/PBS mixture with different volume percentage (vol%) of PBS fractions. (b) Plot of the change in fluorescence intensity of Cou-AIE with the volume fraction of PBS.

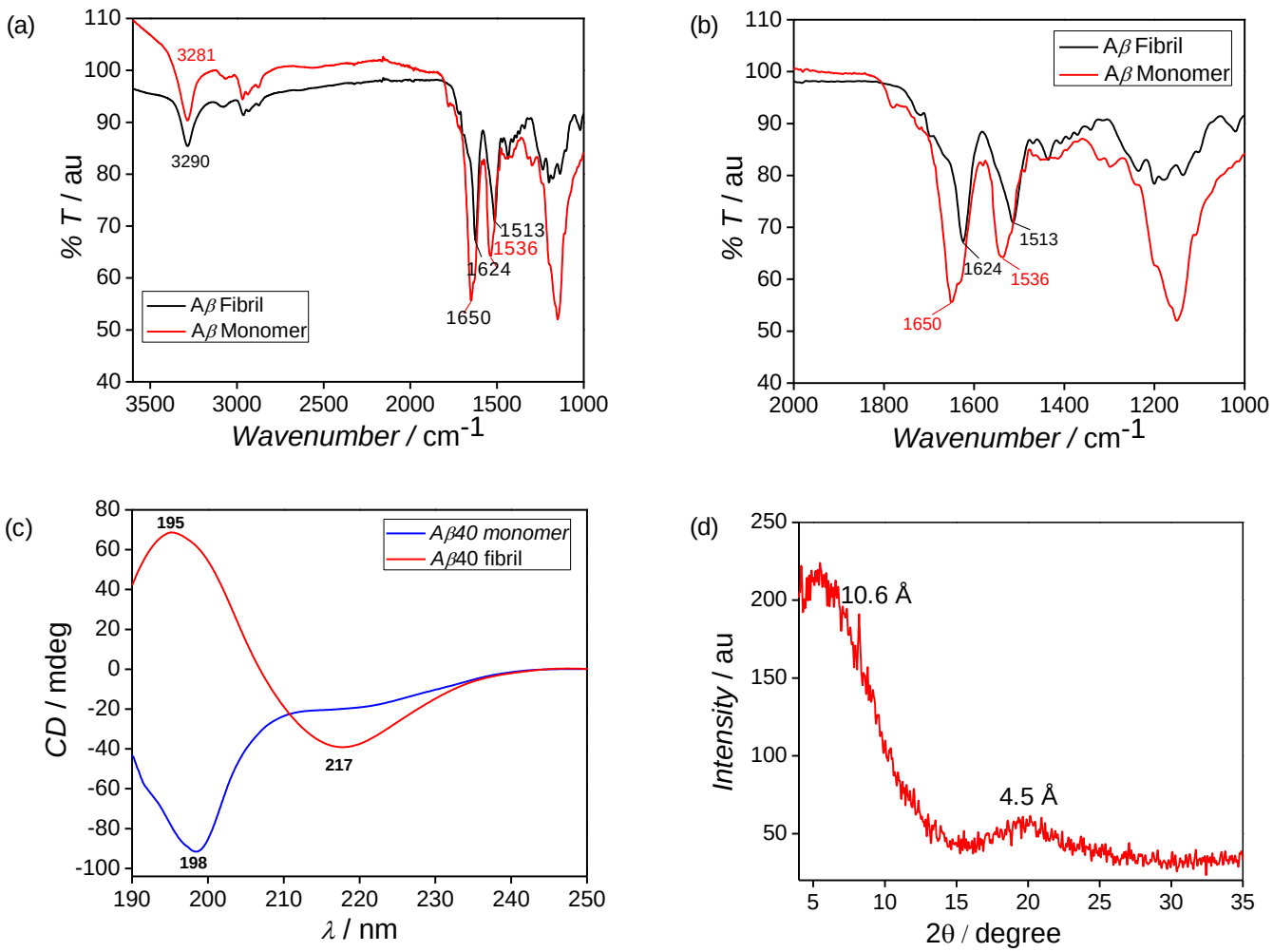

Fig. S30 (a,b) FT-IR spectra of Aβ40 monomer and fibril. (c) CD spectra of Aβ40 monomers and fibrils. (d) XRD of the dried film from Aβ40 fiber.

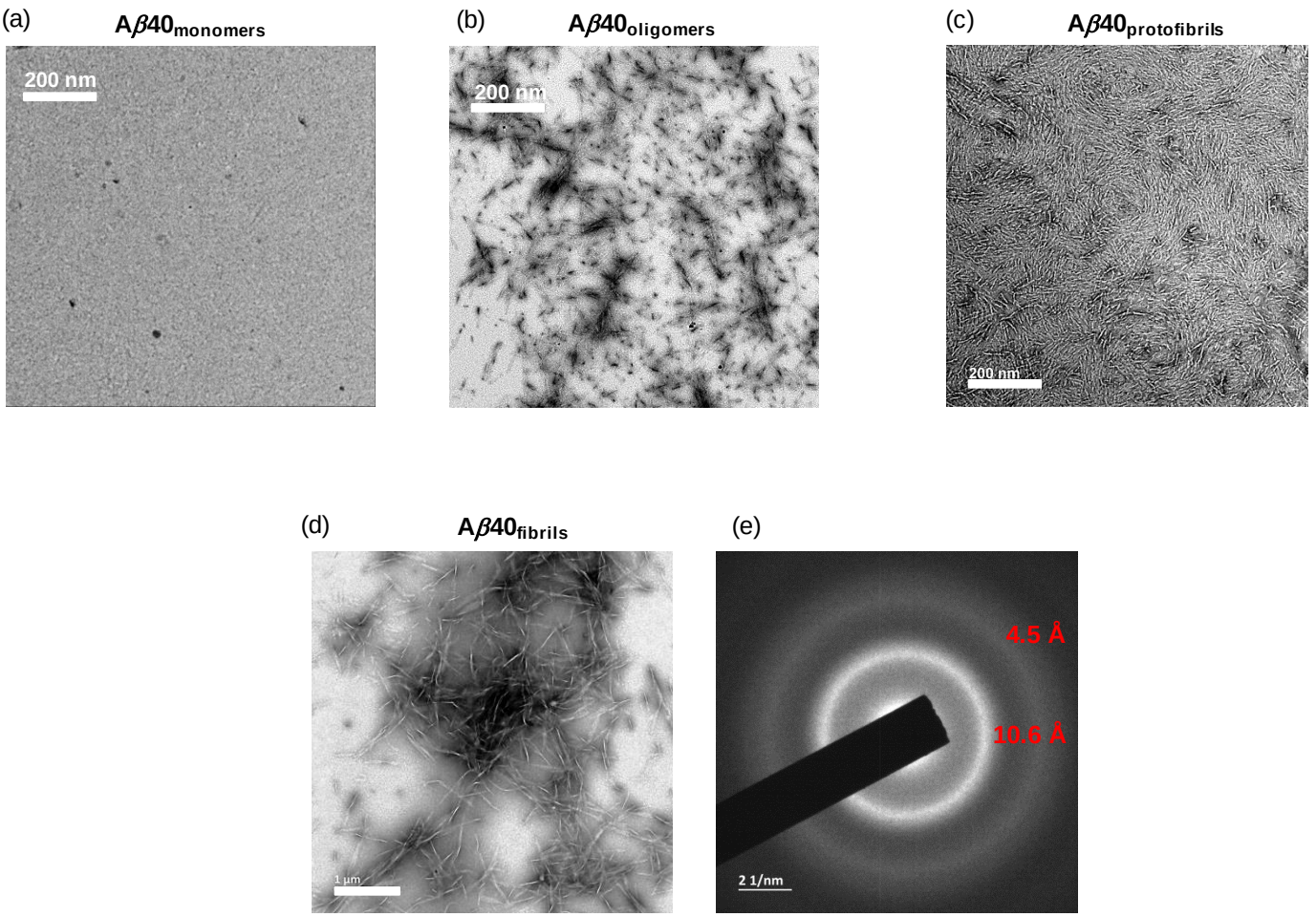

Fig. S31 TEM images of Aβ40 peptide (a) monomers, (b) oligomers, (c) protofibrils, and (d) fibrils. (e) Selected area electron diffraction (SAED) pattern of Aβ40 fibril.

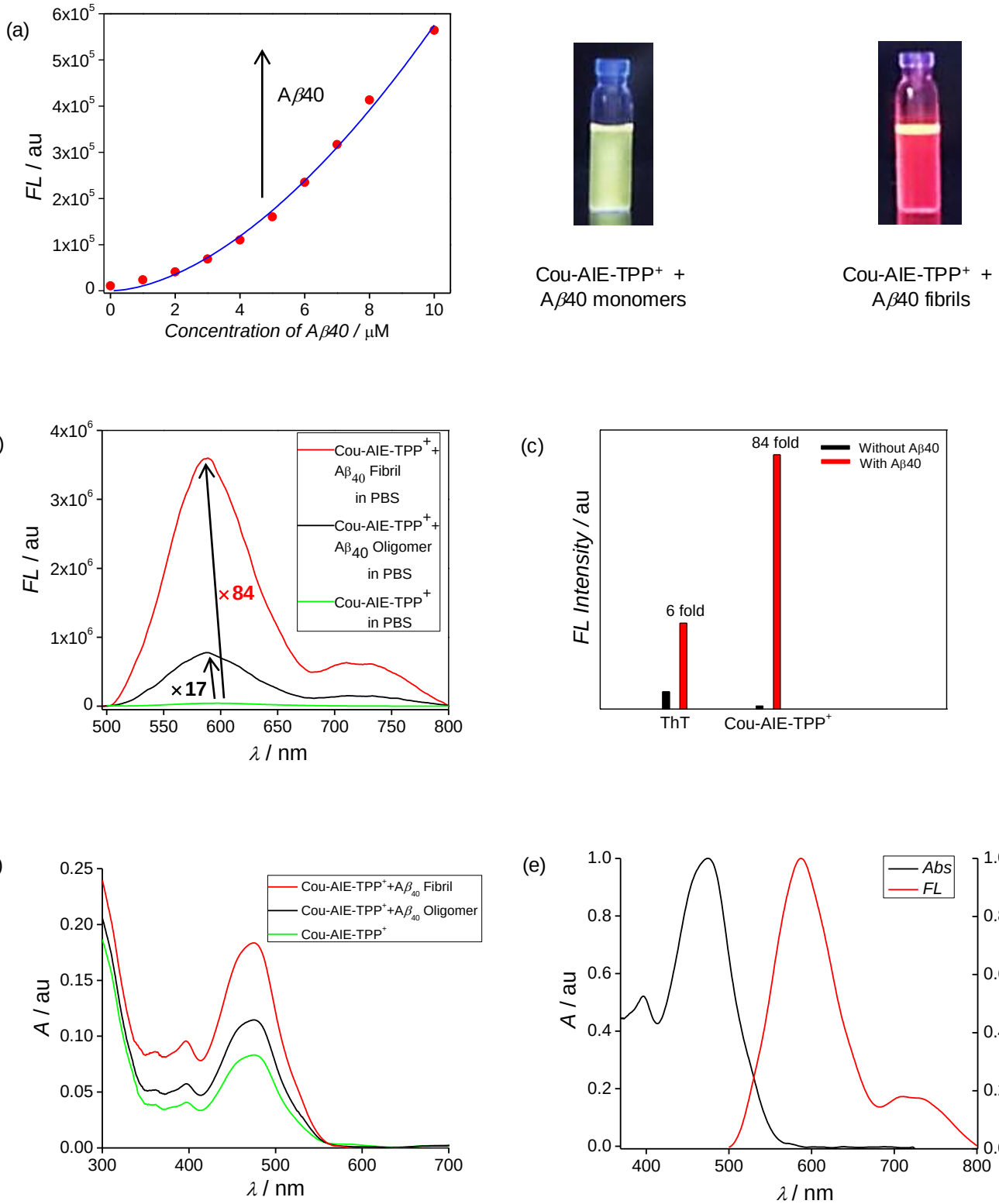

Fig. S32 (a) Plot of fluorescence intensity change of Cou-AIE-TPP$^+$ versus different concentrations of Aβ40 (0-10 μM). (b) Augmentation of fluorescence intensity by 17-fold and 84-fold for Cou-AIE-TPP$^+$ (1 μM) after incubation with Aβ40 oligomers and mature fibrils, respectively with blue shift. (c) Fluorescence emission intensity of ThT (1 μM) and Cou-AIE-TPP$^+$ (1 μM) with or without Aβ40 aggregates (10 μM). (d) Absorption spectra of Cou-AIE-TPP$^+$ and after incubation with Aβ40 oligomer and fibrils in PBS. (e) Normalized absorption and emission spectra of Cou-AIE-TPP$^+$ after binding with Aβ40 fibril in PBS.

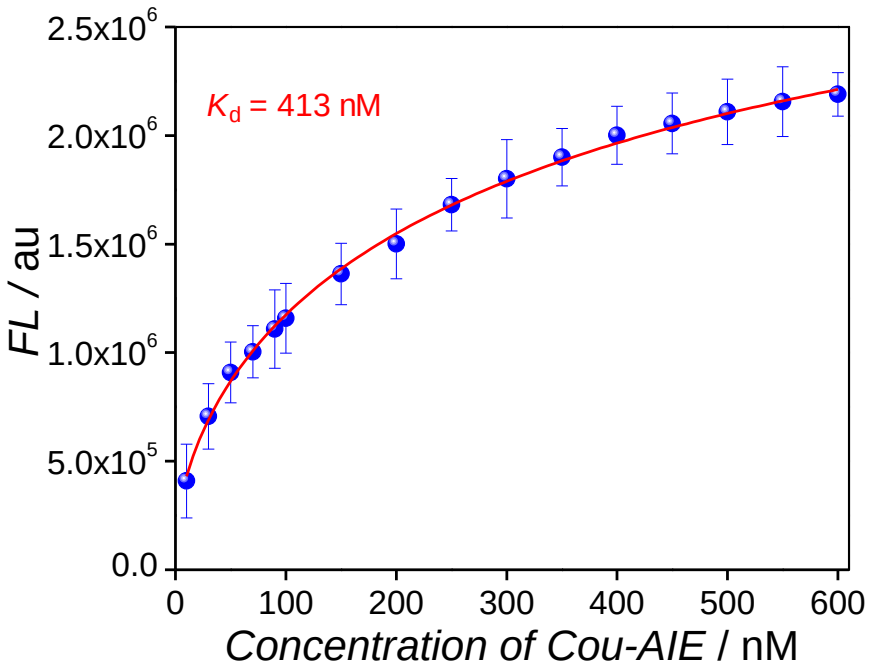

Fig. S33 The dissociation constant (K_d = 413 nM) is determined from the plot of emission intensity change with increasing concentrations (up to 600 nM) of Cou-AIE in Aβ40 aggregate (10 μM). Error bars denote SD of 3 measurements.

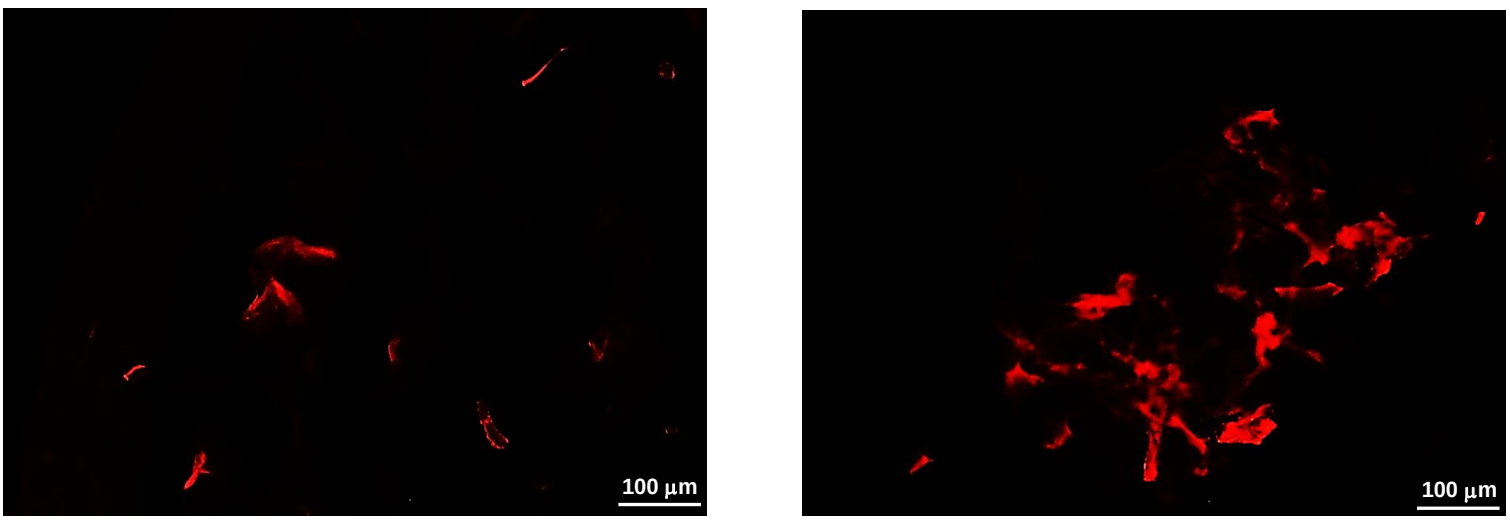

Fig. S34 CLSM image of Aβ40 fibrils stained with Cou-AIE-TPP^{+}.

Table S2 Comparison of our synthesized probe Cou-AIE-TPP$^+$ with the literature reported probes. λ_{em} represents the emission wavelength maximum of the probes after binding to Aβ fibrils. K_d represents the dissociation constants.

Compounds	λ_{em}	K_d (nM)	Reference
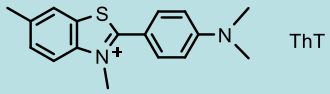 ThT	485 nm	890	*Life Sci*., 2001, **69**, 1471–1484
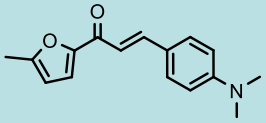	582 nm	2300	*Arch. Pharm. Res*., 2015, **38**, 1992–1998
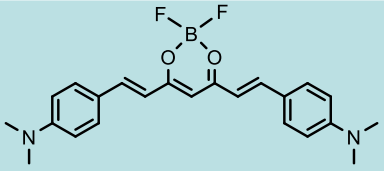	715 nm	38.7	*J. Am. Chem. Soc*., 2009, **131**, 15257–15261
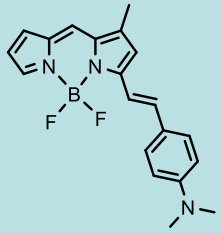	648 nm	44.1	*ACS Chem. Neurosci*., 2012, **3**, 319−324
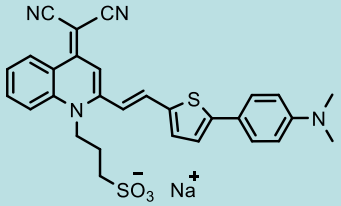	665 nm	NA	*J. Am. Chem. Soc*., 2019, **141**, 3171–3177
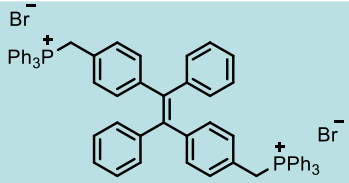	406 nm	8930	*Biochemistry*, 2020, **59**, 1813−1822
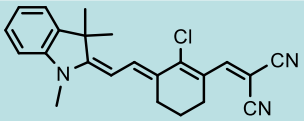	685 nm	59.09	*Chem. Commun*., 2017, **53**, 9910−9913
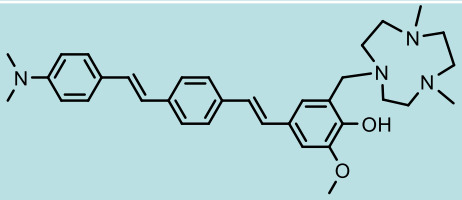	500 nm	58	*J. Am. Chem. Soc.*, 2021, **143**, 10462−10476
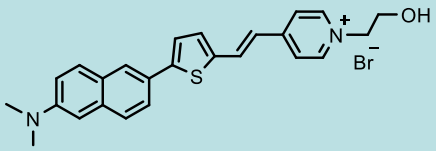	708 nm	143	*Angew. Chem. Int. Ed*., 2023, **62**, e202211550
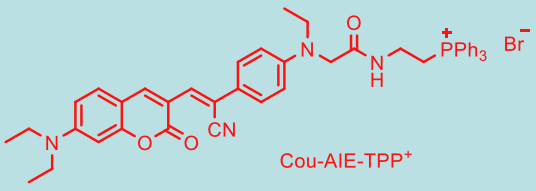 Cou-AIE-TPP$^+$	600 nm	83	In this Work

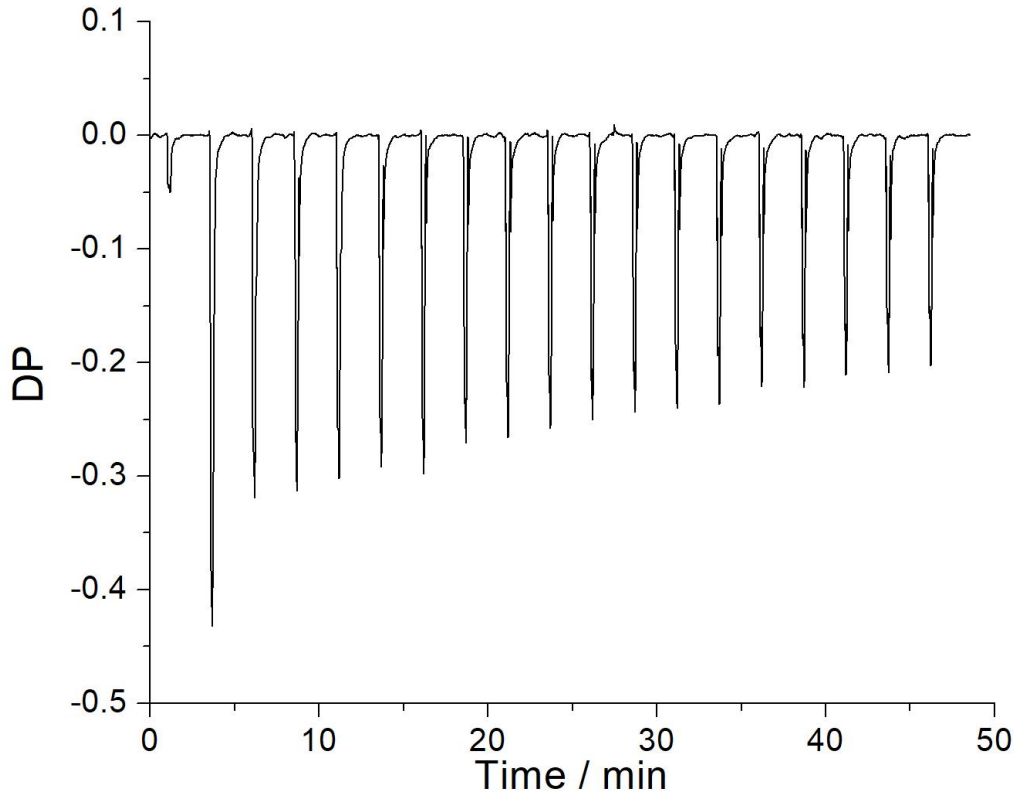

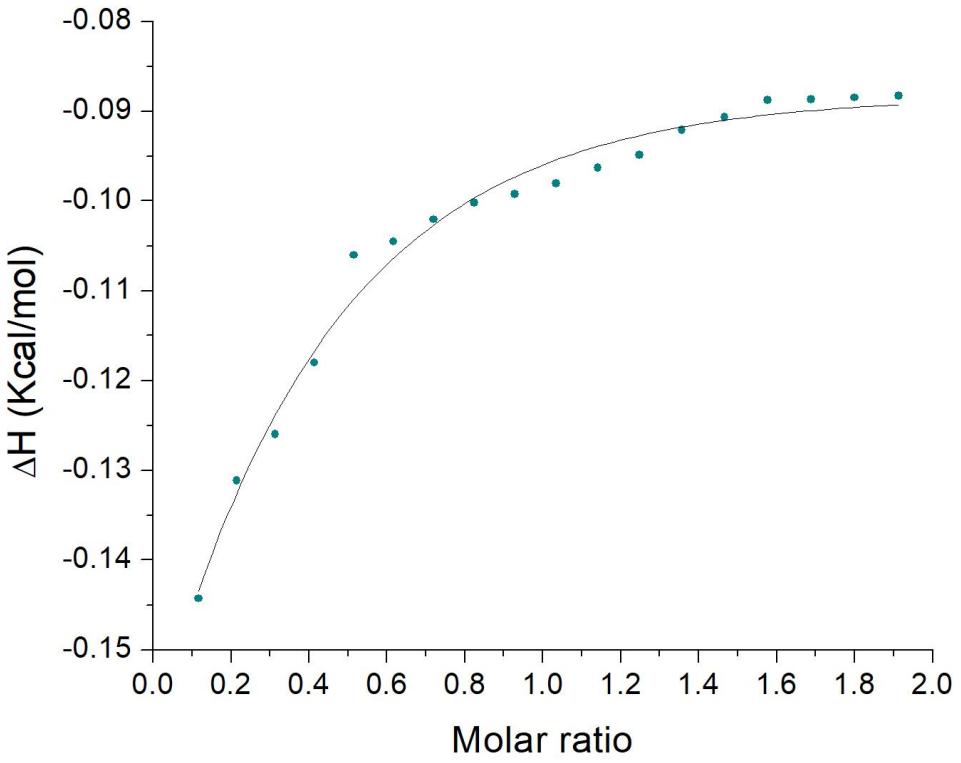

Cell conc.	Syringe conc.	N (Sites)	K_d (nM)	Δ*H* (kcal/mol)	TΔ*S* (kcal/mol)	ΔG (kcal/mol)
20 μM	200 μM	1.1	107	-4.54	-2.24	-2.30

Fig. S35 The upper panels show the raw data for the Aβ40/Cou-AIE-TPP$^+$ titration and the bottom panels represent the binding isotherm. The resultant isotherm is best fitted to a one site binding model to attain the binding affinity (K_d), stoichiometry (n), enthalpy (ΔH), entropy (ΔS), and ΔG of interaction.

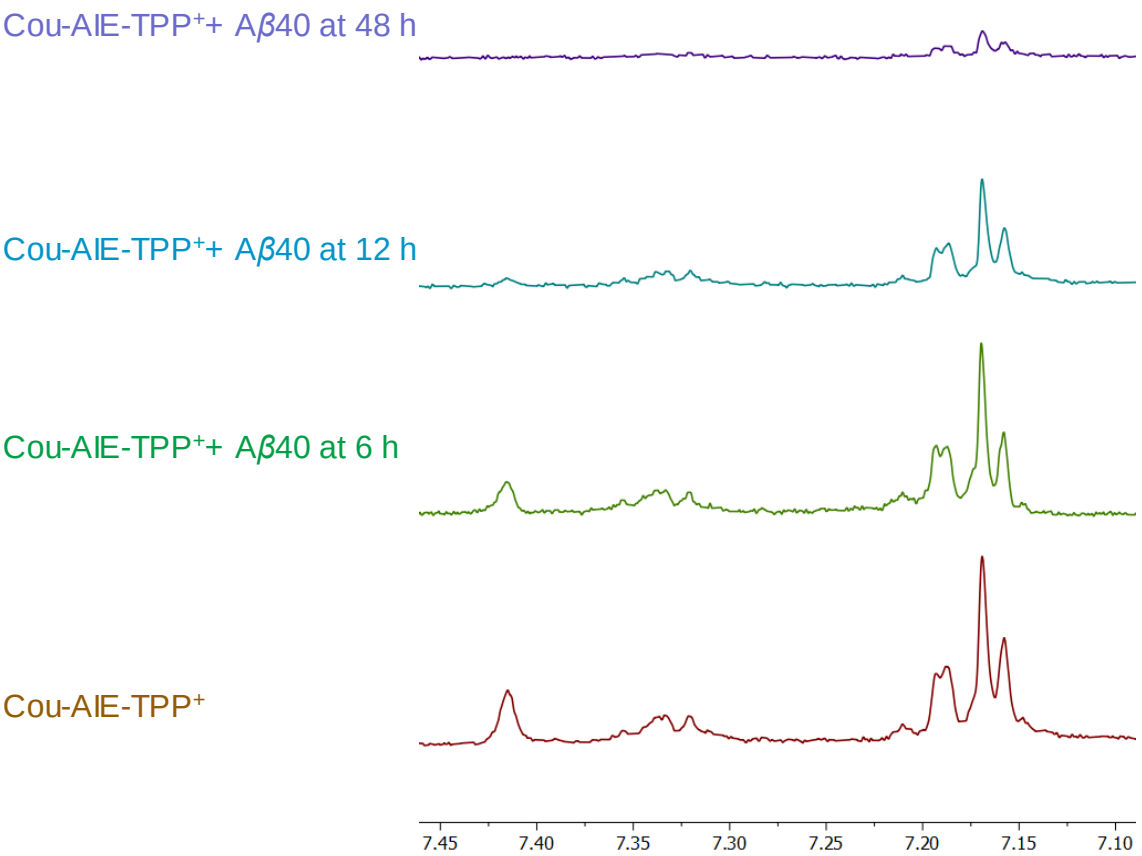

Fig. S36 Relative intensities from diffusion ordered (DOSY-NMR) NMR spectra to investigate the interactions between Cou-AIE-TPP$^+$ and Aβ40 at different time intervals (0-48 h). The diffusivity of Cou-AIE-TPP$^+$ in the presence of 10 μM Aβ40 oligomer is considerably reduced with time in PBS solution.

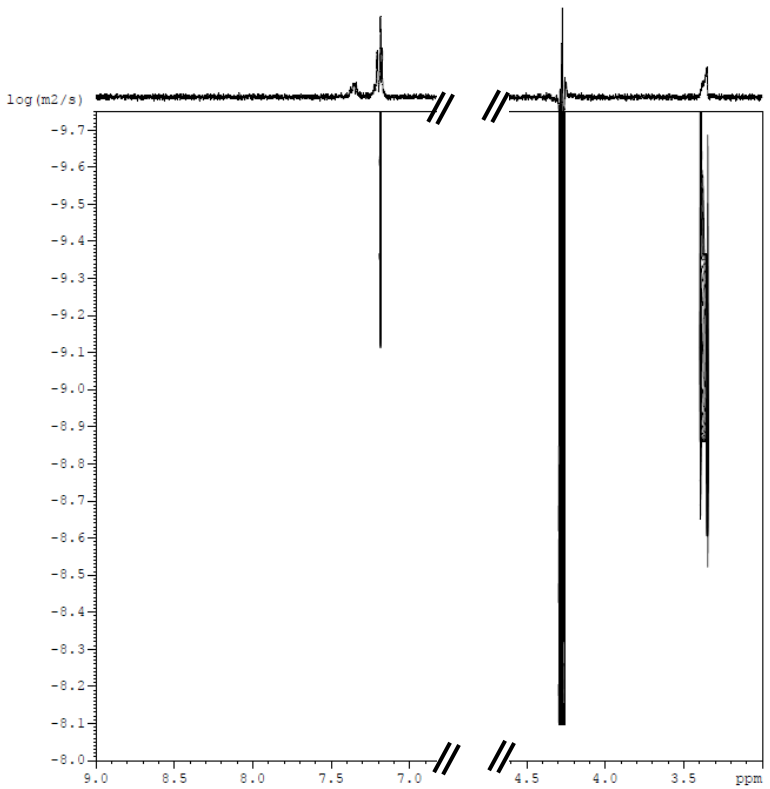

Fig. S37 DOSY spectrum showing the different diffusion behavior of the protons after interactions between Cou-AIE-TPP$^+$ and Aβ40 . The vertical axis log (m^2 / s) represents the diffusion coefficient.

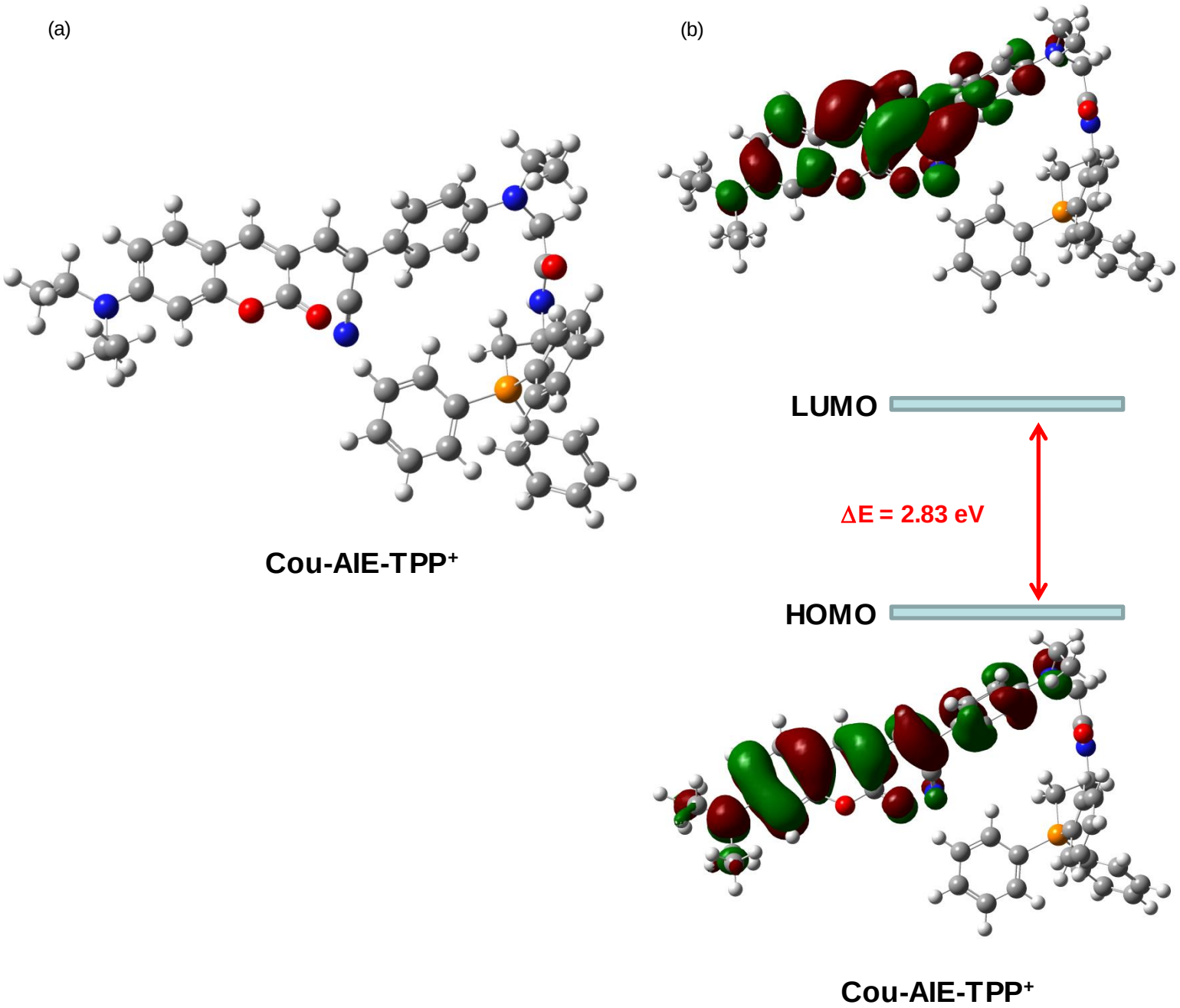

Fig. S38A (a) B3LYP / 6-31G* energy optimized structure of Cou-AIE-TPP$^+$.
(b) HOMO and LUMO of Cou-AIE-TPP$^+$ with a HOMO-LUMO energy gap of 2.83 eV.

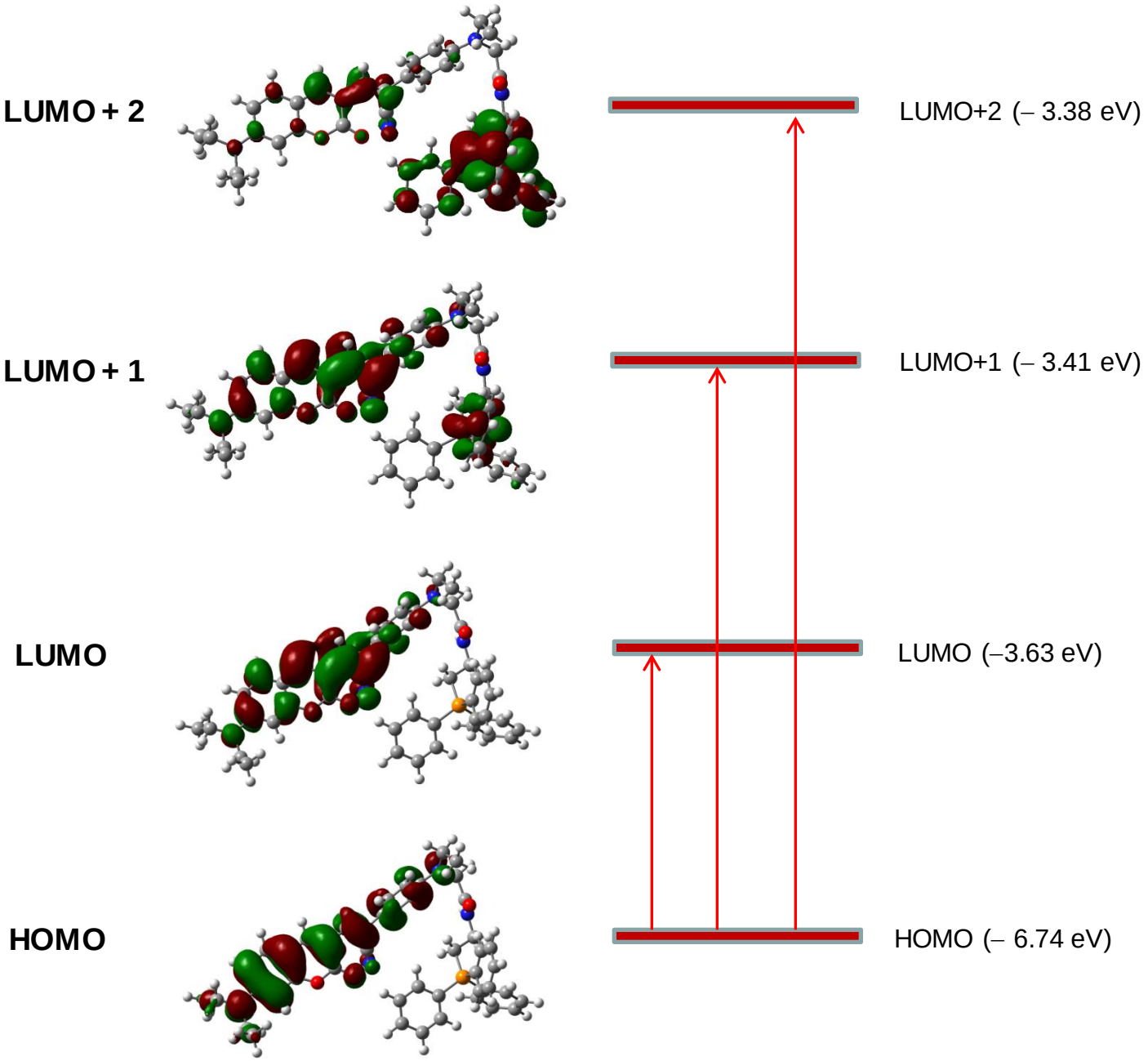

Fig. S38B HOMO, LUMO, LUMO+1, and LUMO+2 diagrams of Cou-AIE-TPP^{+} along with the energy.

Table S3. Molecular parameters derived from TDDFT calculations. Excitation energy, wavelengths (λ_{abs}, nm) of the transition, oscillator strength of the transition, ground to excited state transition dipole moments of Cou-AIE-TPP$^+$ computed using TDDFT method at B3LYP/6-31G* level in H_2O.

Excited States	E[eV]	*f*	λ_{abs}	Character	D_E	D_V
S_1	2.83	0.0016	438	HOMO → LUMO (70%)	0.0233	0.0002
S_2	3.04	0.34	408	HOMO → LUMO+1 (69%)	4.5694	0.0416
S_3	3.06	0.79	405	HOMO → LUMO+1 (10%) HOMO → LUMO+2 (69%)	10.5308	0.0970

E[eV]: Excitation energy.

λ_{abs}: Wavelength of the transition

f: the oscillator strength of the transition

D_E: Ground to excited state transition electric dipole moment

D_V: Ground to excited state transition velocity dipole moment

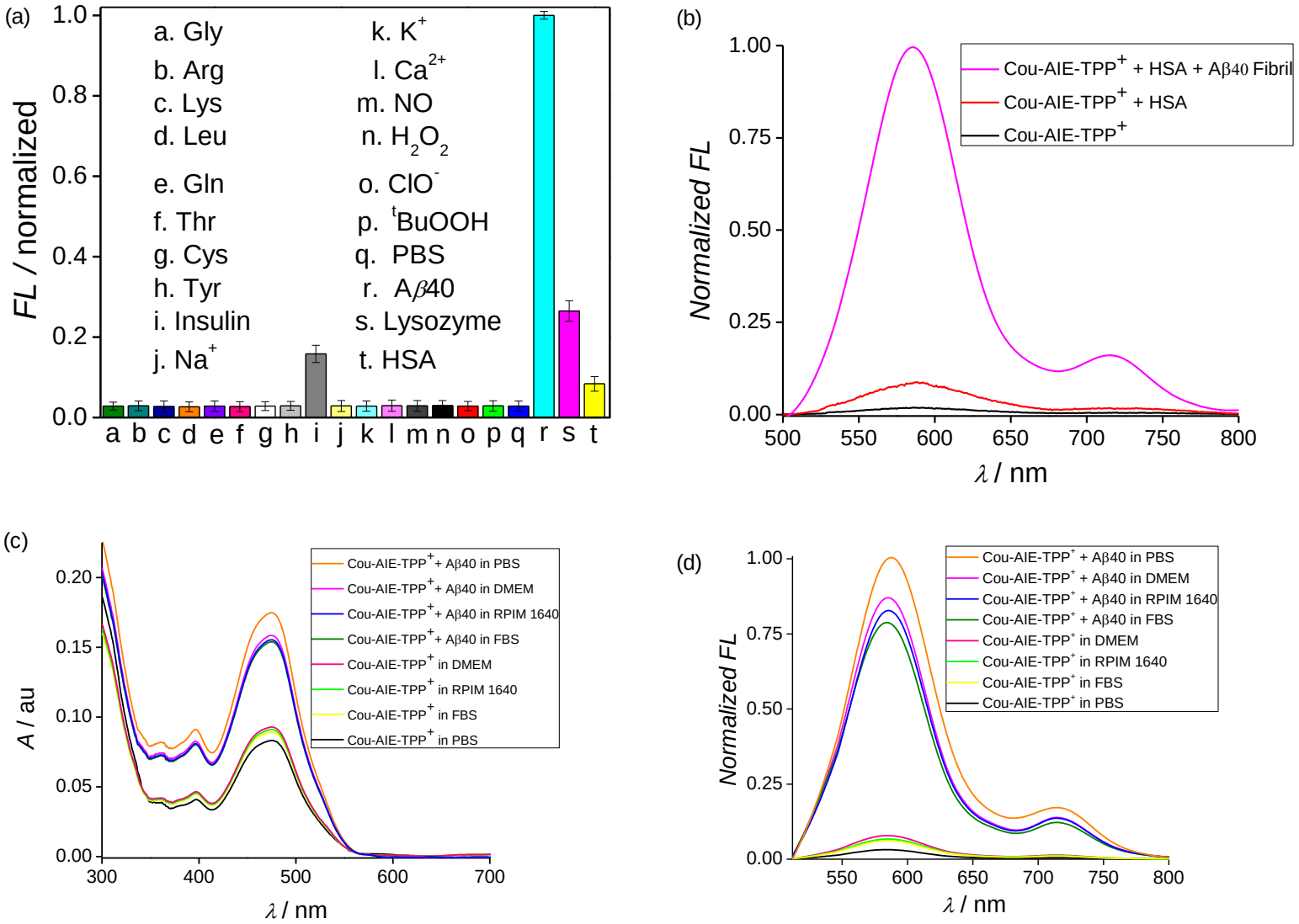

Fig. S39 (a) High selectivity of Cou-AIE-TPP$^+$ towards Aβ40 aggregates over other potential competitive species. Insignificant fluctuations are perceived in the emission of Cou-AIE-TPP$^+$ (1 μM, λ_{em} 604 nm) in the presence of various interferents in PBS, pH 7.4, 37 °C, 24 h. Error bars are ± SD (n = 3). (b) Insignificant fluorescence enhancement of Cou-AIE-TPP$^+$ (1 μM) after incubation with human serum albumin (HSA) protein. Aβ40 can effectively be detected by Cou-AIE-TPP$^+$ in the presence of HSA protein. (c) Absorption and (d) emission plots signify that Aβ40 can efficiently be sensed by Cou-AIE-TPP$^+$ in the presence of various fresh cell culture media, e.g., PBS, FBS-PBS, RPMI 1640, DMEM.

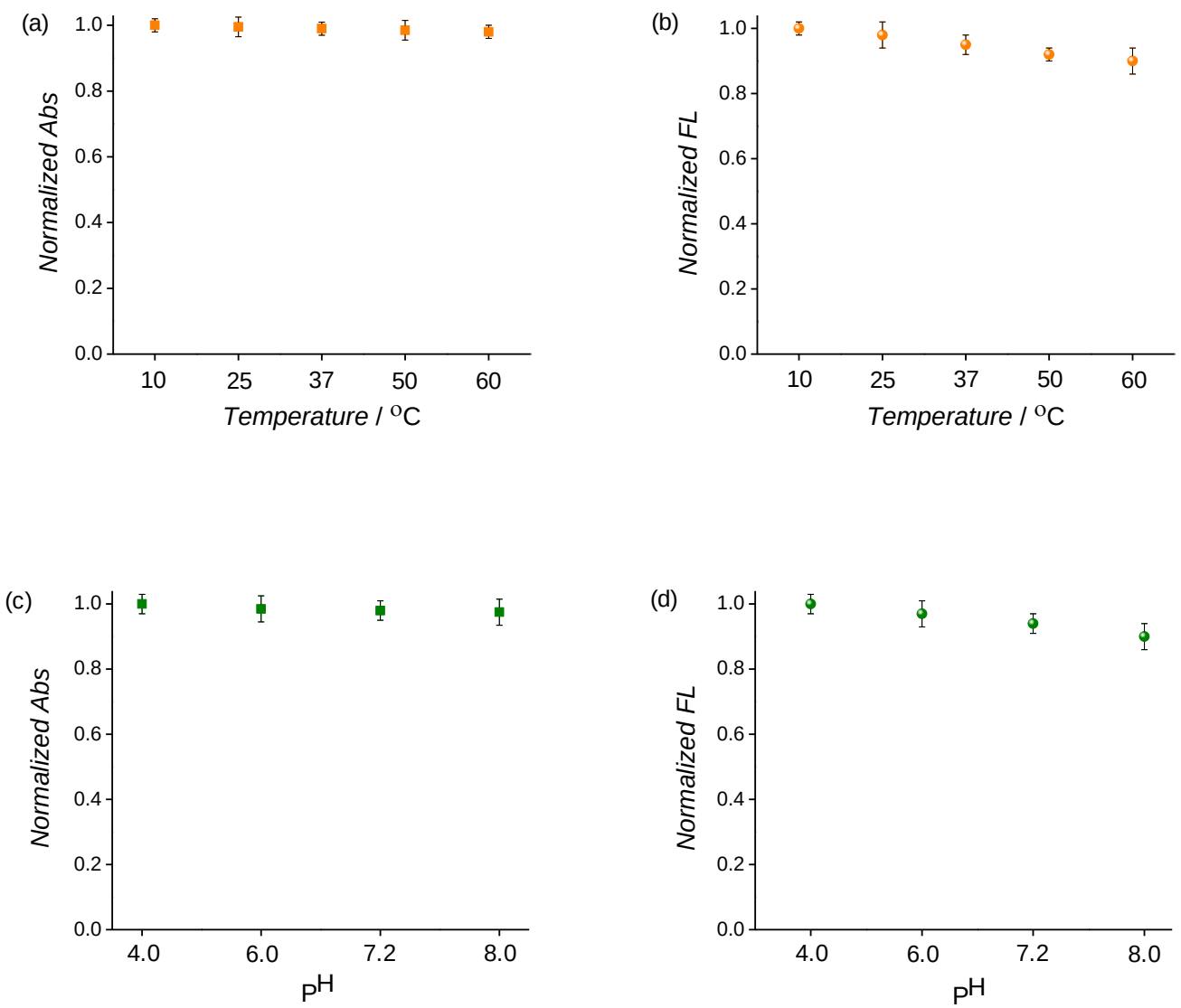

Fig. S40 Trivial (a) absorbance (λ_{abs} = 480 nm) and (b) fluorescence (λ_{em} 600 nm) fluctuation of Cou-AIE-TPP$^+$ (1 μM) at various temperatures (10–60 °C) over 24 h. (b) Insignificant (c) absorbance and (d) fluorescence alteration of Cou-AIE-TPP$^+$ (1 μM) in PBS at different pH values (pH 4–8) over 24 h. Error bars are ± SD (n = 3).

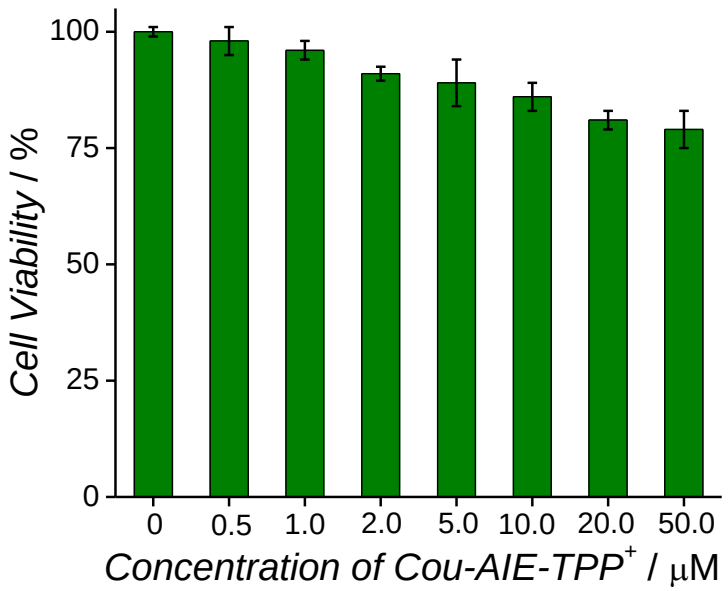

Fig. S41 Cell viability of SH-SY5Y cells at different doses of Cou-AIE-TPP^+ over 72 h exhibits negligible cytotoxicity.

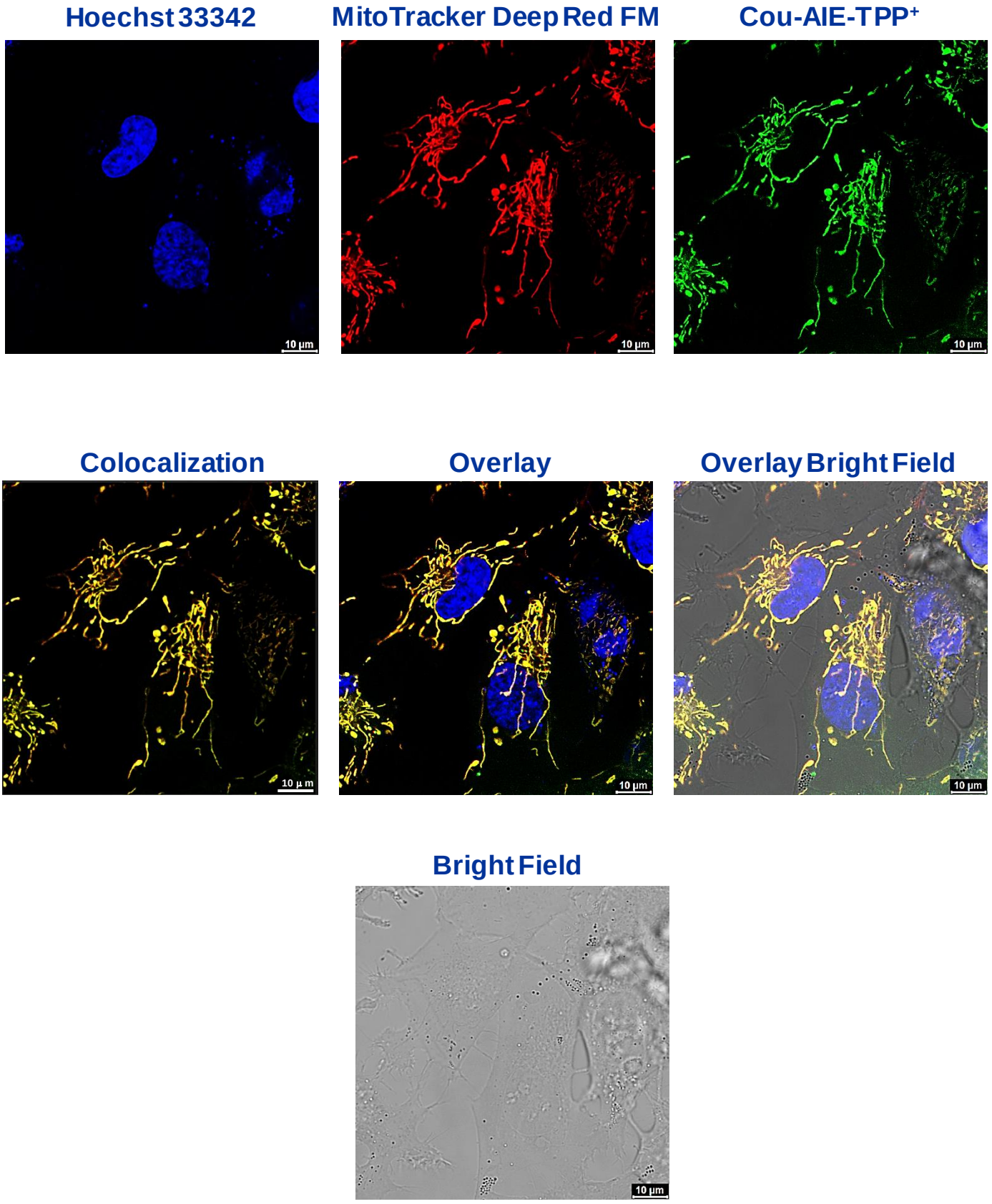

Fig. S42 Confocal microscopic images of Cou-AIE-TPP$^+$ colocalized with MitoTracker Deep Red FM in human neuroblastoma live SH-SY5Y cells. Hoechst 33342 (blue channel), MitoTracker Deep Red FM (red channel), and Cou-AIE-TPP$^+$ (green channel).

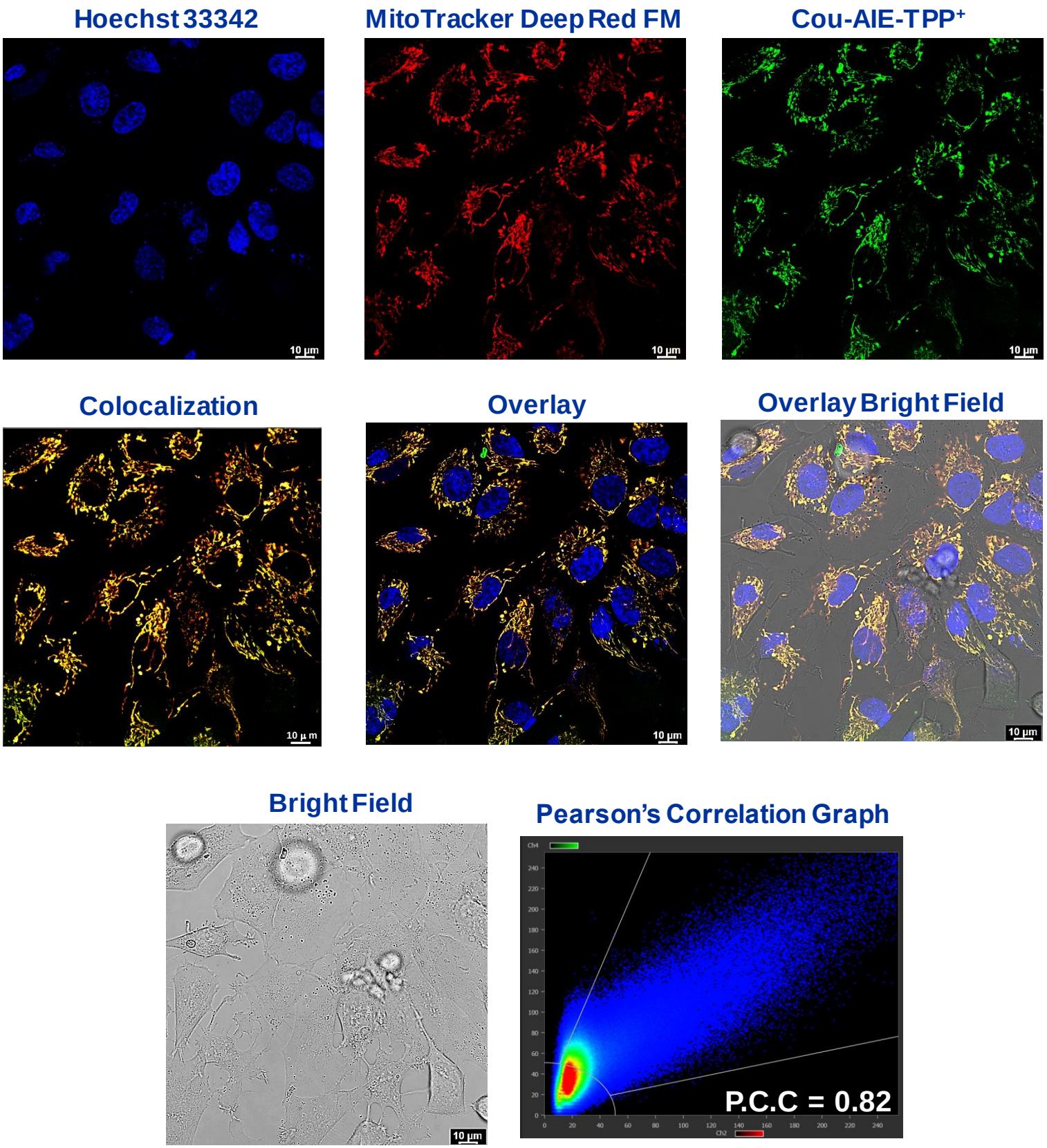

Fig. S43 Confocal microscopic images of Cou-AIE-TPP$^+$ colocalized with MitoTracker Deep Red FM in human neuroblastoma live SH-SY5Y cells. Hoechst 33342 (blue channel), MitoTracker Deep Red FM (red channel), and Cou-AIE-TPP$^+$ (green channel). Colocalization scatter graph displays Pearson's correlation coefficient (PCC) of 0.82.

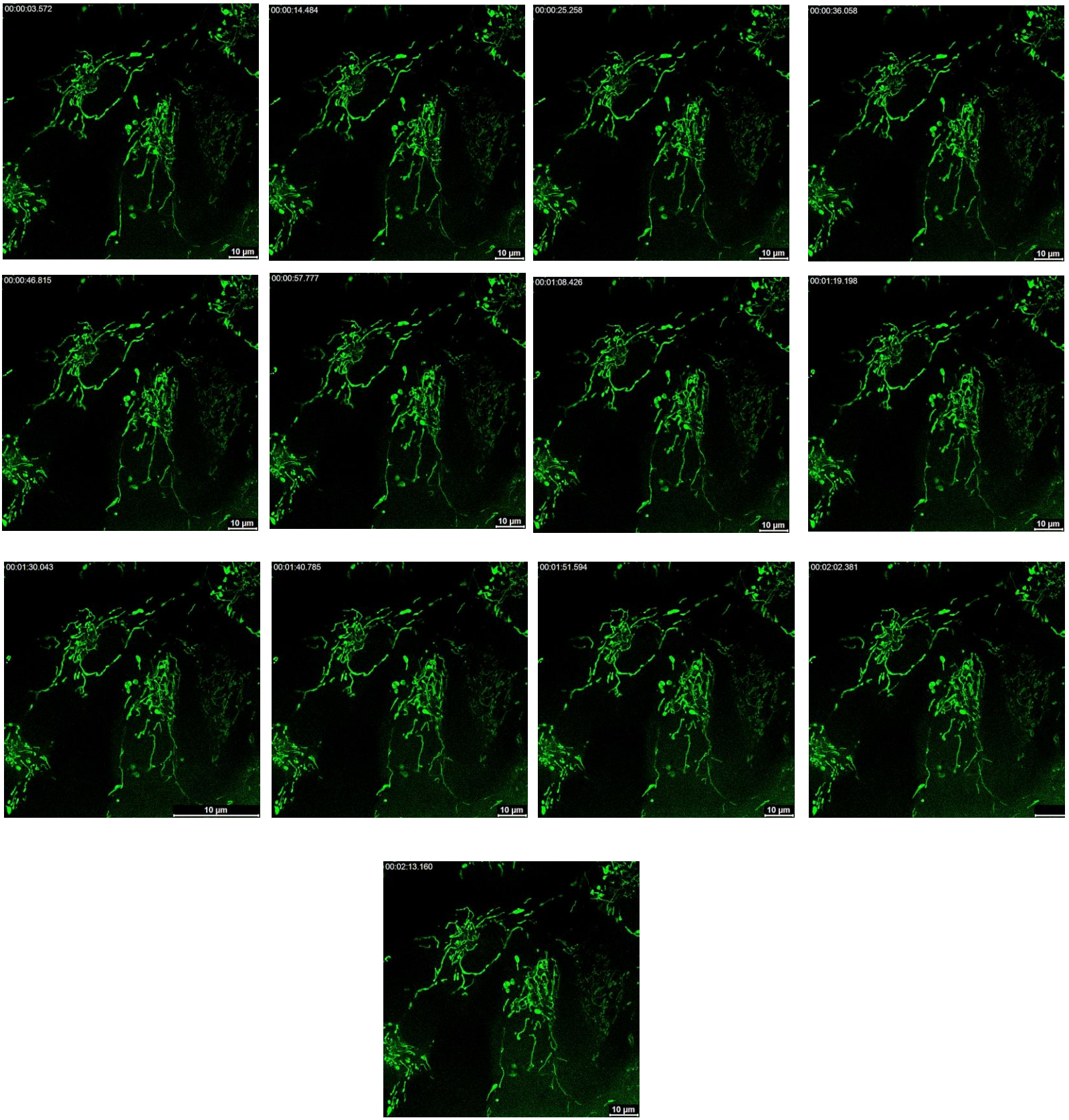

Fig. S44 Real-time mitochondrial tracking inside the human neuroblastoma live SH-SY5Y cells stained with the mitochondria targeting synthesized Cou-AIE-TPP^{+} probe.

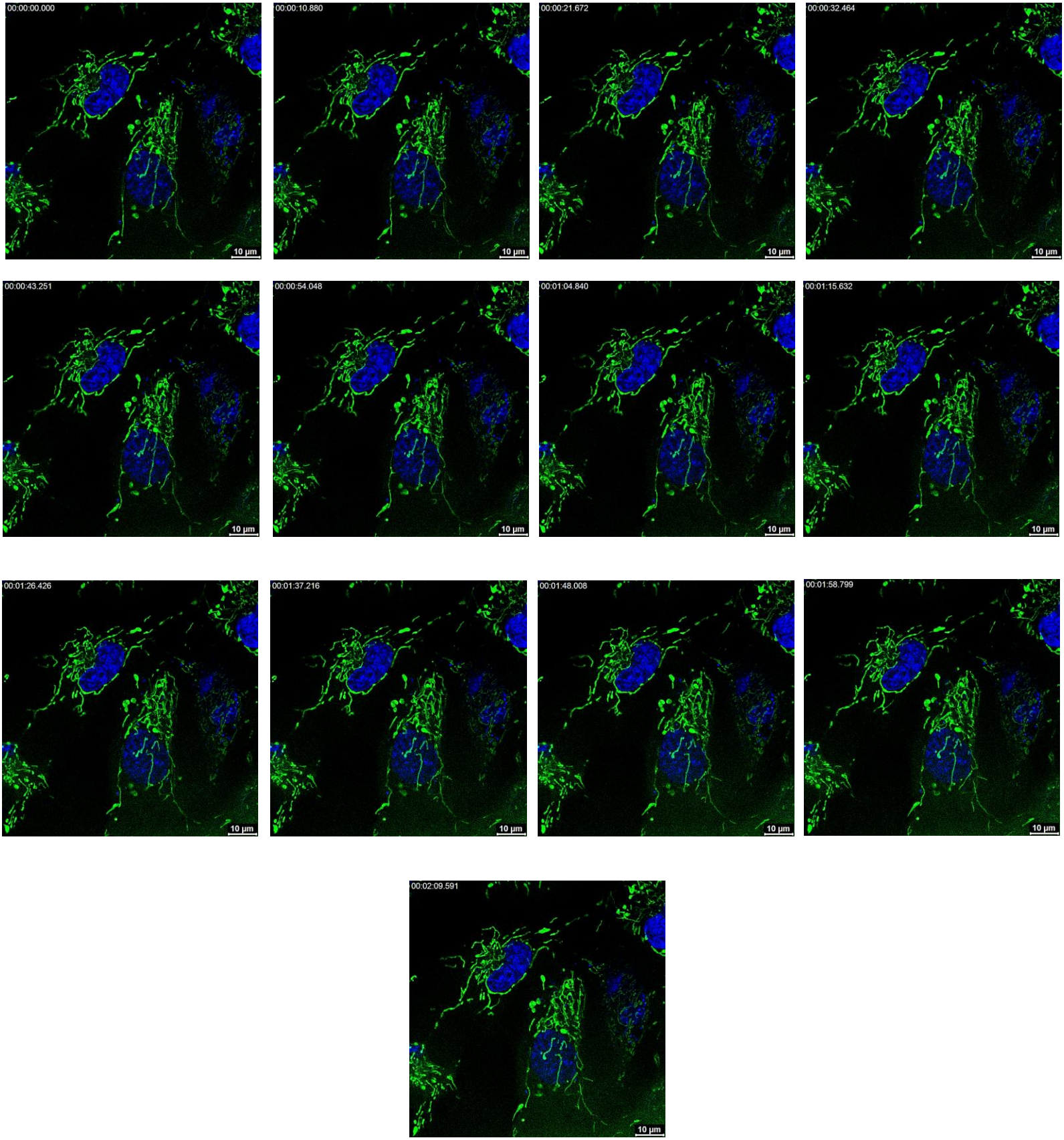

Fig. S45 Real-time mitochondrial tracking inside the human neuroblastoma live SH-SY5Y cells stained with the mitochondria targeting synthesized Cou-AIE-TPP^{+} probe. Blue color signifies nuclear staining by Hoechst 33342.

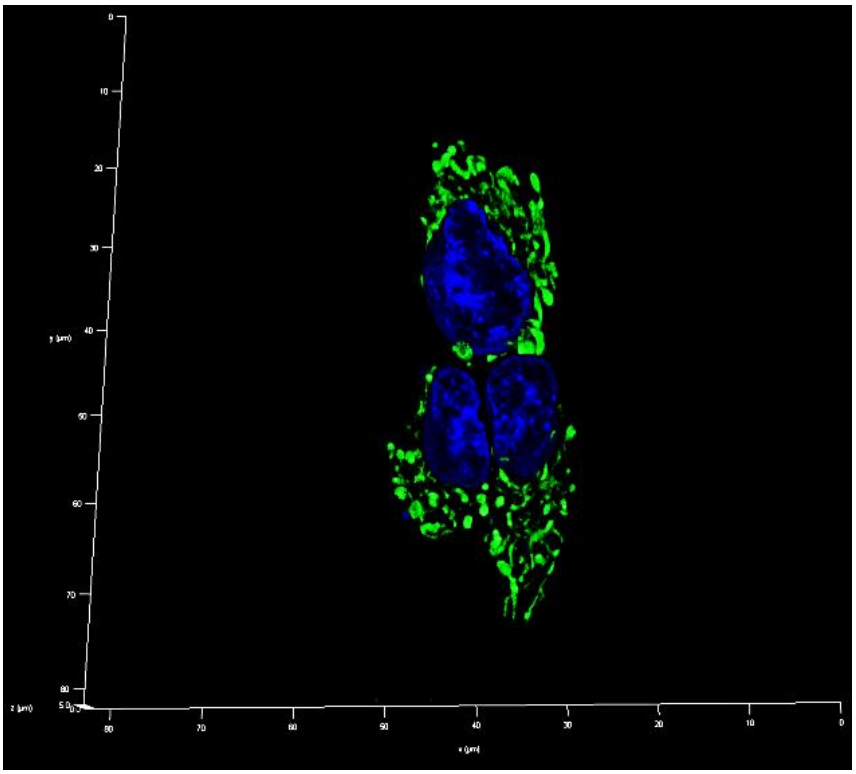

Fig. S46 3D CLSM image of the human neuroblastoma live SH-SY5Y cells stained with our synthesized mitochondria targeting Cou-AIE-TPP^{+} dye (green color). Blue color signifies nuclear staining by Hoechst 33342.

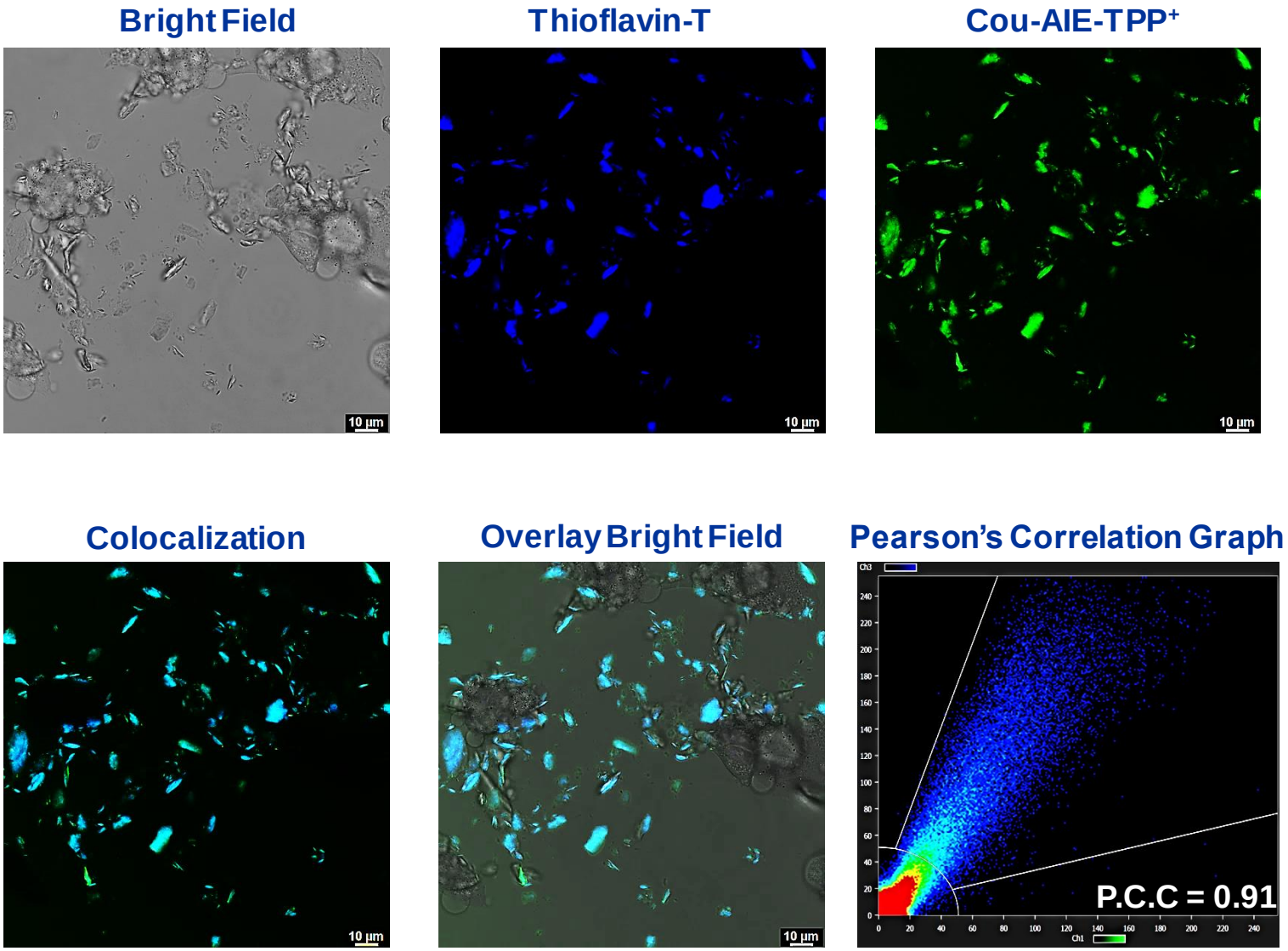

Fig. S47 Confocal microscopic images of human neuroblastoma SH-SY5Y cells incubated for 48 h with Aβ40, stained with Cou-AIE-TPP$^+$ and colocalized with Thioflavin-T (ThT). ThT (blue channel) and Cou-AIE-TPP$^+$ (green channel). Colocalization scatter graph displays PCC of 0.91.

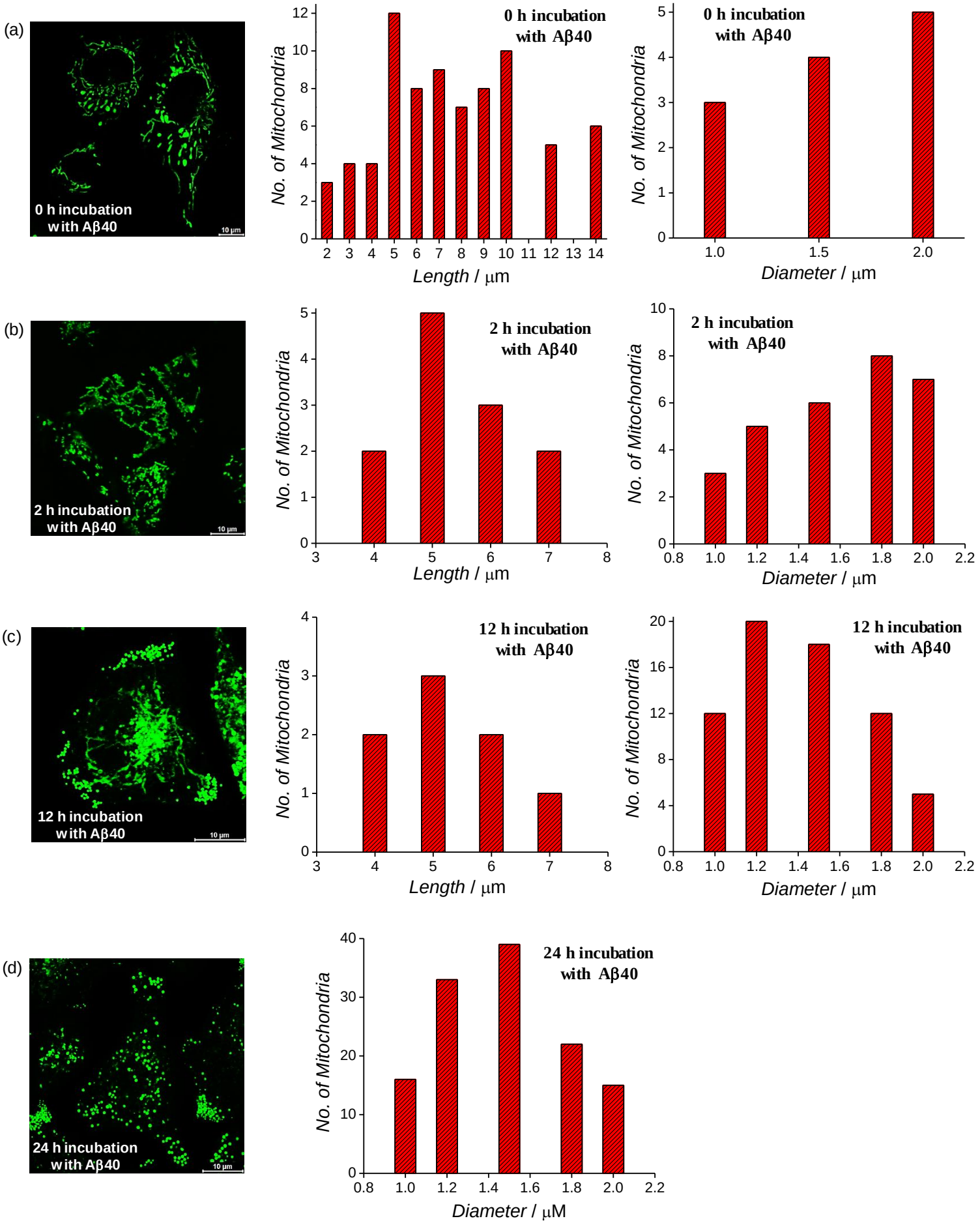

Fig. S48 (a-d) Quantification of mitochondrial morphological changes in human neuroblastoma SH-SY5Y cells using CLSM images through statistical analyses of mitochondrial lengths and diameters after incubation with Aβ40 at various time points.

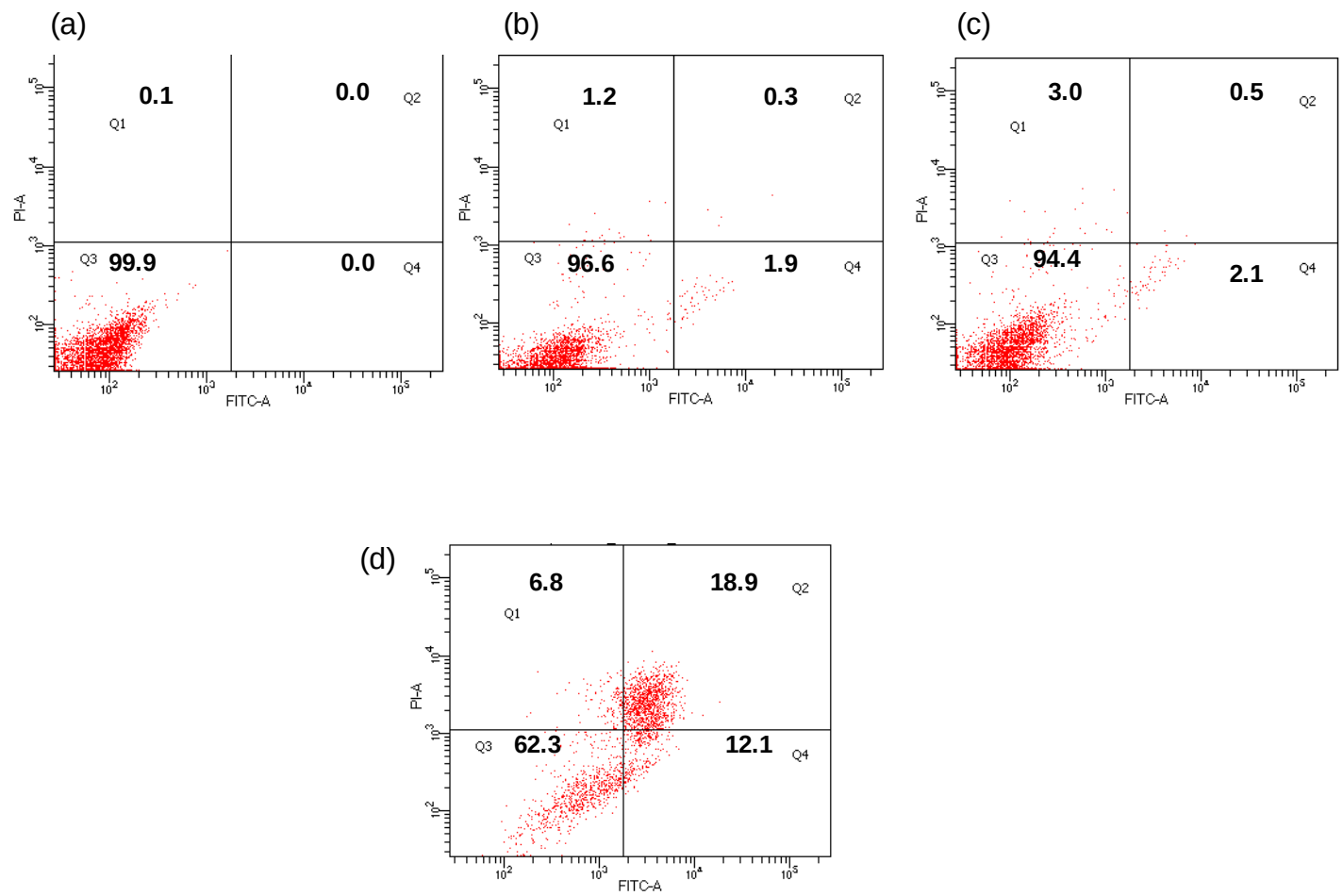

Fig. S49 Time-dependent effect of Aβ40 to monitor early and late apoptosis in SH-SY5Y cells. (a) Control experiment in the absence of Aβ40. (b) Cells treated with Aβ40 (10.0 μM) after 6 h, (c) 12 h, and (d) 24 h. Lower left (Q3) quadrant denotes cell viability, both Annexin V and PI, -Ve; lower right (Q4) quadrant: Annexin V, +Ve and PI, -Ve; upper right (Q2) quadrant: Annexin V, +Ve and PI, +Ve; upper left (Q1) quadrant: Annexin V, -Ve and PI, +Ve.

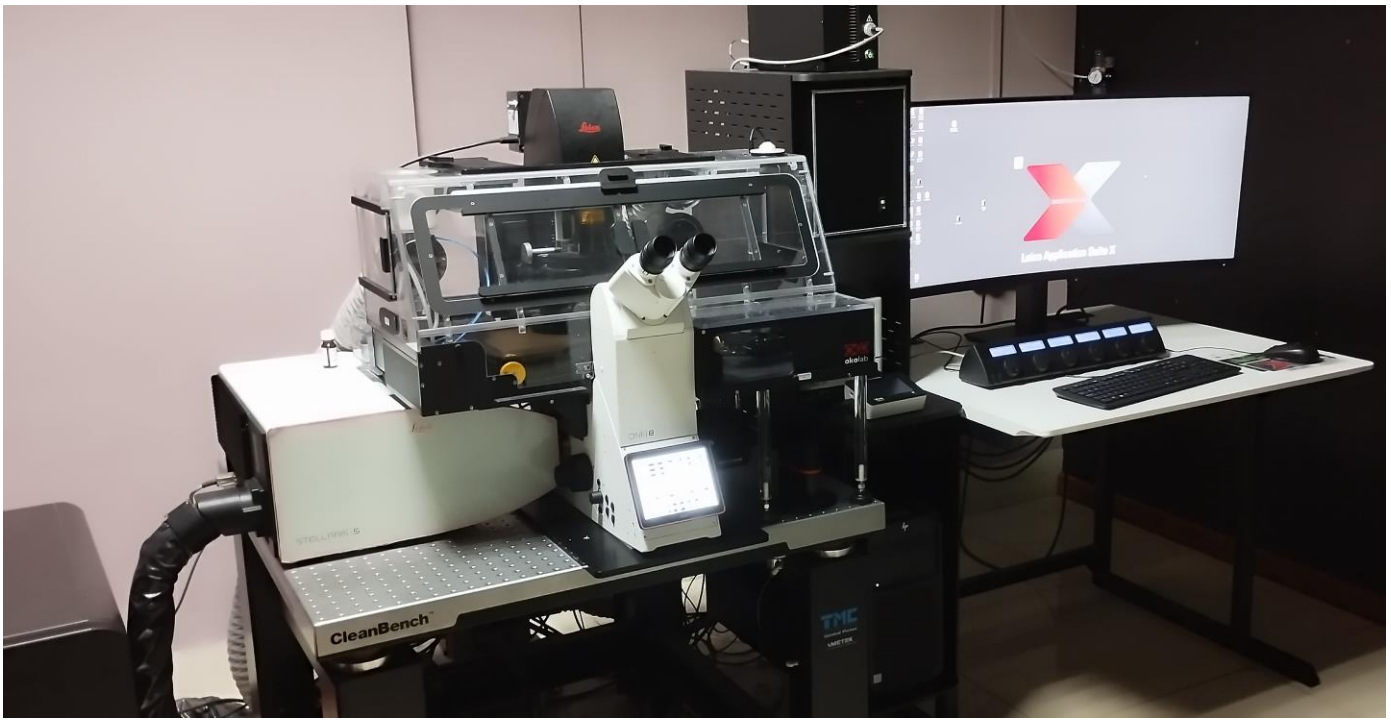

Fig. S50 CLSM device utilized for the live SH-SY5Y cell imaging preserving 5% CO_2 incubation and 37 °C.